

CYCLIC SHEAR LOADING RESPONSE OF FRASER RIVER DELTA SILT

by

MARIA VICTORIA SANÍN

B.Sc. Universidad Nacional de Colombia, 1999

MASc. University of British Columbia, 2005

A THESIS SUBMITTED IN PARTIAL FULFILLMENT OF
THE REQUIREMENTS FOR THE DEGREE OF

DOCTOR OF PHILOSOPHY

in

THE FACULTY OF GRADUATE STUDIES
(Civil Engineering)

THE UNIVERSITY OF BRITISH COLUMBIA
(Vancouver)

November 2010

© Maria Victoria Sanín 2010

ABSTRACT

The cyclic shear response of low-plastic Fraser River silt was investigated using constant-volume direct simple shear testing. Silt specimens, initially consolidated to stress levels at or above the preconsolidation stress, displayed cyclic mobility type strain development during cyclic loading. Liquefaction in the form of strain softening accompanied by loss of shear strength did not manifest regardless of the applied cyclic stress ratio (CSR), or the level of induced excess pore water pressure (Δu). Cyclic mobility type stress-strain behaviour was observed in spite of the initial static shear stress bias. The potential for excess pore water pressure generation and associated shear strain development during cyclic loading was observed to increase with increasing level of initial static shear. Tests on specimens of undisturbed field samples and specimens reconstituted using the same silt material showed that undisturbed silt, despite having a looser density under identical consolidation stress conditions, exhibited more dilative response and larger shear resistance compared to those displayed by reconstituted specimens. In addition to consolidation stress conditions and resulting void ratios, it appears that other naturally inherited parameters such as soil fabric and aging effects would influence the shear response of natural silt.

Studies were also conducted to examine the post-cyclic reconsolidation response of low-plastic

silt using specimens of undisturbed and reconstituted Fraser River silt and reconstituted quartz powder initially subjected to constant volume cyclic loading at different CSR values and then reconsolidated to their initial effective stresses. The volumetric strains during post-cyclic reconsolidation (ϵ_{v-ps}) were noted to increase with the maximum Δu and maximum cyclic shear strain experienced during cyclic loading. The values of ϵ_{v-ps} and maximum excess cyclic pore water pressure ratio (r_{u-max}) were observed to form a coherent relationship regardless of overconsolidation effects, particle fabric, and initial void ratio of the soil. The specimens with high r_{u-max} suffered significantly higher post-cyclic reconsolidation strains. The observed ϵ_{v-ps} versus r_{u-max} relationship, when combined with the observed dependence of r_u on CSR and number of load cycles, seems to provide a reasonable approach to estimate post-cyclic reconsolidation strains of low-plastic silt.

TABLE OF CONTENTS

Abstract	ii
Table of Contents	ii
List of Tables	viii
List of Figures	ix
Acknowledgements	xvii
1 Introduction.....	1
1.1 Background.....	1
1.2 Response of soils to earthquake loading.....	2
1.3 Objectives of the thesis	3
1.4 Scope of work	4
2 Literature Review	6
2.1 General mechanical response of soils to cyclic shear loading.....	7
2.1.1 Response of sands.....	7
2.1.1.1 Monotonic response.....	7
2.1.1.2 Cyclic response	10
2.1.2 Response of clays	16
2.1.3 Response of silts	20
2.2 Earthquake-induced settlements	23
2.3 Closure	25

3	Material Tested and Experimental Aspects	26
3.1	Material tested	26
3.2	Specimen reconstitution method.....	30
3.3	Direct simple shear apparatus.....	31
3.3.1	DSS loading system.....	32
3.3.2	Data acquisition, control system and measurement resolution.....	35
3.3.3	DSS Test procedure	36
3.3.3.1	Specimen extrusion and setup	36
3.3.3.2	Consolidation phase.....	37
3.3.3.3	Static shear bias application phase	39
3.3.3.4	Shear loading phase	39
3.3.3.5	Post-cyclic reconsolidation	40
3.4	Test program.....	40
4	Cyclic Shear Response of Fraser River Delta Silt.....	43
4.1	Monotonic shear loading response	47
4.1.1	Effect of initial effective confining stress.....	47
4.1.2	Effect of initial static shear stress bias.....	50
4.2	Cyclic response.....	53
4.2.1	Effects of initial effective confining stress	53
4.2.1.1	General stress strain pore water pressure response.....	53
4.2.1.2	Cyclic shear resistance.....	63
4.2.2	Effects of initial static shear loading	66
4.2.2.1	General stress strain pore water pressure response.....	66
4.2.2.2	Cyclic shear resistance.....	76
4.2.3	Effects of overconsolidation	77

4.2.3.1	General stress strain pore water pressure response.....	77
4.2.3.2	Cyclic shear resistance.....	79
4.3	Other considerations and discussion.....	81
4.3.1	Sensitivity of cyclic shear resistance to strain criteria.....	81
4.3.2	Comparison with cyclic shear response of sand.....	83
4.4	Observations on the cyclic shear response of other fine-grained soils.....	84
4.4.1	Cyclic shear response	85
4.4.2	Cyclic shear resistance.....	89
4.5	Comparison of experimental observations with empirical criteria for liquefaction	91
4.6	Summary and principal findings.....	93
5	Effects of Particle Structure in the Mechanical Response of Fine-Grained Soils.....	95
5.1	Mechanical response of undisturbed and reconstituted Fraser River silt	96
5.1.1	Monotonic shear response	96
5.2	Cyclic shear response	103
5.3	Comparison of cyclic shear response between reconstituted and undisturbed Fraser River silt.....	105
5.3.1	Effects of “ageing” of reconstituted soils on the cyclic shear resistance.....	109
5.3.2	Cyclic shear resistance.....	111
5.3.3	Observations on the cyclic shear response between undisturbed and reconstituted specimens on different materials.....	111
5.4	Summary and principal findings.....	115
6	Post-Cyclic Reconsolidation Strains in Low Plastic Fraser River Silt.....	118
6.1	Experimental observations.....	119
6.1.1	Post-cyclic reconsolidation response.....	119
6.1.2	An approach for estimation of post-cyclic volumetric strains.....	126
6.2	Summary and principal findings.....	128

7 Summary and Conclusions	130
7.1 Cyclic shear response of Fraser River silt	131
7.1.1 Cyclic shear response of other fine-grained soils	132
7.2 Comparison of the response of undisturbed versus reconstituted specimens of Fraser River silt.....	132
7.3 Post-cyclic reconsolidation response of low-plastic silt.....	134
7.4 Recommendations for future research	135
References.....	137

LIST OF TABLES

Table 3.1. Index parameters of Fraser River delta silt.....	29
Table 3.2 Measurement resolution of UBC-DSS device.....	36
Table 3.3 Test program.....	42
Table 4.1 Test parameters and summary results.....	44
Table 4.2 Summary of index properties of the materials used for observations of effects of plasticity on the cyclic response of fine-grained materials.....	84

LIST OF FIGURES

Figure 2.1 Typical shear response of loose and dense sand observed during drained monotonic loading in the direct shear apparatus (Modified from Schofield and Wroth, 1968).	9
Figure 2.2 Typical undrained monotonic loading response of sand. a) Stress-strain response. b) Stress path (after Vaid and Chern, 1985).	9
Figure 2.3 Typical “liquefaction” response during undrained cyclic loading. a) Stress-Strain response. b) Stress Path. c) Shear strain development (after Vaid and Chern, 1985).	11
Figure 2.4 Typical “limited liquefaction due to cyclic loading” type of response during undrained cyclic loading. a) Stress-Strain response. b) Stress Path. c) Shear strain development (after Vaid and Chern, 1985).	12
Figure 2.5 Typical “cyclic mobility” type of response during undrained cyclic loading. a) Stress-Strain response. b) Stress Path. c) Shear strain development (after Vaid and Chern, 1985).	13
Figure 2.6 (a) Field and laboratory model cases and (b) stress conditions for an element of soil.	15
Figure 2.7 Stress-strain and stress path response of Cloverdale clay during undrained cyclic loading (Zergoun and Vaid 1994).	17
Figure 2.8 Cyclic stress ratios required to cause failure or some strain criteria versus number of uniform cycles at a frequency of 1 Hz in different clays. (Boulanger and Idriss 2008)	18
Figure 2.9. Effects of preshearing: Cyclic resistance ratio versus number of cycles to reach $\gamma=3.75\%$ on first and second cyclic loading phases from constant volume DSS tests on Fraser River silt (Sanin 2005).	21
Figure 2.10 Schematic diagram explaining contractive and dilative shear behaviour during undrained monotonic and cyclic loading (Hyde et al. 2006)	22

Figure 3.1 Cone penetration test profile of the site at No. 3 Road in Richmond BC. – Depth horizon of the channel fill Fraser River silt used in the present study identified. ...	28
Figure 3.2 Grain size analysis of different samples of Fraser River silt.....	29
Figure 3.3 Comparison of stress conditions in (a) Simple Shear testing – DSS and (b) Triaxial testing – CTX.....	33
Figure 3.4 Schematic diagram of UBC simple shear test device (Modified from Sriskandakumar, 2004).....	34
Figure 3.5. Sample preparation and set up in DSS equipment.....	38
Figure 4.1 Constant volume monotonic DSS test on undisturbed specimens of Fraser River Delta silt at varying confining stress levels: Stress-strain curves; $\sigma'_{vc} = 100$, 200, 300, 400 and 500 kPa.....	48
Figure 4.2 Constant volume monotonic DSS test on undisturbed specimens of Fraser River Delta silt at varying confining stress levels: Stress path curves; $\sigma'_{vc} = 100$, 200, 300, 400 and 500 kPa.....	49
Figure 4.3 Constant volume monotonic DSS test on undisturbed specimens of Fraser River Delta silt at varying confining stress levels: Normalized stress path curves; $\sigma'_{vc} = 100$, 200, 300, 400 and 500 kPa.....	49
Figure 4.4. Application of static shear prior to monotonic shear in constant volume DSS test on undisturbed specimens of Fraser River Delta silt at varying initial static shear bias (α): $\sigma'_{vc} = 100$; $\alpha=0.05$, 0.10, 0.15. a) Stress-Strain curve, b) Volumetric strain versus shear strain.....	51
Figure 4.5 Constant volume monotonic DSS test on undisturbed specimens of Fraser River Delta silt at varying initial static shear bias (α): Stress-strain curves; $\sigma'_{vc} = 100$; $\alpha=0.05$, 0.10, 0.15.....	52
Figure 4.6 Constant volume monotonic DSS test on undisturbed specimens of Fraser River Delta silt at varying initial static shear bias (α): Stress path curves; $\sigma'_{vc} = 100$; $\alpha=0.05$, 0.10, 0.15.....	52
Figure 4.7 Constant volume cyclic simple shear DSS test on undisturbed specimen of normally consolidated Fraser River Delta silt: Stress strain and stress path curves; $\sigma'_{vc} = 100$; CSR = 0.14.....	54
Figure 4.8 Constant volume cyclic simple shear DSS test on undisturbed specimen of normally consolidated Fraser River Delta silt: Stress strain and stress path curves; $\sigma'_{vc} = 100$; CSR = 0.17.....	55
Figure 4.9. Constant volume cyclic simple shear DSS test on undisturbed specimen of	

normally consolidated Fraser River Delta silt: Stress strain and stress path curves; $\sigma'_{vc} = 100$; CSR = 0.20.....	55
Figure 4.10 Constant volume cyclic simple shear DSS test on undisturbed specimen of normally consolidated Fraser River Delta silt: Stress strain and stress path curves; $\sigma'_{vc} = 100$; CSR = 0.29.....	56
Figure 4.11 Constant volume cyclic simple shear DSS test on undisturbed specimen of normally consolidated Fraser River Delta silt: Stress strain and stress path curves; $\sigma'_{vc} = 300$; CSR = 0.12.....	56
Figure 4.12 Constant volume cyclic simple shear DSS test on undisturbed specimen of normally consolidated Fraser River Delta silt: Stress strain and stress path curves; $\sigma'_{vc} = 300$; CSR = 0.15.....	57
Figure 4.13 Constant volume cyclic simple shear DSS test on undisturbed specimen of normally consolidated Fraser River Delta silt: Stress strain and stress path curves; $\sigma'_{vc} = 300$; CSR = 0.17.....	57
Figure 4.14 Constant volume cyclic simple shear DSS test on undisturbed specimen of normally consolidated Fraser River Delta silt: Stress strain and stress path curves; $\sigma'_{vc} = 300$; CSR = 0.20.....	58
Figure 4.15 Constant volume cyclic simple shear DSS test on undisturbed specimen of normally consolidated Fraser River Delta silt: Stress strain and stress path curves; $\sigma'_{vc} = 400$; CSR = 0.12.....	58
Figure 4.16 Constant volume cyclic simple shear DSS test on undisturbed specimen of normally consolidated Fraser River Delta silt: Stress strain and stress path curves; $\sigma'_{vc} = 400$; CSR = 0.17.....	59
Figure 4.17 Constant volume cyclic simple shear DSS test on undisturbed specimen of normally consolidated Fraser River Delta silt: Stress strain and stress path curves; $\sigma'_{vc} = 400$; CSR = 0.19.....	59
Figure 4.18 Constant volume cyclic simple shear DSS test on undisturbed specimen of normally consolidated Fraser River Delta silt: Excess pore water pressure vs. number of loading cycles for different CSR values; $\sigma'_{vc} = 100$ kPa.	60
Figure 4.19 Constant volume cyclic simple shear DSS test on undisturbed specimen of normally consolidated Fraser River Delta silt: Excess pore water pressure vs. number of loading cycles for different CSR values; $\sigma'_{vc} = 300$ kPa.	61
Figure 4.20 Constant volume cyclic simple shear DSS test on undisturbed specimen of normally consolidated Fraser River Delta silt: Excess pore water pressure vs. number of loading cycles for different CSR values; $\sigma'_{vc} = 400$ kPa.	61

Figure 4.21 Cyclic resistance ratio (τ_{cy}/σ'_{vc}) from constant volume cyclic DSS tests on undisturbed specimens of normally consolidated Fraser River Delta silt at varying initial confining stress levels.	64
Figure 4.22. Cyclic strength ratio (τ_{cy}/s_u^{DSS}) from constant volume cyclic DSS tests on undisturbed specimens of normally consolidated Fraser River Delta silt at varying initial confining stress levels.	65
Figure 4.23 Constant volume cyclic simple shear DSS test on undisturbed specimen of normally consolidated Fraser River Delta silt: Stress strain and stress path curves; $\sigma'_{vc} = 100$ kPa; CSR = 0.12; $\alpha=0.05$	66
Figure 4.24 Constant volume cyclic simple shear DSS test on undisturbed specimen of normally consolidated Fraser River Delta silt: Stress strain and stress path curves; $\sigma'_{vc} = 100$ kPa; CSR = 0.15; $\alpha=0.05$	67
Figure 4.25 Constant volume cyclic simple shear DSS test on undisturbed specimen of normally consolidated Fraser River Delta silt: Stress strain and stress path curves; $\sigma'_{vc} = 100$ kPa; CSR = 0.19; $\alpha=0.05$	67
Figure 4.26 Constant volume cyclic simple shear DSS test on undisturbed specimen of normally consolidated Fraser River Delta silt: Stress strain and stress path curves; $\sigma'_{vc} = 100$ kPa; CSR = 0.21; $\alpha=0.05$	68
Figure 4.27 Constant volume cyclic simple shear DSS test on undisturbed specimen of normally consolidated Fraser River Delta silt: Stress strain and stress path curves; $\sigma'_{vc} = 100$ kPa; CSR = 0.09; $\alpha=0.10$	68
Figure 4.28 Constant volume cyclic simple shear DSS test on undisturbed specimen of normally consolidated Fraser River Delta silt: Stress strain and stress path curves; $\sigma'_{vc} = 100$ kPa; CSR = 0.13; $\alpha=0.10$	69
Figure 4.29 Constant volume cyclic simple shear DSS test on undisturbed specimen of normally consolidated Fraser River Delta silt: Stress strain and stress path curves; $\sigma'_{vc} = 100$ kPa; CSR = 0.12; $\alpha=0.10$	69
Figure 4.30 Constant volume cyclic simple shear DSS test on undisturbed specimen of normally consolidated Fraser River Delta silt: Stress strain and stress path curves; $\sigma'_{vc} = 100$ kPa; CSR = 0.17; $\alpha=0.10$	70
Figure 4.31 Constant volume cyclic simple shear DSS test on undisturbed specimen of normally consolidated Fraser River Delta silt: Stress strain and stress path curves; $\sigma'_{vc} = 100$ kPa; CSR = 0.19; $\alpha=0.10$	70
Figure 4.32 Constant volume cyclic simple shear DSS test on undisturbed specimen of normally consolidated Fraser River Delta silt: Stress strain and stress path curves; $\sigma'_{vc} = 100$ kPa; CSR = 0.20; $\alpha=0.10$	71

Figure 4.33 Constant volume cyclic simple shear DSS test on undisturbed specimen of normally consolidated Fraser River Delta silt: Stress strain and stress path curves; $\sigma'_{vc} = 100$ kPa; CSR = 0.12; $\alpha=0.15$.	71
Figure 4.34 Constant volume cyclic simple shear DSS test on undisturbed specimen of normally consolidated Fraser River Delta silt: Stress strain and stress path curves; $\sigma'_{vc} = 100$ kPa; CSR = 0.15; $\alpha=0.15$.	72
Figure 4.35 Constant volume cyclic simple shear DSS test on undisturbed specimen of normally consolidated Fraser River Delta silt: Stress strain and stress path curves; $\sigma'_{vc} = 100$ kPa; CSR = 0.19; $\alpha=0.15$.	72
Figure 4.36 Constant volume cyclic simple shear DSS test on undisturbed specimen of normally consolidated Fraser River Delta silt: Stress strain and stress path curves; $\sigma'_{vc} = 100$ kPa; CSR = 0.16; $\alpha=0.15$.	73
Figure 4.37 Constant volume cyclic simple shear DSS test on undisturbed specimen of normally consolidated Fraser River Delta silt: Stress strain and stress path curves; $\sigma'_{vc} = 100$ kPa; CSR = 0.11; $\alpha=0.15$.	73
Figure 4.38 Constant volume cyclic simple shear DSS test on undisturbed specimen of normally consolidated Fraser River Delta silt: Pore water pressure development at different initial static shear values and constant CSR = 0.15.	75
Figure 4.39 Constant volume cyclic simple shear DSS test on undisturbed specimen of normally consolidated Fraser River Delta silt: Pore water pressure development at different initial static shear values and constant CSR = 0.20.	75
Figure 4.40 Cyclic resistance ratio from constant volume cyclic DSS tests on undisturbed specimens of normally consolidated Fraser River Delta silt at varying initial static shear bias.	76
Figure 4.41 Constant volume cyclic simple shear DSS test on undisturbed specimen of overconsolidated Fraser River Delta silt: Stress strain and stress path curves; $\sigma'_{vc} = 100$ kPa; CSR = 0.21; OCR=1.3.	77
Figure 4.42 Constant volume cyclic simple shear DSS test on undisturbed specimen of overconsolidated Fraser River Delta silt: Stress strain and stress path curves; $\sigma'_{vc} = 100$ kPa; CSR = 0.21; OCR=1.7	78
Figure 4.43. Comparison of constant volume cyclic simple shear DSS test on specimens of Fraser River Delta silt at different overconsolidation ratios. First and eleventh loading cycles: Stress strain and stress path curves; $\sigma'_{vc} = 100$ kPa; CSR = 0.21.	79
Figure 4.44 Cyclic resistance ratio from constant volume cyclic DSS tests on undisturbed specimens of Fraser River Delta silt at varying overconsolidation ratios.	80

Figure 4.45	Cyclic resistance ratio from constant volume cyclic DSS tests on undisturbed specimens of Fraser River Delta: Effect of overconsolidation ratio.....	81
Figure 4.46	Cyclic resistance ratio from constant volume cyclic DSS tests on undisturbed specimens of Fraser River Delta: Effect of overconsolidation ratio.....	82
Figure 4.47	Grain size analyses of fine-grained soils analyzed in this study	85
Figure 4.48	Constant volume cyclic simple shear DSS test on undisturbed specimen of natural Kitimat clay: Stress strain and stress path curves; $\sigma'_{vc} = 80$ kPa; CSR = 0.24.	86
Figure 4.49	Constant volume cyclic simple shear DSS test on undisturbed specimen of natural Kitimat clay: Stress strain and stress path curves; $\sigma'_{vc} = 80$ kPa; CSR = 0.26.	87
Figure 4.50	Constant volume cyclic simple shear DSS test on undisturbed specimen of natural Kitimat clay: Stress strain and stress path curves; $\sigma'_{vc} = 80$ kPa; CSR = 0.17.	87
Figure 4.51	Constant volume cyclic simple shear DSS test on specimen of quartz rock powder: Stress strain and stress path curves; $\sigma'_{vc} = 100$ kPa; CSR = 0.09.	88
Figure 4.52	Constant volume cyclic simple shear DSS test on specimen of quartz rock powder: Stress strain and stress path curves; $\sigma'_{vc} = 100$ kPa; CSR = 0.12.	88
Figure 4.53	Constant volume cyclic simple shear DSS test on specimen of quartz rock powder: Stress strain and stress path curves; $\sigma'_{vc} = 100$ kPa; CSR = 0.14.	89
Figure 4.54	Cyclic resistance ratio from constant volume cyclic DSS tests on undisturbed specimens of fine-grained materials with different plasticity.....	90
Figure 4.55	Application to Bray et al (2006) criteria for liquefaction susceptibility to Fraser River Delta silt.....	91
Figure 5.1	Constant volume monotonic DSS test on reconstituted and undisturbed specimens of Fraser River Delta silt at varying confining stress levels: Stress-strain curves; $\sigma'_{vc} = 100, 200, 300$ and 400 kPa.	97
Figure 5.2	Constant volume monotonic DSS test on reconstituted and undisturbed specimens of Fraser River Delta silt at varying confining stress levels: Stress path curves; $\sigma'_{vc} = 100, 200, 300$ and 400 kPa.	97
Figure 5.3	Constant volume monotonic DSS test on reconstituted and undisturbed specimens of Fraser River Delta silt at varying confining stress levels: Normalized stress path curves; $\sigma'_{vc} = 100, 200, 300$ and 400 kPa.....	99
Figure 5.4	e-log σ'_v relationships for undisturbed and reconstituted specimens of Fraser River silt immediately after initial consolidation compared with those after reaching 15% shear strain in monotonic direct simple shear.	101

Figure 5.5 Constant volume cyclic simple shear DSS test on reconstituted specimen of normally consolidated Fraser River Delta silt: Stress strain and stress path curves; $\sigma'_{vc} = 100$ kPa; CSR = 0.10; consolidation time = 3hrs.	103
Figure 5.6 Constant volume cyclic simple shear DSS test on reconstituted specimen of normally consolidated Fraser River Delta silt: Stress strain and stress path curves; $\sigma'_{vc} = 100$ kPa CSR = 0.12; consolidation time = 3hrs.	104
Figure 5.7 Constant volume cyclic simple shear DSS test on reconstituted specimen of normally consolidated Fraser River Delta silt: Stress strain and stress path curves; $\sigma'_{vc} = 100$ kPa; CSR = 0.15; consolidation time = 3hrs.	104
Figure 5.8 Comparison of constant volume cyclic simple shear DSS test on reconstituted and undisturbed specimens of normally consolidated Fraser River Delta silt. First and twenty-ninth loading cycles: Stress strain and stress path curves; $\sigma'_{vc} = 100$ kPa; CSR = 0.10.....	106
Figure 5.9 Comparison of constant volume cyclic simple shear DSS test on reconstituted and undisturbed specimens of normally consolidated Fraser River Delta silt. First and fourth loading cycles: Stress strain and stress path curves; $\sigma'_{vc} = 100$ kPa; CSR = 0.15.....	107
Figure 5.10 Constant volume cyclic simple shear DSS test on undisturbed and reconstituted specimens of normally consolidated Fraser River Delta silt: Pore water pressure development at different CSR; $\sigma'_{vc} = 100$ kPa.	108
Figure 5.11 Constant volume cyclic simple shear DSS test on reconstituted specimen of normally consolidated Fraser River Delta silt, aged specimen: Stress strain and stress path curves; $\sigma'_{vc} = 100$ kPa CSR = 0.12, consolidation time=24hours.....	110
Figure 5.12 Constant volume cyclic simple shear DSS test on reconstituted specimen of normally consolidated Fraser River Delta silt, aged specimen: Stress strain and stress path curves; $\sigma'_{vc} = 100$ kPa CSR = 0.12, consolidation time=7 days.	110
Figure 5.13 Cyclic resistance ratio from constant volume cyclic DSS tests on undisturbed and reconstituted specimens of normally consolidated Fraser River Delta silt: Nominal initial effective confining stress $\sigma'_{vc} = 100$ kPa.	112
Figure 5.14 Constant volume cyclic simple shear DSS test on reconstituted specimen of Kitimat clay: Stress strain and stress path curves; $\sigma'_{vc} = 80$ kPa CSR = 0.25.	113
Figure 5.15 Constant volume cyclic simple shear DSS test on reconstituted specimen of Kitimat clay: Stress strain and stress path curves; $\sigma'_{vc} = 80$ kPa CSR = 0.20.	113
Figure 5.16 Constant volume cyclic simple shear DSS test on reconstituted specimen of Kitimat clay: Stress strain and stress path curves; $\sigma'_{vc} = 80$ kPa CSR = 0.17.	114

Figure 5.17. Comparison of constant volume cyclic simple shear DSS test on reconstituted and undisturbed specimens of normally consolidated Kitimat clay. First and third loading cycles: Stress strain and stress path curves; $\sigma'_{vc} = 80$ kPa; CSR = 0.24.	114
Figure 5.18. Comparison of constant volume cyclic simple shear DSS test on reconstituted and undisturbed specimens of normally consolidated Kitimat clay. First and 24 th loading cycles: Stress strain and stress path curves; $\sigma'_{vc} = 80$ kPa; CSR = 0.17.	115
Figure 5.19. Cyclic resistance ratio from constant volume cyclic DSS tests on undisturbed and reconstituted specimens of normally consolidated Fraser River Delta silt and Kitimat clay.	116
Figure 6.1. Typical volumetric strain (ϵ_{v-ps}) versus square-root-time characteristics of normally consolidated natural Fraser River silt during post-cyclic consolidation (Test Series Ib).	120
Figure 6.2. Typical volumetric strain (ϵ_{v-ps}) versus square-root-time characteristics of overconsolidated natural Fraser River silt during post-cyclic consolidation (Test Series Ic).	120
Figure 6.3. Typical volumetric strain (ϵ_{v-ps}) versus square-root-time characteristics of quartz rock powder during post-cyclic consolidation (Test Series IVa).	121
Figure 6.4. Post-cyclic volumetric strain (ϵ_{v-ps}) versus maximum cyclic excess pore water pressure ratio (r_{u-max}) during cyclic loading for Fraser River Silt (Test Series Ib).	122
Figure 6.5. Post-cyclic volumetric strain versus (ϵ_{v-ps}) versus maximum cyclic shear strain (γ_{max}) during cyclic loading for Fraser River Silt (Test Series Ib).	123
Figure 6.6. Post-cyclic volumetric strain (ϵ_{v-ps}) versus maximum cyclic excess pore water pressure ratio (r_{u-max}) during cyclic loading using data from all tested soils in this program forming the proposed curve to estimate post cyclic volumetric strain based on maximum pore water pressure during cyclic loading.	124

ACKNOWLEDGEMENTS

Many people contributed in some way to the culmination of this thesis. I would like to express my sincere appreciation to those who supported me throughout this process. Without their assistance this research would not have been possible.

First, I wish to express my most sincere gratitude to my research supervisor, Dr. Dharma Wijewickreme, for his constant guidance and encouragement throughout this journey. His experience, knowledge and positive attitude made possible the culmination of this work. His friendship and unconditional support, made the path easier and enjoyable.

I also wish to thank the members of the supervisory committee: Dr. John Howie and Dr. Peter Byrne for their constructive comments and encouragement. Their lessons, input and support during the preparation of this thesis and during my years at UBC are deeply appreciated.

Financial support provided by the National Research Council of Canada (NSERC), the University of British Columbia and Thurber Engineering Ltd. through the Al Insley Scholarship Award is deeply appreciated.

I am grateful to my colleagues at the Geotechnical group for interesting, critical and enjoyable conversations regarding this research, laboratory techniques and extracurricular activities. Technical assistance of Messrs Harald Schremp, Bill Leung, Scott Jackson and John Wong of

the Department of Civil Engineering Workshop is also acknowledged with deep regard.

Finally, I wish to thank my husband, Jose Roberto, for his constant support, encouragement and understanding. His positive attitude helped me enjoy the good times and kept me focused during the difficult times. The patience of my kids, Emilio and Adelaida, is endless. The unconditional love of my family made it all possible and worthwhile.

1 INTRODUCTION

1.1 Background

Fine-grained silty soils with high levels of saturation are commonly found as natural deposits and also originate as a man-made waste product in tailings derived from the processing of ore in the mining industry. Evidence of ground failure in fine-grained soils during strong earthquakes has suggested that certain saturated low plastic fine-grained soils can be as much susceptible to earthquake-induced softening and strength reduction as relatively clean sands (Boulanger et al. 1998; Boulanger and Idriss 2006; Bray and Sancio 2006). Although wide-ranging studies have been undertaken to understand the performance of sands over the past 40 years, the available published information on the undrained shear response of fine-grained soils with respect to cyclic loading is limited (Polito and Martin 2001; Bray and Sancio 2006; Sanin and Wijewickreme 2006; Wijewickreme et al. 2005). In particular, there is a need for understanding the response of low plastic silts in a more fundamental manner, and laboratory testing plays an important role in this regard.

In addition to the shear deformations associated with loss of stiffness and/or strength in some situations, another key mechanism of earthquake-induced deformations is the overall volume changes in the soil mass that take place due to the dissipation of shear-induced excess pore

water pressures. These volume changes manifest in the field as post-liquefaction settlements, and they may occur both during and after earthquake shaking. Recent evidence of ground failure during strong earthquakes has indicated that certain saturated fine-grained soils can be susceptible to earthquake-induced softening and strength reduction, in turn, leading to post-cyclic settlements, foundation sliding, tilting, and collapsing of structures (Bray et al. 2004b; Bray and Sancio 2006; Boulanger et al. 1998; Boulanger and Idriss 2006; Boulanger and Idriss 2007).

1.2 Response of soils to earthquake loading

The response of a given soil to cyclic loading is controlled by many parameters such as packing density, microstructure, fabric, level/duration of cyclic loading, confining stress, initial static bias, etc. These parameters have been noted to primarily govern the development of excess pore water pressures, stiffness, and strength in a soil mass during earthquake shaking and, in turn, controlling the overall seismic response. While cyclic shear tests are valuable in assessing the performance of soils under seismic loading conditions, data from monotonic shear tests have often provided insight into the fundamental soil behaviour and assisted interpretation of the behavioural patterns observed in cyclic shear tests (Vaid and Chern 1985).

Due to the difficulties associated with field sampling, most of the laboratory research on sands has been conducted using reconstituted soil specimens. The influence of specimen reconstitution technique on laboratory observed soil behaviour, and the differences in the fabric and mechanical response between undisturbed and reconstituted samples of sand and silty sands have been widely studied (e.g., Oda 1972; Vaid et al. 1999). The effect of specimen

reconstitution on the performance of silty soils has also been studied and significant differences in behaviour have been found between undisturbed and reconstituted specimens (e.g., Høeg et al. 2000; Long et al. 2001).

In general, it is fair to state that the mechanical behaviour of a given field soil condition is best examined in the laboratory by element testing of good quality undisturbed soil specimens. The possibility to obtain reasonably undisturbed samples of certain low-plastic silts has been already demonstrated (e.g., Bray et al. 2004a, Sanin and Wijewickreme 2006); in spite of this, due to increased costs and difficulties with such undisturbed field sampling, there is a tendency to use reconstituted specimens for assessing the shear response of silts. Controlled laboratory studies conducted with the purpose of advancing the understanding and knowledge of the response of silts to earthquake loading are very few; the limited available studies have also focused mainly on reconstituted specimens on silty sands (Thevanayagam et al. 2002; Polito and Martin 2001). These studies cannot be directly extended to understand the behaviour of natural silt deposits without a framework of comparison between undisturbed and reconstituted specimens.

1.3 Objectives of the thesis

The main goal of this study is to develop a fundamental understanding of the shear response of low plastic silts, and to generate data that contributes to the understanding of the response of silts to earthquake induced loading. In this regard, the mechanical response of low plastic Fraser River silt was investigated using the direct simple shear (DSS) device and in particular included the following components:

- Undrained monotonic response of normally consolidated silt;
- cyclic shear loading response of normally consolidated silt;
- effects of initial confining stress level on the monotonic and cyclic loading response;
- effects of initial static shear bias on the monotonic and cyclic loading response;
- effects of particle structure in the context of mechanical behavioural pattern between undisturbed and reconstituted specimens;
- consolidation response of silt due to dissipation of pore water pressures following cyclic loading.

1.4 Scope of work

In recognition of the above, a detailed laboratory element testing research program concentrated on the cyclic shear response of undisturbed samples of Fraser River Delta silt was undertaken at the University of British Columbia. The testing was mainly focused on obtaining results by the NGI type cyclic direct simple shear device (Bjerrum and Landva, 1966), which has been considered more effective than other devices in simulating effects of earthquake loading. This research work is an in depth extension to the scope of research undertaken during the masters studies completed by the author (Sanin 2005). In the present study, the behaviour of low plastic Fraser River silt was investigated over a wide range of confining stress levels and initial static shear. Moreover, a comparison of the behavioural patterns of undisturbed and reconstituted specimens was undertaken to examine the effects of

particle structure. The post-cyclic volumetric consolidation response of this material following cyclic loading was also investigated.

Chapter 2 of the thesis compiles the previous research on the topic and summarizes the behaviour of sands, clays and silts to earthquake loading. The experimental procedures and description of apparatus used in the present study are presented in Chapter 3 along with a description of the test soil material, methods of soil sampling, and specimen preparation. Chapter 4 presents the experimental results from the main testing program and discussion of the relevant findings. In particular, laboratory findings on the following aspects of the mechanical response of low plastic silt are presented and discussed: (i) monotonic loading response, (ii) cyclic loading response (iii) effects of initial static shear, and (iv) effect of plasticity (based on limited study of a number of materials). Chapter 5 presents the main findings on the effects of particle structure studied in the context of mechanical behavioural pattern between undisturbed and reconstituted specimens. The post-cyclic recompression of Fraser River delta silt is presented on Chapter 6, and the summary and conclusion derived from this investigation are presented in Chapter 7.

2 LITERATURE REVIEW

Understanding the response of soils to field loading conditions is fundamental to developing meaningful constitutive models for numerical modeling and, in turn, for effective geotechnical design of engineering structures. Laboratory testing plays an essential role in framing this understanding as it allows characterization of basic element behaviour of soils. One of the areas of major interest to the engineers has been the design of structures to withstand earthquake loading. Geotechnical performance of foundations, soils, or structures made of soils is considered of particular concern due to the potential for reduction of strength and stiffness of soils when subjected to earthquake loading. Because of the widely observed adverse effects, much of the research over the past 40 years has been on the performance of sands. Through these efforts, a fundamental understanding of the behaviour of sand has been developed, and a detailed approach for engineering design has been proposed (Youd et al. 2001). Evidence from recent earthquakes shows that low plastic fine-grained soils are susceptible to earthquake induced softening and strength reduction (Boulanger and Idriss 2006; Bray and Sancio 2006). However, in comparison to sands, the available published data of undrained response of low-plastic, fine-grained soils are very limited (Bray and Sancio 2006, Wijewickreme and Sanin 2006, Bray et al 2004). Bray and Sancio (2006) reported that the consequences of liquefaction in fine-grained soils are different from those that occur in loose

saturated sands, as silts undergo a transient loss of shear strength (cyclic mobility) rather than a permanent loss of shear strength.

This chapter is intended to present a review of literature of the main aspects of the cyclic behaviour of sands, clays and silts as well as a discussion of the approaches that are currently available for the assessment of cyclic shear performance of fine-grained soils.

2.1 General mechanical response of soils to cyclic shear loading

2.1.1 Response of sands

Drained and undrained static behaviour of sands has been studied by several researchers (Casagrande, 1936a; Roscoe et al., 1963; Castro, 1969, Vaid and Chern, 1985; Vaid and Thomas, 1995). Typical response of sand observed during drained monotonic loading in the direct shear apparatus under constant effective confining stress is shown in Figure 2.1. Volumetric response has been observed as contractive (compression) or dilative (expansion). At large strains, the angle of friction at which the soil deforms at constant void ratio is called the constant volume friction angle (ϕ_{cv}).

2.1.1.1 Monotonic response

Typical undrained monotonic loading response of sand is presented in Figure 2.2. The behaviour has been interpreted in three types of responses:

- Type 1 response is characterized by reaching a maximum shear strength followed by continuous strain softening. This brittle response has been defined as liquefaction by

Castro (1969), Casagrande (1975), and Seed (1979) and as true liquefaction by Chern (1985). This type of response is considered to result in flow failure under field conditions.

- Type 2 response shows maximum peak of shear strength followed by initial strain-softening and immediate strain-hardening (dilation). This typical behaviour was named as limited liquefaction by Castro (1969). After reaching the critical stress ratio, the soil starts to strain soften followed by deformation at constant stress ratio and subsequent dilative response. The deformation at constant stress ratio has been called quasi-steady-state (QSS) by Ishihara et al. (1975). In terms of stress path (see Figure 2.2), the term phase transformation (PT) is the point at which the soil changes its behaviour from contractive to dilative (point of maximum excess pore water pressure). The mobilized friction angle at PT, ϕ_{PT} , has been noted to be unique for a given sand (Ishihara, 1975; Vaid and Chern, 1985; Kuerbis et al., 1988). It has been also found that the friction angle at phase transformation (ϕ_{PT}) is essentially the same as the constant volume friction angle (ϕ_{cv}) for a given sand (Chern, 1985; Negussey et al., 1988).
- In Type 3 response, the soil exhibits increasing shear resistance with increasing deformation with no strain-softening. The excess pore water pressure initially shows an increase (contractive response), then followed by a decrease (dilative response) with increasing strain.

Figure 2.1 Typical shear response of loose and dense sand observed during drained monotonic loading in the direct shear apparatus (Modified from Schofield and Wroth, 1968).

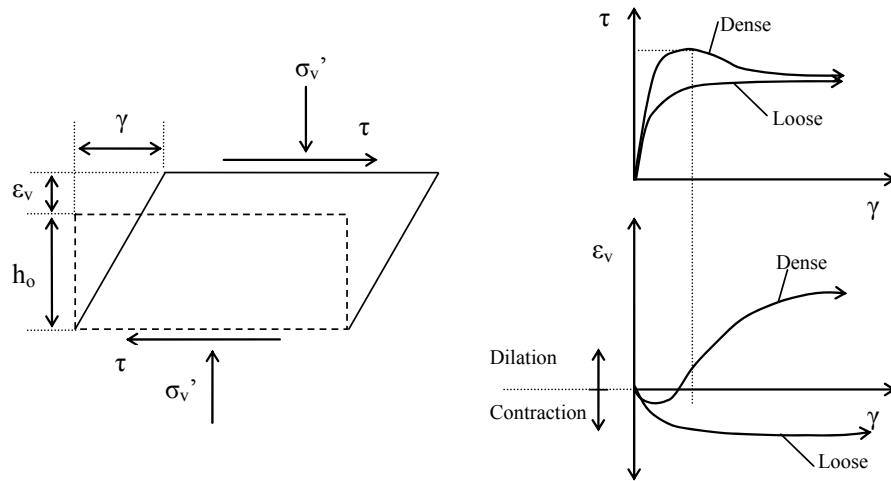
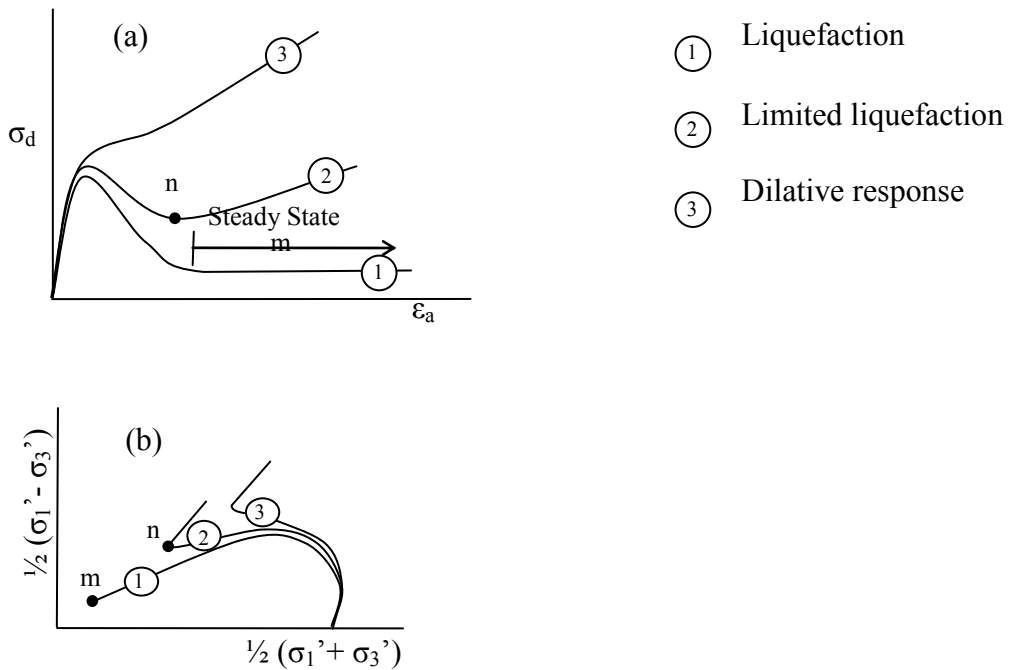


Figure 2.2 Typical undrained monotonic loading response of sand. a) Stress-strain response. b) Stress path (after Vaid and Chern, 1985).



2.1.1.2 Cyclic response

Although cyclic loading can induce significant volumetric strains in unsaturated sands, most of the research focus has been on the performance of saturated sands because of their noted potential for generation of excess pore water pressures and associated strength and stiffness degradation under cyclic loading. In this regard, undrained behaviour of saturated sands has been understood via laboratory cyclic tests. As in the case of monotonic undrained loading, three types of response have been identified (Castro, 1969, Vaid and Chern, 1985), and they are schematically presented in Figure 2.3 through Figure 2.5. In the “liquefaction” type of response, as per Figure 2.3, the soil experiences contractive deformation until reaching the steady state.

The second type of response is called cyclic mobility with limited liquefaction (see Figure 2.4). Herein, once the stress ratio has reached PT , the soil starts to behave in a dilative manner. During the unloading part of the cycle, larger excess pore water pressures are developed producing a state of zero effective stress. The loading cycles that follow cause a dilative response leading to a strain-hardening tendency. In the third type of response (Figure 2.5), with increasing number of load cycles, the shear strains increase gradually and there is gradual build up of pore water pressure although there is no strain-softening. This type of response has been called “cyclic mobility” by many researchers (Vaid and Chern 1985, Bray et al. 2004, Boulanger and Idriss 2006). This terminology has been used to describe similar behavioural patterns observed during testing undertaken herein.

Figure 2.3 Typical “liquefaction” response during undrained cyclic loading. a) Stress-Strain response. b) Stress Path. c) Shear strain development (after Vaid and Chern, 1985).

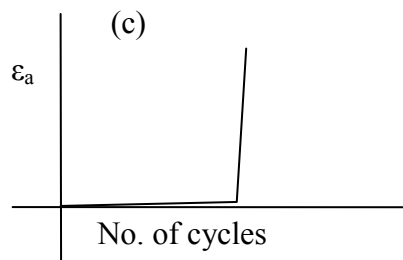
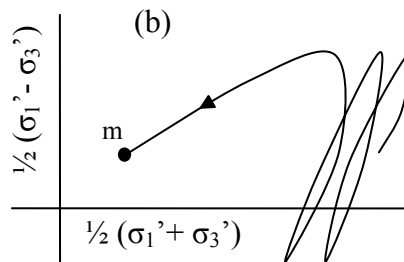
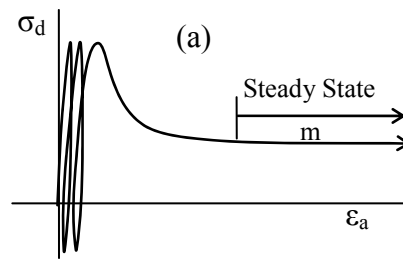


Figure 2.4 Typical “limited liquefaction due to cyclic loading” type of response during undrained cyclic loading. a) Stress-Strain response. b) Stress Path. c) Shear strain development (after Vaid and Chern, 1985).

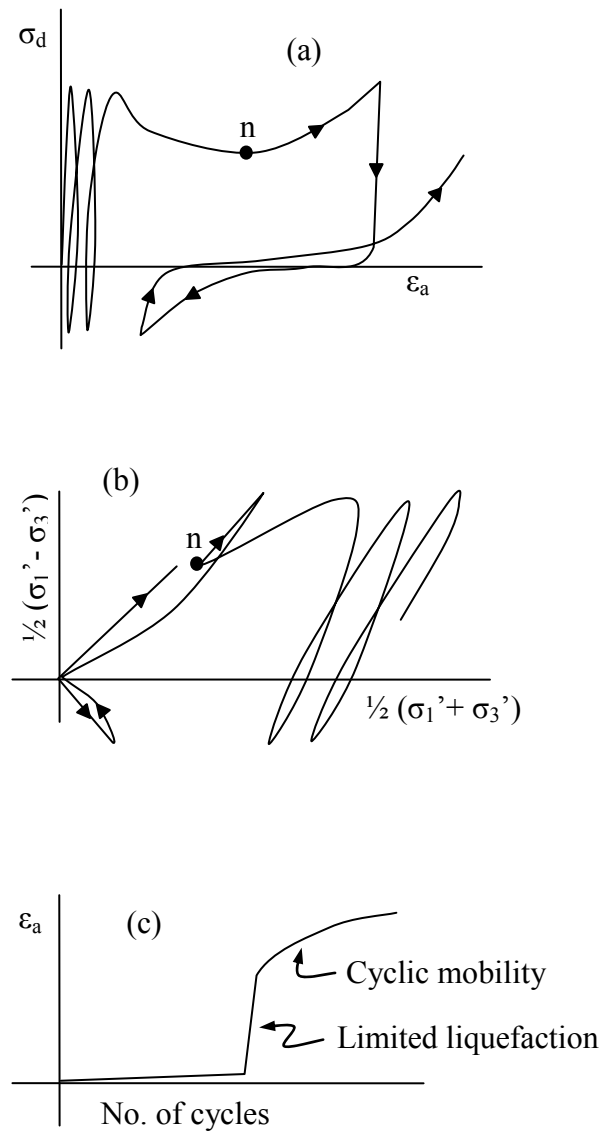
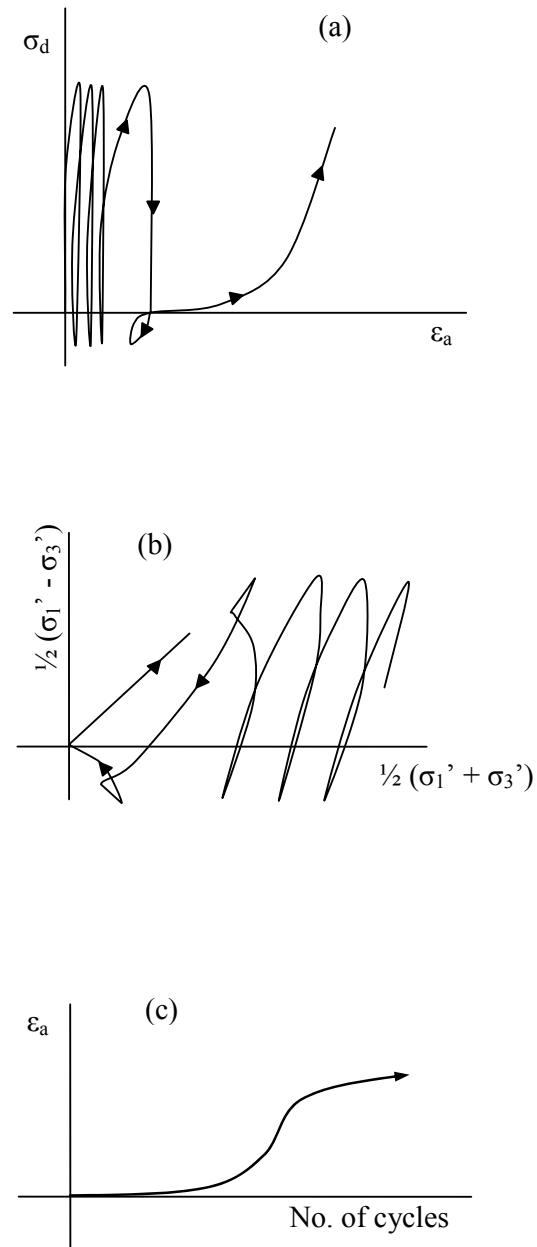


Figure 2.5 Typical “cyclic mobility” type of response during undrained cyclic loading. a) Stress-Strain response. b) Stress Path. c) Shear strain development (after Vaid and Chern, 1985).



Effects of static shear

Earthquake geotechnical problems generally involve level ground as well as sloping configurations. For level ground conditions, “no static shear bias” is commonly used to indicate the condition with no initial shear stresses on the horizontal plane prior to earthquake loading (Seed and Peacock, 1971; Vaid and Finn, 1979). To simulate field conditions with configuration of sloping ground, samples are consolidated with an applied static shear stress prior to cyclic loading, and these tests are typically referred to as cyclic shear tests with “initial static shear stress bias”.

Figure 2.6 schematically shows the field and laboratory models of the stress field conditions with and without initial static shear bias. It has been found that the presence of initial static shear stress has a profound influence on the cyclic resistance of sands although the findings have not always been in agreement. While some researchers have found that the presence of initial static shear increases the cyclic resistance to liquefaction (Lee and Seed, 1967; Seed et al., 1975), others have observed that the increase in static shear stress would decrease the cyclic resistance to liquefaction (Castro, 1969; Casagrande, 1975; Castro et al., 1982). Vaid and Finn (1979), Vaid and Chern (1985), Seed and Harder (1990), Vaid et al. (2001) and Sriskandakumar (2004) have found that the effect of static shear stress on the cyclic resistance of sands is influenced by the initial density; thus, loose sands would experience reduction in the cyclic resistance with the presence of static shear, while the cyclic resistance of dense (dilative) sands would increase if applied initial static shear.

Figure 1 consists of two parts, (a) and (b), illustrating the stress conditions during earthquake loading.

(a) Geometry of the slope and dam. The left diagram shows a slope with two rectangular blocks, labeled 1 and 2, positioned on its surface. The right diagram shows a dam cross-section with a vertical centerline labeled ζ . Two rectangular blocks, labeled 1 and 2, are positioned within the dam body.

(b) Initial static stress conditions and stress conditions during earthquake loading. The left diagram shows the initial static stress conditions for block 1. It is a rectangular block with vertical effective stress $\sigma'_v = \text{Initial}$ acting downwards, horizontal effective stress $\sigma'_h = \text{Initial}$ acting horizontally, and vertical effective stress σ'_v acting upwards. The right diagram shows the initial static stress conditions for block 2. It is a rectangular block with vertical effective stress σ'_v acting downwards, horizontal effective stress σ'_h acting horizontally, and vertical effective stress σ'_v acting upwards. The initial static shear stress $\tau_{st} = \text{Initial Static Shear Stress}$ is also indicated. The bottom diagrams show the stress conditions during earthquake loading. The left diagram shows block 1 with vertical effective stress σ'_v acting downwards, horizontal effective stress σ'_h acting horizontally, and cyclic shear stress τ_{cyc} acting horizontally. The right diagram shows block 2 with vertical effective stress σ'_v acting downwards, horizontal effective stress σ'_h acting horizontally, and cyclic shear stress τ_{cyc} acting horizontally. The cyclic shear stress is represented by a double-headed arrow labeled τ_{cyc} . The bottom right diagram also shows the cyclic shear stress τ_{cyc} acting horizontally, with the text $\{T_{cyc} = \text{Cyclic Shear Stress}\}$ below it.

Cyclic resistance of sands has also been noted to be significantly affected by past liquefaction or pre-shearing (Finn et al., 1970; Seed et al., 1977; Ishihara and Okada, 1978; Suzuki and Toki, 1984; Vaid et al., 1989; Sriskandakumar, 2004). Finn et al. (1970) found that previously liquefied samples exhibited significantly less cyclic shear resistance than virgin samples, despite a significant increase in density following consolidation after the first liquefaction stage. Similar results were found by Sriskandakumar (2004) based on tests conducted on loose Fraser River Sand in the direct simple shear. Small pre-shearing improves the soil fabric and increases the cyclic resistance of sand to liquefaction during a second cyclic loading phase, while large pre-shearing weakens the soil fabric and decreases the cyclic resistance to liquefaction in the following cyclic loading.

2.1.2 Response of clays

Cyclic shear response of clays has been widely studied (Zergoun and Vaid 1994, Vucetic and Dobry 1991, Chu et al, 2008, Boulanger and Idriss 2006, 2007). Ground failures in deposits of clays have been observed during earthquakes but are considered less common than in saturated sands. Zergoun and Vaid (1994) investigated the cyclic response of natural Cloverdale clay with slow (low frequency) undrained cyclic loading tests. Their tests have shown that a threshold cyclic stress level separates the response of clay into two different patterns: at low cyclic stress levels, shear strains and pore water pressure development tend to reach equilibrium with continuing cyclic loading. At higher cyclic stress levels, strain development undergoes three phases: the rate of strain development per cycle initially decreases followed by constant rate per cycle; the final stage is characterized by strain development at increasing rate

per cycle. This final stage occurs at a constant effective stress ratio regardless of the cyclic stress level.

The potential for cyclic loading to produce increasing strains in clays is shown in Figure 2.7 (Zergoun and Vaid 1994). Cyclic loading causes a progressive increase in excess pore water pressure accompanied by increasing strains potentially leading to significant ground deformation during an earthquake (Idriss and Boulanger 2008). This type of behaviour is called “cyclic softening” to differentiate it from the term liquefaction used for the effect of cyclic loading in saturated sands. The cyclic strength of clays has been generally expressed as a relatively unique function of the soil’s undrained monotonic shear strength as shown in Figure 2.8 for different fine-grained soils (modified from Idriss and Boulanger 2008).

Figure 2.7 Stress-strain and stress path response of Cloverdale clay during undrained cyclic loading (Zergoun and Vaid 1994).

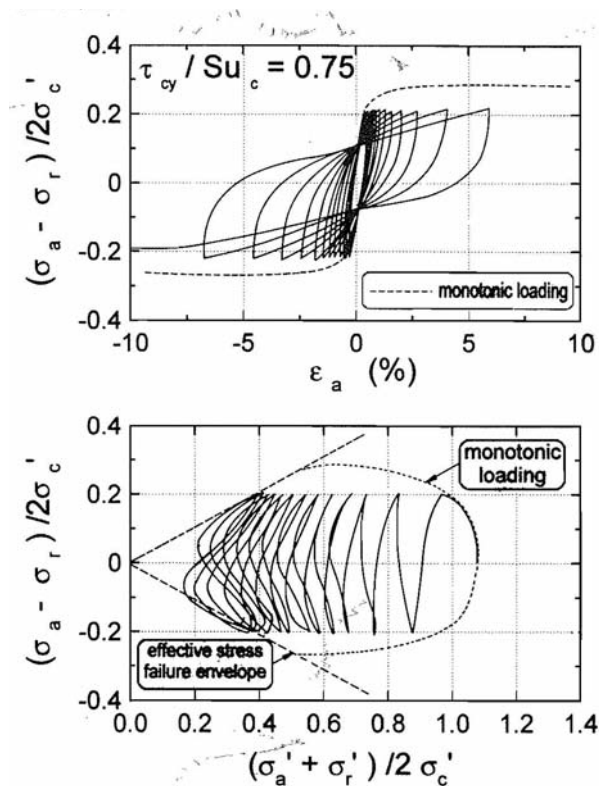
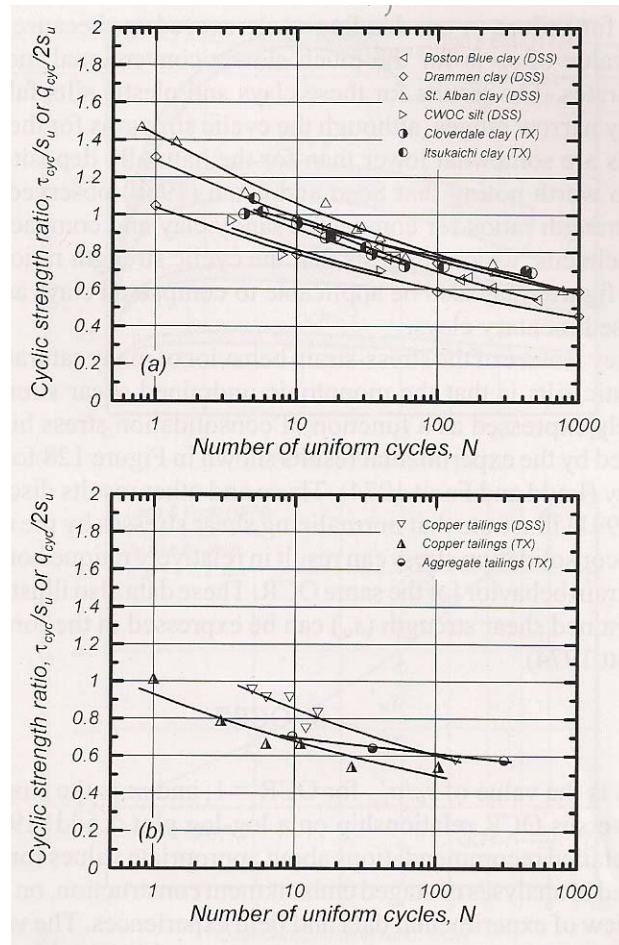


Figure 2.8 Cyclic stress ratios required to cause failure or some strain criteria versus number of uniform cycles at a frequency of 1 Hz in different clays. (Boulanger and Idriss 2008)



Consequences of cyclic softening in clays depend on the soil sensitivity (defined as the ratio of intact undrained shear strength to the remoulded undrained shear strength). Soft, normally consolidated clays with generally large natural water contents will have higher sensitivity and will be most prone to loss of strength during earthquake loading compared to those of stiff, overconsolidated clays.

The undrained cyclic strength of clays can be expressed as a function of the soil's undrained monotonic shear strength as shown in Figure 2.8. Cyclic stress ratios in this plot are represented by the ratio of cyclic shear (τ_{cy} , in direct simple shear and $q_{cyc}/2$ in triaxial shear) to

the undrained shear strength under monotonic loading, s_u . In addition, the monotonic shear strength of clays is a function of the consolidation stress history of the clay as follows

$$\frac{s_u}{\sigma'_{vc}} = S \cdot OCR^m \quad \text{Equation 1}$$

where S is the value of s_u/σ'_{vc} for $OCR=1$, and m is the slope of the s_u/σ'_{vc} vs. OCR relationship on a log-log plot. The above relationships that define the mechanical behaviour of clays are the basis for the evaluation of its cyclic shear strength (Idriss and Boulanger, 2008). The loading of clay by a magnitude $M=7.5$ earthquake can be represented by an average of about 30 uniform loading cycles at 65% of peak stress. In sands, this value has been computed to be 15 cycles. Boulanger and Idriss also presented magnitude scaling factor and a static shear correction factor, K_α for clays. The approaches for estimating the cyclic resistance ratio (CRR) in clays are the direct measurement of CRR in the laboratory, measuring the shear strength (s_u) in the field or in the laboratory or empirically estimating the CRR based on the stress history profile and the estimated values for the normalized CSR. Details of the latter approach are presented in Boulanger and Idriss (2008).

Andersen (2009) presented a variety of tests in diagrams where the number of cycles to failure (defined as a strain criterion) is plotted as a function of average and cyclic shear stresses. These diagrams also contain the failure mode (permanent and/or cyclic shear strains at failure). Throughout this work, Andersen noted that there is tendency for the normalized shear strength to increase with the plasticity index, similar to the findings by Guo and Prakash (1999) and Ishihara et al. (1981).

2.1.3 Response of silts

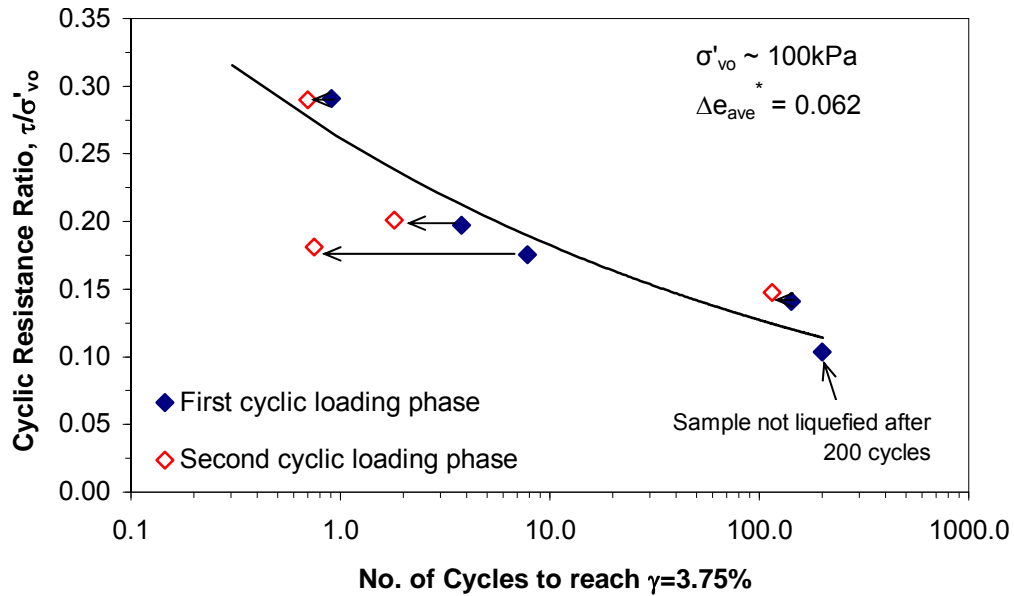
Cyclic shear response of silts has been recently studied by many authors (Sanin 2005, Wijewickreme et al. 2005, Sanin and Wijewickreme 2006, Bray et al. 2004a, 2004b, Hyde et al. 2006, Polito et al. 2008). In general, low-plastic silts subject to cyclic loading are susceptible to cyclic mobility manifesting an increase in pore water pressure ratio accompanied by loss in shear resistance and stiffness. Consequences are different from those in loose saturated sands as silts do not undergo permanent loss of shear strength (Bray et al. 2004b).

Sanin (2005) noted that, under cyclic loading, normally consolidated specimens of channel-fill Fraser River silt would exhibit progressive increase in equivalent excess pore water pressure ratio (r_u) with degradation of shear modulus in all tests conducted at different cyclic stress ratios (CSR). This is essentially the “cyclic-mobility” type of response that has been observed previously in dense sands. The specimens generally exhibited initially contractive response followed by dilative response. Specimens tested under more severe CSR levels manifested phase transformation at early stages of cyclic loading, and reached r_u of approximately 100% in a lesser number of cycles than those subjected to low CSR values. The cyclic resistance ratio versus number of cycles to liquefaction relationship for the tested channel-fill silt is not sensitive to the initial confining stress, for stress levels below 200 kPa (Sanin 2005, Sanin and Wijewickreme 2006).

Effects of pre-shearing had also been studied by Sanin (2005). In this study, specimens of Fraser River silt that were initially subjected to cyclic loading were re-consolidated and subjected to a second cyclic loading phase. During the second cyclic loading phase following re-consolidation, samples exhibited a rapid drop in effective stress (rise in pore water pressure)

and performed softer than in the first cyclic loading phase as shown in Figure 2.9. Despite the densification that had taken place during re-consolidation after first cyclic phase, the specimens reached the liquefaction triggering ($\gamma = 3.75\%$) in a fewer number of load cycles than those required for the first phase. This work illustrates that the decrease in cyclic shear resistance (CRR) due to degradation of particle fabric as a result of previous shearing has overshadowed any gain in CRR that would have taken place due to reduction of void ratio during consolidation. Observations by Andersen (2009) show an effect contrary to this observation by Sanin (2005), where the cyclic shear strength of sands has been noted to increase after preshearing. Destructuration of the soil particle structure due to large shear strains during cyclic loading may be the cause of the discrepancy between these two findings.

Figure 2.9. Effects of preshearing: Cyclic resistance ratio versus number of cycles to reach $\gamma=3.75\%$ on first and second cyclic loading phases from constant volume DSS tests on Fraser River silt (Sanin 2005).

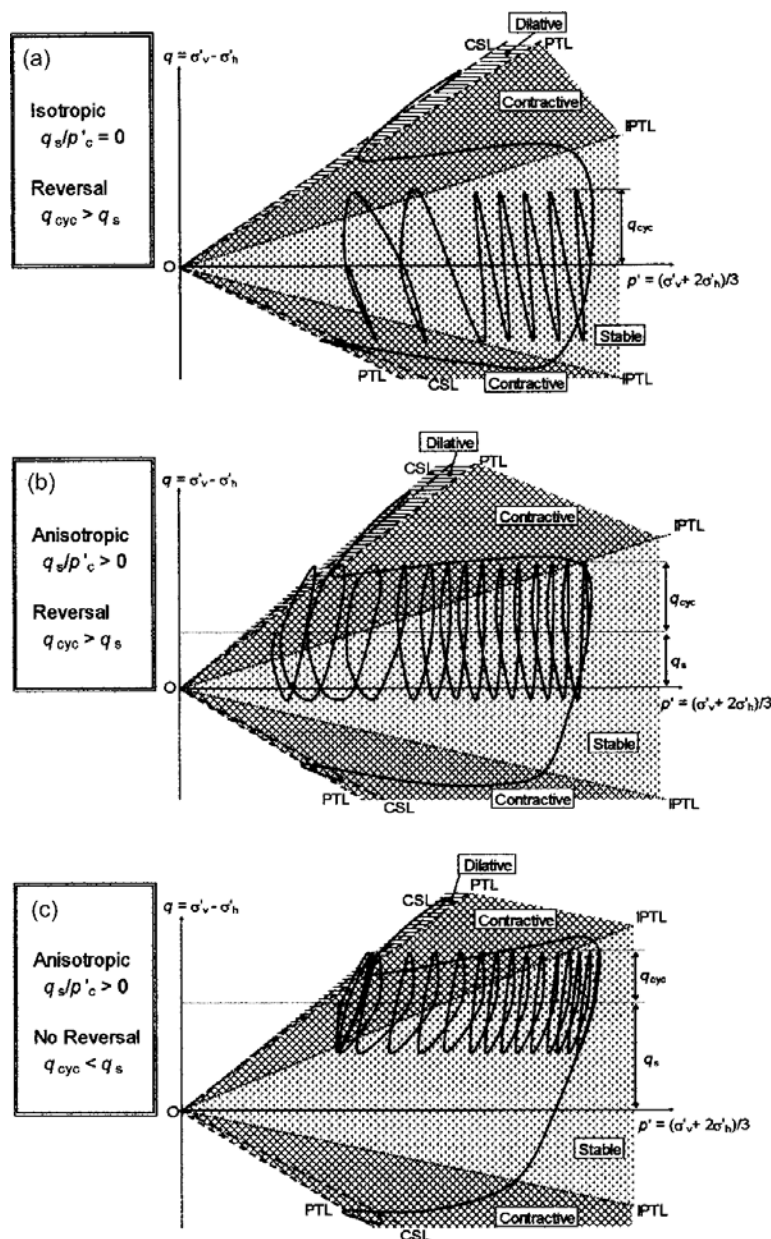


*: Average change in void ratio after first cyclic loading phase

Hyde et al. (2006) investigated the effects of cyclic loading on reconstituted samples of low plastic, silt-size, powdered limestone on cyclic triaxial testing. Their findings showed that for

isotropically consolidated samples, the initial phase transformation determined by monotonic shear loading in extension tests was the boundary between stable and contractive behaviour. For anisotropically consolidated samples this boundary was defined by monotonic compression tests. Figure 2.10 shows the three schematic diagrams that explain the contractive and dilative shear behaviour during undrained monotonic and cyclic loading.

Figure 2.10 Schematic diagram explaining contractive and dilative shear behaviour during undrained monotonic and cyclic loading (Hyde et al. 2006)



Hyde et al. (2007) also investigated the post cyclic recompression and post-cyclic behaviour of silt with respect to the effect of initial anisotropic consolidation. Triaxial testing showed that compressibility during post-cyclic recompression was similar for both isotropic and anisotropic initial stress conditions. Second cyclic loading, following recompression showed that cyclic strength increased with increasing anisotropy while isotropically consolidated specimens resulted in a weaker soil structure, similar to the findings of Sanin (2005).

2.2 Earthquake-induced settlements

In addition to the shear deformations associated with loss of stiffness and/or strength in some situations, another key mechanism of earthquake-induced deformations is the overall volume change in the soil mass that takes place due to the dissipation of shear-induced excess pore water pressures. These volume changes manifest in the field as post-liquefaction settlements, and they may occur both during and after earthquake shaking. The adverse impacts of these settlements on the performance of structural foundations and linear lifelines (such as buried pipelines, bridges) have been well documented (Bray et al. 2004; Bray and Sancio 2006; Boulanger and Idriss 2006, 2007).

Studies conducted to evaluate volume change after cyclic loading have shown that, in general, the key factors that control post-cyclic settlements in sands are the cyclic excess pore water pressures and cyclic shear strains (Tokimatsu and Seed, 1987). Due to the direct connection with excess pore water pressure development, the potential for volumetric strains has been often linked with the field density. Several simplified methods have been proposed to estimate probable settlements of sands with the knowledge of the field penetration resistance (i.e.,

standard penetration resistance (SPT) N-value or cone penetration testing (CPT) resistance) and the cyclic stress ratio (CSR) applied by the design earthquake (Lee and Albaisa, 1974; Tokimatsu and Seed, 1987; Ishihara and Yoshimine, 1992; Wu 2002; and Zhang et al. 2002).

Unlike the wide range of data available on the response of sands, there is only very limited available information on the post-liquefaction settlements of fine-grained soils. Yasuhara et al. (2001) proposed a method to estimate settlements based on the cyclic excess pore water pressure, plasticity index, and bearing capacity factor of safety. Sanin and Wijewickreme (2006) noted that silt specimens that experienced high equivalent excess cyclic pore water pressure ratios seemed to experience considerable volumetric strains during post-cyclic reconsolidation, suggesting the need to further study this topic.

Limited consolidation tests conducted at UBC by Sanin (2005) on specimens initially subjected to constant volume cyclic loading indicate that post-cyclic volumetric strains (ϵ_{v-ps}) increase with the maximum pore water pressure generated during cyclic loading as well as with the maximum cyclic shear strain to which the specimens were subjected during cyclic loading (Sanin and Wijewickreme, 2006). The values of ϵ_{v-ps} arising from the specimens of Fraser River silt correlated well with the maximum excess pore water pressure ratio (r_{u-max}). Additional research testing work along with data from past earthquake performance, is needed to confirm the validity of the above observations.

2.3 Closure

Fine-grained silty soils with high levels of saturation are commonly found in natural river deposits and also originate as a man-made waste product in tailings derived from the processing of ore in the mining industry. Recent evidence of ground failure during strong earthquakes has indicated that certain saturated fine-grained soils can be susceptible to earthquake-induced softening and strength reduction, in turn, leading to post-cyclic settlements, foundation sliding, tilting and collapsing of structures.

Although there are major advances in the understanding of the shear loading response of sands, our understanding of the mechanical response of silts is still very limited. For example, despite increasing interest in this topic, still there are no standard procedures to assess the potential for cyclic softening/ liquefaction. Clearly, there is a strong need to investigate the behaviour of fine-grained soils and laboratory element testing has a key role to play in this regard.

In recognition of the above, it was decided to undertake a detailed laboratory research program on the cyclic shear response of undisturbed samples of Fraser River Delta silt, thus forming the basis for the doctoral research presented herein. In this research, the behaviour of low plastic Fraser River silt was investigated over a wide range of confining stress levels and initial static shear stress levels. A comparison of the behavioural patterns of undisturbed and reconstituted specimens of low plastic silt to examine the effects of particle structure was included as a part of this work. The post-cyclic volumetric consolidation response of this material following cyclic loading was also investigated.

The scope of this research work and the organization of the thesis are presented in Section 1.4 of Chapter 1.

3 MATERIAL TESTED AND EXPERIMENTAL ASPECTS

3.1 Material tested

The mechanical response of soils is dependent on a multitude of factors including particle fabric, microstructure, density, and age. As pointed out by Leroueil and Hight (2003), testing of undisturbed samples of soils is critically important in representing soil conditions in-situ, and, in turn, in understanding the field response of natural soils. Significant differences in the response of soils have been observed between undisturbed and reconstituted samples of sands (Vaid et al. 1999) and silt and sandy silt (Høeg et al., 2000). These differences are mainly attributed to the differences in fabric between the undisturbed and reconstituted specimens.

A channel-fill silt obtained from the Fraser River Delta of British Columbia, Canada, was selected for the investigation of the cyclic response of silts. The choice of silt from this area is considered relevant since it is located in one of the most seismically active regions in Canada (NBCC, 1995) and the area is experiencing rapid urban and industrial growth. The general ground surface elevation in the area is below the high-tide level; as such, the area is now protected by dikes. In addition, deltaic silts are compressible and susceptible to settlements under building loads (Crawford and Morrison, 1996).

Deposits of the delta are Holocene in age and have a maximum known thickness of 305 m (Clague et al., 1996). The deltaic deposits can be subdivided into topset, foreset and bottomset units (Monahan et al., 1997), and the upper part of the topset comprises flood-plain silts and peat (Monahan et al., 2000).

The subject site for the present testing program is located immediately north of the South Arm of the Fraser River, on the river dyke at the southern foot of No. 3 Road in Richmond, B.C. A channel-fill silt deposit is overlain by about 3.5 m thickness of dyke-fill materials at the site. Available data from in-situ cone penetration testing, CPT (see Figure 3.1), suggested that the upper part of this channel fill silt between depths of 5.6 m and 9.3 m below the ground surface is relatively uniform, and, therefore, this deposit was considered suitable as the source of test material for the present study.

A fixed-piston tube sampling conducted in a conventional mud-rotary drill hole was used to obtain a number of undisturbed samples from the silt deposit (from the same horizon identified above). A specially fabricated ~75-mm diameter, 0.9-m long tubes (with no inside clearance, a 5-degree cutting edge, and 1.5 mm wall thickness) were used for this purpose. As noted by Leroueil and Hight (2003), piston sampling using thin, sharp-edged tubes offers a suitable and acceptable means of obtaining relatively undisturbed samples of fine-grained soils. Figure 3.2 show the gradation curves for several samples obtained from the silt deposit. As may be noted, the generally homogeneous samples have an average clay content of 10% and sand content of 13%. Parameters obtained from index tests are presented in Table 3.1. These observations also confirm the uniformity of the deposit previously noted based on field cone penetration test data.

Figure 3.1 Cone penetration test profile of the site at No. 3 Road in Richmond BC. – Depth horizon of the channel fill Fraser River silt used in the present study identified.

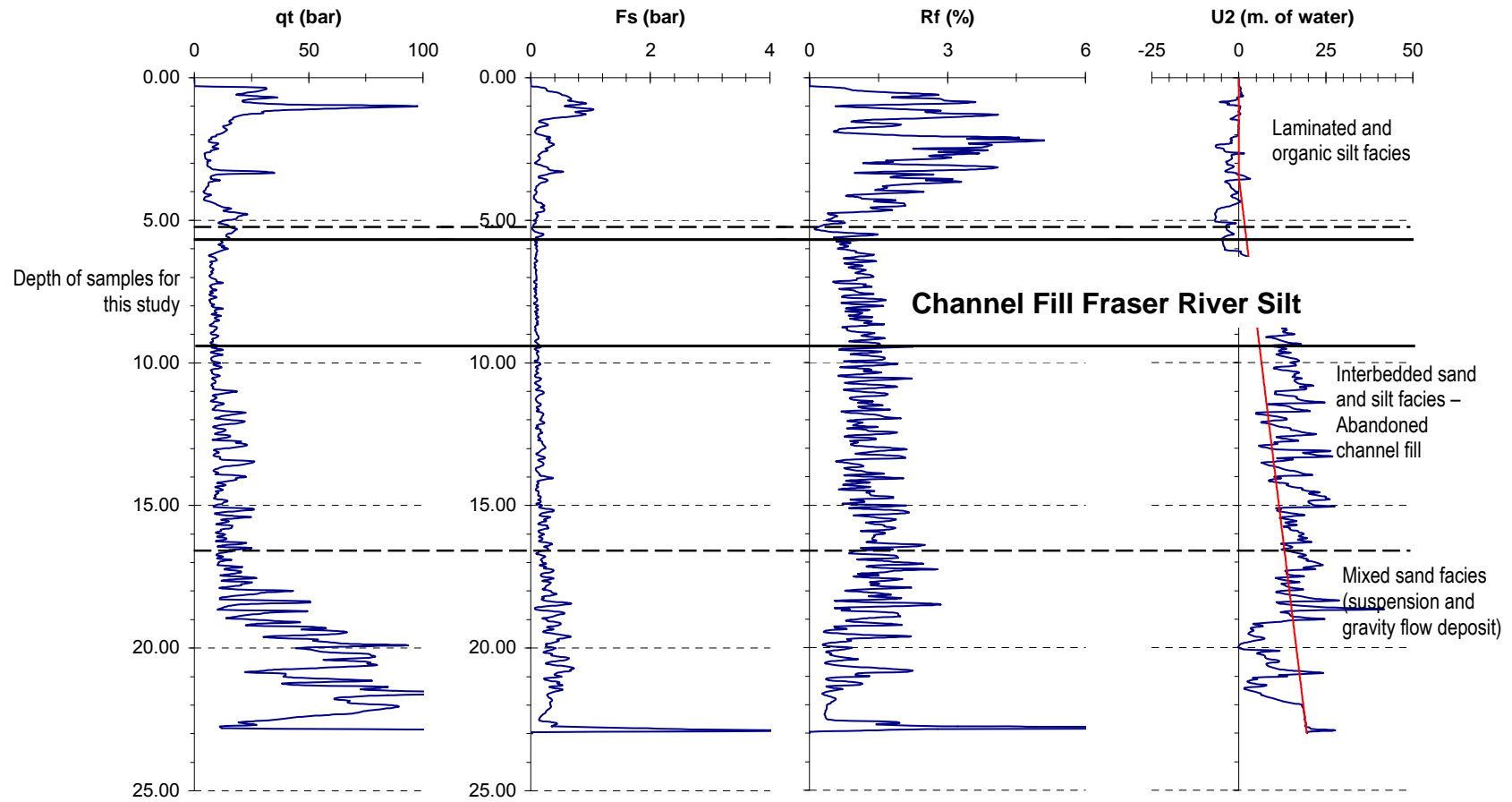


Figure 3.2 Grain size analysis of different samples of Fraser River silt.

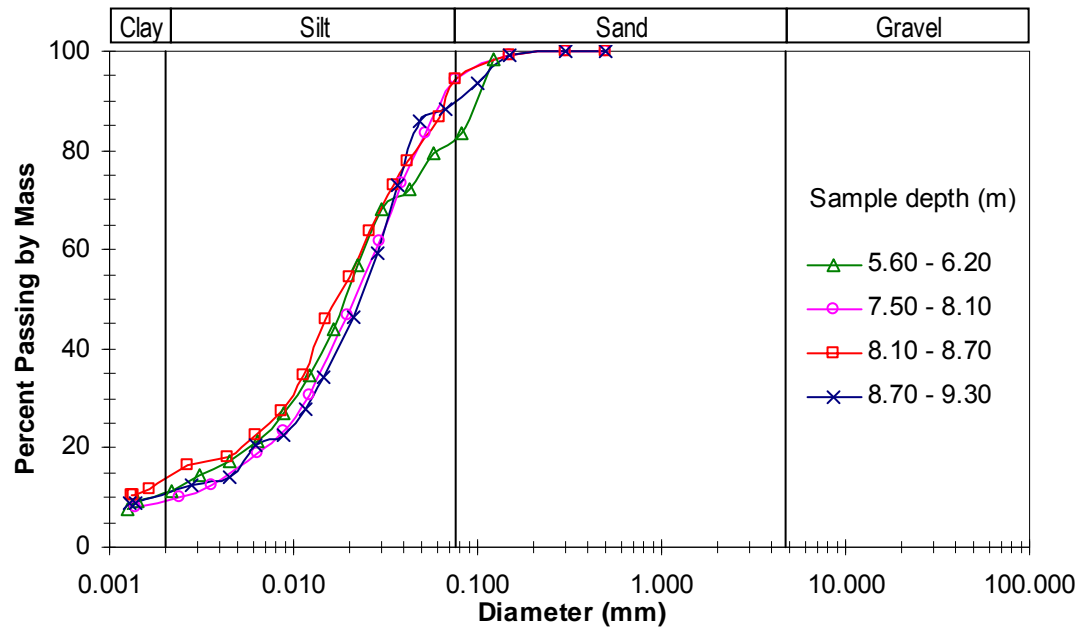


Table 3.1. Index parameters of Fraser River delta silt

Soil Property	Values
Depth range below ground surface	5.60 to 8.7 m
Water content, W_c (%)	34.8 to 39.6
Liquid limit, LL (%)	30.4 ^a (0.41) ^b
Plastic limit, PL (%)	26.3 ^a (0.90) ^b
Plasticity Index, PI	4.1 ^a (—1.3) ^b
Unified soil classification	ML
Specific gravity, G_s	2.69
Estimated range of effective overburden stress in situ	80 – 85 kPa
*CPT cone penetration resistance, q_t	1.2 – 1.8 MPa
* CPT friction sleeve resistance, f_s	0.006 – 0.012 MPa
*Field vane shear strength, S_u	40 kPa
Preconsolidation stress **	85 – 95 kPa

Note: a= Average value; b= Standard deviation; * = Based on past (unpublished) in situ testing data available from others; ** Data from Sanin (2005)

3.2 Specimen reconstitution method

Most of the specimens tested were performed on undisturbed samples of Fraser River silt. A limited number of tests were also performed on reconstituted specimens to compare the results. The reconstituted specimens were formed from a saturated slurry as follows. The material was mixed with de-aired water and left under vacuum for about 24 hours. The samples, while under vacuum were stirred occasionally to minimize entrapped air bubbles and with the objective of obtaining a saturated homogeneous slurry. Each sample was then transferred to a 500-mm beaker, where it was left to consolidate under its own weight for about 24 hours. The clear water accumulated at the top was removed and the remaining material was carefully stirred. Moisture content was measured at this time and the slurry was spooned to the DSS mould. The DSS test specimens were secured with o-rings and loaded to the desired vertical effective stress in an incremental manner to avoid any loss of material due to squeezing.

The slurry deposition method does not allow varying the density of the specimen to match that of the undisturbed specimens. Other methods, as the modified moist tamping technique, have been developed to change and target specific densities within the reconstituted specimen (Bradshaw and Baxter 2007). The slurry deposition method for sample reconstitution as described above, was selected for the present study since it is considered to better mimic the in-situ natural deposition of the silt in a river environment.

3.3 Direct simple shear apparatus

Cyclic triaxial (CTX) and cyclic direct simple shear (CDSS) tests have been used by many researchers for the study of cyclic shear response of soils. While the CTX has been widely used because of its simplicity and common availability, the CDSS loading is considered to effectively mimic the anticipated stress conditions under seismic loading (Finn et al., 1978). This can be more readily explained with respect to Figure 3.3 where the differences between the CTX and CDSS loading modes are presented. In addition, the DSS apparatus allows for constant volume tests, which avoids the errors associated with compliance and make the testing procedure simpler and eliminates the saturation requirements (Finn and Vaid, 1977; Finn et al., 1978). Considering the above, the cyclic direct simple shear apparatus at the University of British Columbia (UBC) was selected for the characterization of the cyclic loading response of Fraser River Delta silt.

The UBC simple shear apparatus is of the NGI type (Bjerrum and Landva, 1966). A schematic diagram of the apparatus is given in Figure 3.4. The cylindrical soil specimen, 70 mm in nominal diameter and approximately 20 mm height, is placed in a reinforced rubber membrane. The reinforced rubber membrane would constrain the specimen from deforming laterally; as such, the soil specimen would be in a state of zero lateral strain during consolidation and cyclic loading, which is considered to simulate the anticipated field stress conditions. Simple shear tests can be performed in undrained or constant volume condition. The latter constant volume DSS test is an alternative to the former where all drainage in a saturated sample would be suspended. In a constant volume test, the specimen diameter is constrained by the reinforced membrane, and any vertical deformation is restricted by clamping the top and bottom loading

caps against vertical movement. It has been shown that the decrease (or increase) of vertical stress in a constant volume DSS test is essentially equivalent to the increase (or decrease) of excess pore water pressures in an undrained test (Finn et al., 1978; Dyvik et al., 1987) where the near constant volume condition is sustained by keeping the mass of water unchanged. As such, the direct measurement of the change in vertical stress in a constant volume DSS test corresponds to the equivalent excess pore water pressure change. Throughout the thesis the term “pore water pressure” is used when reference is made to the “equivalent pore water pressure”.

3.3.1 DSS loading system

The UBC-DSS apparatus consists of horizontal and vertical loading systems as shown in Figure 3.4. The vertical loading system, located at the bottom of the apparatus, consists of a simple single-acting air piston controlled manually by an external pressure regulator. Horizontal load is applied by a double-acting frictionless air piston coupled in series with a constant speed motor drive. This horizontal loading system allows a smooth transition from stress-controlled to strain-controlled loading and vice versa, as required.

Figure 3.3 Comparison of stress conditions in (a) Simple Shear testing – DSS and (b) Triaxial testing – CTX.

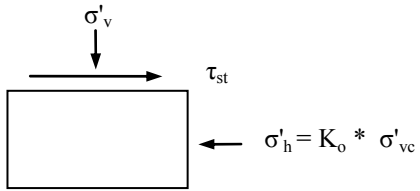
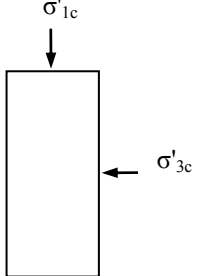
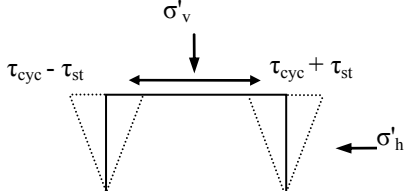
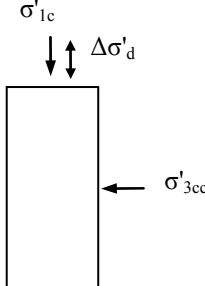
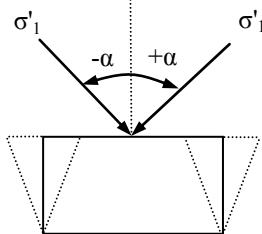
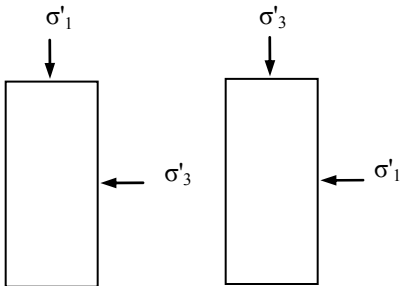
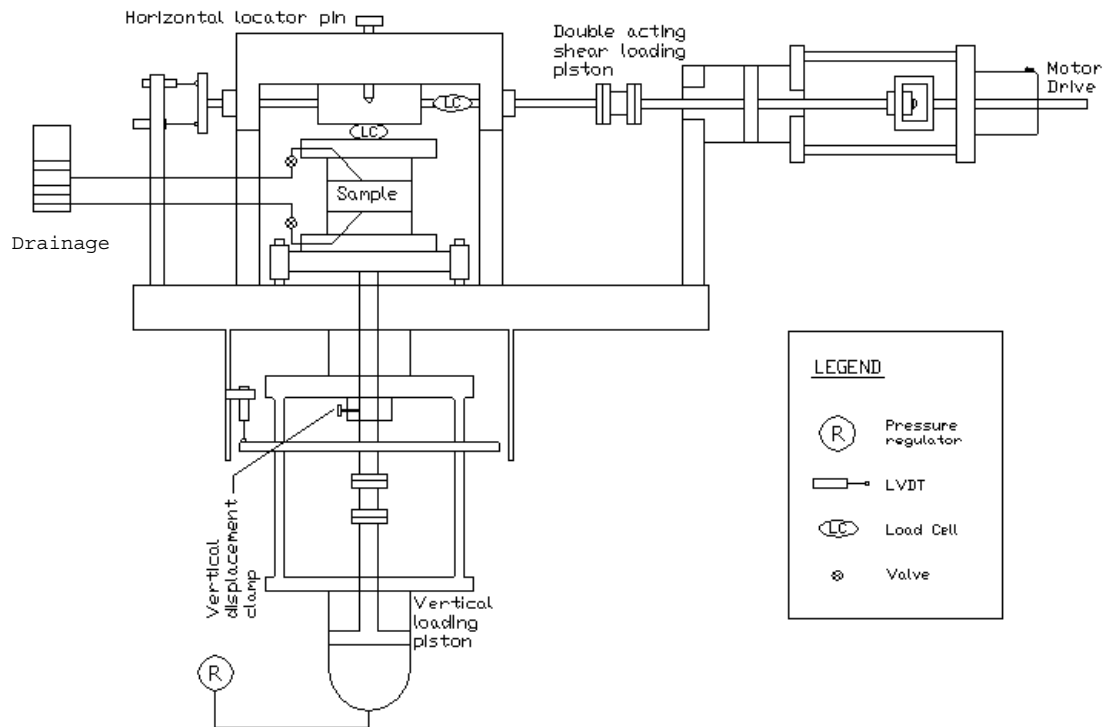
(a) DSS	(b) CTX	Stress status
		Initial (static) condition
		Cyclic loading condition
		Principal stress direction during cyclic loading

Figure 3.4 Schematic diagram of UBC simple shear test device (Modified from Sriskandakumar, 2004)



Stress-controlled cyclic loading is applied by changing the pressure on one side of the double acting piston with an electro-pneumatic regulator and maintaining the pressure on the other side constant. The electro-pneumatic regulator enables applying any prescribed form of cyclic loading by the coupling with a data acquisition system and computer. A sinusoidal wave form is generally chosen for the cyclic loading, and the magnitude and duration of the wave can be changed during the test if required.

In strain-controlled monotonic or cyclic loading, since the loading arm is coupled to a constant speed motor, the direction and speed can be changed manually as required.

3.3.2 Data acquisition, control system and measurement resolution

The UBC DSS apparatus is equipped with a high speed data acquisition and control system. A 12-bit “PCL718” high speed data acquisition card is used for signal input and output. This card consists of five A/D input channels and a D/A output channel.

Two load cells and three linear variable displacement transducers (LVDTs) are monitored by the input channels. One of the load cells is dedicated to measure the vertical load, and the second one is for the horizontal load. One LVDT measures the vertical displacement and the other two are assigned to monitor the horizontal displacements. The use of two LVDTs allows measuring both small and large displacements. All transducers are excited with a 5V d.c voltage supply. Input signals from load cells are amplified by a factor of 1000. The measurements are further refined by averaging 60 readings for each data channel. The high speed data acquisition system is able to gather about 500 sets of data per second.

The D/A channel is used to control the electro-pneumatic transducer that regulates the air pressure to one of the chambers of the horizontal loading double acting air piston. The electro-pneumatic transducer is “SMC IT2051-N33” type, and it is capable of delivering 90 kPa full scale pressure output for a 1000 kPa input pressure. A high resolution of measurements is obtained by the above carefully selected measurement devices (transducers) and a sophisticated data acquisition system. Shaft friction on the horizontal loading ram, stiffness of reinforced membrane, and spring forces arising from the LVDTs are also accounted for in the data reduction program.

Table 3.2 presents the resolution of each measurement for a typical 70 mm diameter and 20 mm height sample.

Table 3.2 Measurement resolution of UBC-DSS device

Measurement		Resolution
Vertical/Normal stress		± 0.25 kPa
Horizontal/Shear stress		± 0.25 kPa
Horizontal/Shear strain	Small range (<13%)	± 0.01 %
	Large range (>13%)	± 0.05 %
Vertical strain		± 0.01 %

3.3.3 DSS Test procedure

3.3.3.1 Specimen extrusion and setup

The DSS test device was set up in advance to prepare for receiving the silt specimen upon completion of extrusion and trimming. A saturated porous stone was initially placed in the bottom pedestal of the DSS device. The reinforced rubber membrane was placed in position and the bottom of the membrane was sealed with the bottom pedestal using an o-ring. The split mould was then kept in position and vacuum was subsequently applied to stretch the membrane and create a cavity in the DSS device to receive the specimen.

Specimens for DSS testing were carefully extruded from the tube samples retrieved from the field (as per Section 3.1). For a given specimen, silt material of approximately 40 mm in thickness was extruded from the sampling tube. A stainless steel ring with a sharp cutting-edge and essentially having a diameter slightly smaller than the tube sample was gently pushed into the extruded specimen. The sharp edge of the stainless steel ring, while “trimming” the

specimen to a 70-mm diameter, allowed securing silt material against disturbance during the next steps in sample setup. The specimen secured as per above, was then trimmed at the top and bottom using a wire saw to obtain a specimen height of approximately 20 mm. Trimmings obtained from the top, bottom and sides were collected for water content measurements.

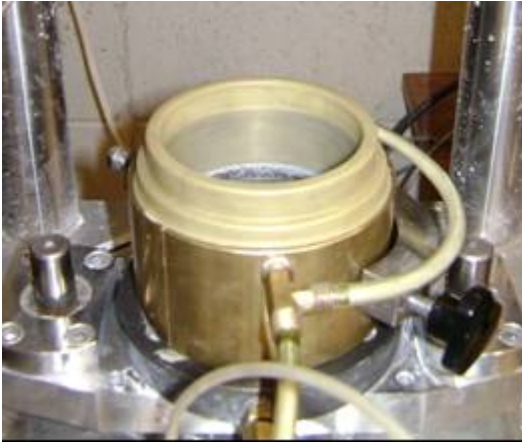
Upon completion of the above process, the stainless steel ring that contains the specimen was placed over the cavity of the DSS device and then set into the cavity by applying a slight uniform pressure with a plastic plunger. Once the sample was in position in the DSS device, the top cap was placed and a pressure of ~ 10 kPa was applied using the vertical loading system. The rubber membrane was sealed with the top cap using an o-ring. Figure 3.5 illustrates the steps for sample preparation and set-up in the DSS.

All the transducers were properly positioned and initial outputs were set to zero values prior to commencement of testing. The split mould was removed while all transducer readings were monitored to assess that no undesirable movements or loads were imparted during this process.

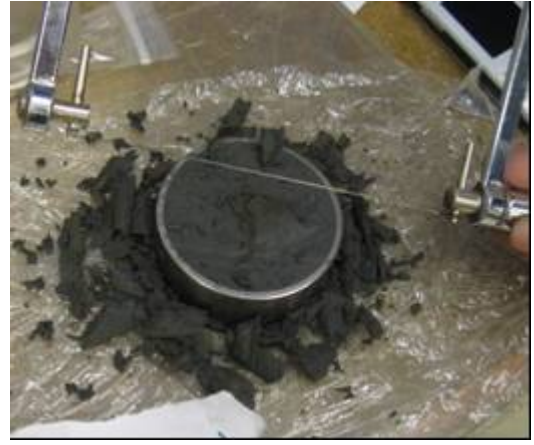
3.3.3.2 Consolidation phase

After completion of specimen setup, the vertical confining stress was increased to the target value corresponding to the test to be performed. The change in height of the specimen (proportional to the volume change) with respect to the elapsed time was recorded using the data acquisition system. The samples were kept at the stress condition for about 3 hours or 10,000 seconds. This time duration was adequate to obtain essentially unchanging vertical deformation of the specimen (i.e., adequate time allowed for completion of primary consolidation of Fraser River silt specimen).

Figure 3.5. Sample preparation and set up in DSS equipment.



1. Split mould and reinforced rubber membrane positioned in bottom pedestal prior to sample set-up



2. Specimen in stainless steel ring and being trimmed for set up in DSS



3. Specimen placed in mould



4. Specimen in DSS secured with O-rings (mould removed) prior to testing

3.3.3.3 Static shear bias application phase

After consolidation, for those tests requiring initial static shear bias, the desired shear stress was applied slowly in 5 kPa increments and under drained conditions until vertical and shear strains were stable.

3.3.3.4 Shear loading phase

After completion of the consolidation phase, the specimen was constrained against vertical strains by clamping the vertical loading ram (see Figure 3.4). This ensured constant volume conditions during cyclic loading. The horizontal shear loading was applied either using a double acting piston or a constant speed motor depending on whether the test was stress-controlled or strain-controlled, respectively. For cyclic stress-controlled tests, the shear load was applied in the form of a sinusoidal wave with a frequency of 0.1 Hz at the desired amplitude. This frequency is less than most of the frequencies encountered in typical earthquake loading. However, it allows a better control of loading as well as data acquisition. Zergoun and Vaid (1994) noted that the behaviour of clay in undrained cyclic triaxial shear loading cannot be confidently interpreted in fast loading tests because of unreliable measured pore water pressures (due to inadequate time for pore water pressure equalization in fast tests). In the DSS tests performed for this study, the constant volume condition is achieved by controlling the external boundaries, and pore water does not participate in volume control. Hence, there is no need for measurement of pore water pressure as the vertical effective stress on the sample at any given time is directly obtained from the measured load at the vertical stress boundary. With this consideration together with the need to obtain accurate control of applied stresses, the chosen loading frequency of 0.1 Hz is considered suitable, and this

approach has been in use for constant volume cyclic DSS testing of silty and sandy soils at UBC over the last 20 years.

In monotonic strain-controlled loading, the tests were performed at a rate of 10% strain per hour. In cyclic tests, loading was conducted until a shear strain of approximately 15% was reached. Monotonic shear tests were terminated after reaching shear strains of approximately 20%.

3.3.3.5 Post-cyclic reconsolidation

After completion of the constant volume cyclic loading stage as per above, specimens were re-consolidated to the initial confining stresses to assess potential post-cyclic volumetric deformations. Since the specimens generally had a residual shear strain at the end of cyclic loading, the specimen top cap position was manually reset to reach an approximate shear strain of zero prior to reconsolidation.

3.4 Test program

A systematic testing program was undertaken with the main objective of characterizing the fundamental mechanical response of Fraser River Delta silt at the location shown in Figure 3.1, mainly on undisturbed samples. The material was tested varying different parameters to investigate the following:

- undrained monotonic response of normally consolidated Fraser River delta silt in direct simple shear;

- cyclic shear loading response of normally consolidated silt in the direct simple shear;
- effects of initial confining stress level in monotonic and cyclic loading;
- effects of initial static shear bias in monotonic and cyclic loading;
- effects of particle structure and comparison between undisturbed and reconstituted specimens;
- post-cyclic reconsolidation response of Fraser River Delta silt.

Table 3.3 presents a summary of the proposed test program describing each of the test series and the parameters investigated.

Table 3.3 Test program

Test Series		Material / Tests	Nominal σ'_{vc}	CSR = τ_{cy}/σ'_{vc}	Static Bias, $\alpha = \tau_o/\sigma'_{vc}$	No. of tests
			(kPa)			
I	a	Natural Fraser River silt (NC): Effects of initial effective confining stress, post-cyclic consolidation response	100-500	MONOTONIC	0.0	5
	b		85,100,200, 300,400	0.10 – 0.30		21
	c	Natural Fraser River silt (OC): Effects of OCR, post-cyclic consolidation response	100	0.10 – 0.30	0.0	12
II	a	Natural Fraser River silt: Effects of initial static bias.	100	MONOTONIC	0.05 – 0.15	3
	b			0.10 – 0.30	0.05 - 0.15	15
III	a	Fraser River silt – Reconstituted: effects of particle structure.	100 - 400	MONOTONIC	0.00	4
	b		100	0.10 – 0.20		5
IV	a	Quartz rock powder : post-cyclic consolidation response	100	0.08 – 0.15	0.00	4
				0.12		
	b	Natural Kitimat clay: Effect of particle structure, effect of plasticity	80	0.16 – 0.25		3
	c	Reconstituted Kitimat clay: Effect of particle structure	80	0.16 – 0.25	0.00	3

Total No. of tests 75

4 CYCLIC SHEAR RESPONSE OF FRASER RIVER DELTA SILT

This chapter presents a detailed examination of the results obtained from the testing work undertaken with the primary motivation of characterizing the cyclic shear response of natural low plastic Fraser River Delta silt and of developing a database for use by the engineering profession. In particular, experimental findings on the effects of confining stress, overconsolidation, initial static shear stress bias, and level and duration of loading on the characteristic cyclic direct simple shear response of specimens prepared from the undisturbed tube samples of the silt are presented.

The presentation also includes observations made from limited experimental work to study the behavioural characteristics derived from monotonic shear loading of the natural silt material. Although these tests formed only a minor component of this research in terms of number of investigative tests, the monotonic loading results have been presented to provide some basic reference parameters and behavioural information for comparison with the results from the cyclic loading tests mentioned above and those from tests conducted on reconstituted specimens of Fraser River silt (described in Chapter 5). Data from monotonic shear tests are initially presented then followed by data derived from cyclic tests. Table 4.1 summarizes the tests parameters and key results.

Table 4.1 Test parameters and summary results

Test series	Test ID	(w _i) _{ave}	e _i	OCR	σ'_{vc} (kPa)	e _c	Cyclic tests					PCC* ε_{v-pc} (%)
							$\alpha = \tau_o/\sigma'_{vc}$	τ_{cy}/σ'_{vc}	$N_{(\gamma=3.75\%)}$	γ_{max} (%)	r_{u-max}	
la	FRN-100-M	40.9%	1.096	1.0	101.9	1.018	0.00	MONOTONIC				N/A
	FRN-200-M	39.7%	1.068	1.0	199.6	0.949						N/A
	FRN-300-M	40.8%	1.097	1.0	296.4	0.885						N/A
	FRN-400-M	37.9%	1.019	1.0	401.7	0.851						N/A
	FRN-500-M	37.3%	1.004	1.0	501.3	0.843						N/A
lb	FRS85-010	38.5%	1.076	1.0	86.9	0.939	0.00	0.10	N/A	1.04	0.53	0.52
	FRS85-015	37.8%	1.017	1.0	84.9	0.945		0.15	65	15.03	0.98	4.06
	FRS85-025	38.2%	1.027	1.0	85.0	0.985		0.24	2	15.19	0.94	3.37
	FRS85-029	39.1%	1.052	1.0	87.2	0.981		0.29	1	18.98	0.91	3.63
	FRS100-010	36.9%	0.991	1.0	92.4	0.921	0.00	0.10	N/A	0.31	0.59	0.54
	FRS100-014	38.7%	1.042	1.0	101.2	0.969		0.14	143	5.06	0.95	3.28
	FRS100-017	36.8%	0.990	1.0	101.3	0.892		0.17	8	21.45	0.92	2.43
	FRS100-020	36.2%	0.974	1.0	97.2	0.884		0.20	4	15.52	0.91	4.13
	FRS100-029	38.7%	1.041	1.0	101.1	0.990		0.29	1	7.75	1.00	3.47
	FRN100-016	38.3%	1.029	1.0	99.0	0.942		0.15	26	3.82	0.91	1.83
	FRSV100-01	37.5%	1.001	1.0	100.7	0.953		0.15	N/A	1.16	0.69	0.90
	FRS200-015	38.9%	1.047	1.0	199.3	0.900	0.00	0.15	13	15.40	0.91	1.67
	FRS200-020	36.8%	0.989	1.0	199.8	0.855		0.20	3	18.49	0.94	4.46
	FRS200-011	37.0%	0.997	1.0	198.6	0.882		0.11	164	15.42	0.97	5.11
	FRN300-017	40.1%	1.078	1.0	303.1	0.890	0.00	0.17	7	19.28	0.94	N/A
	FRN300-012	40.3%	1.083	1.0	299.0	0.895		0.12	47	11.74	0.93	N/A
	FRN300-020	41.7%	1.121	1.0	299.4	0.932		0.19	1	18.17	0.91	N/A
	FRN300-015	40.1%	1.078	1.0	300.2	0.882		0.15	10	11.84	0.93	N/A
	FRN400-012	38.3%	1.031	1.0	398.5	0.854	0.00	0.12	32	10.98	0.96	N/A
	FRN400-017	37.9%	1.020	1.0	399.8	0.818		0.17	11	20.44	0.94	N/A
	FRN400-019	41.2%	1.109	1.0	399.0	0.890		0.19	2	12.45	0.84	N/A

* PCC: Post cyclic consolidation test data

Table 4.1 Test parameters and summary results

Test series	Test ID	(w _i) _{ave}	e _i	OCR	σ'_{vc} (kPa)	e _c	Cyclic tests					PCC* ε_{v-pc} (%)
							$\alpha = \tau_o/\sigma'_{vc}$	τ_{cy}/σ'_{vc}	$N_{(\gamma=3.75\%)}$	γ_{max} (%)	r_{u-max}	
Ic	FROC1.3-021	38.6%	0.983	1.3	95.5	0.912	0.00	0.21	6	15.86	0.90	3.66
	FROC1.5-021	37.5%	1.001	1.5	98.0	0.900		0.21	18	15.06	0.92	2.58
	FROC2.1-021	35.4%	0.945	2.1	106.0	0.863		0.21		0.89	0.55	0.21
	FROC1.9-020	38.9%	1.046	1.9	104.5	0.908		0.20	136	15.47	0.96	3.67
	FROC1.4-021	34.8%	0.936	1.4	109.4	0.853		0.21	14	15.15	0.96	4.10
	FROC1.7-021	37.4%	1.006	1.7	104.5	0.894		0.21	37	18.23	0.98	3.17
	FROC1.2-030	38.5%	1.036	1.2	106.5	0.936		0.30	1	15.09	0.86	3.33
	FROC1.4-030	36.4%	0.980	1.4	105.5	0.894		0.30	2	15.40	0.90	3.21
	FROC1.9-031	36.6%	0.985	1.9	104.9	0.846		0.31	7	16.49	0.89	3.51
	FROC1.6-030	38.4%	1.032	1.6	111.0	0.929		0.30	3	15.08	0.89	3.60
	FROC1.2-015	37.8%	1.016	1.2	104.1	0.919		0.15	78	15.61	0.98	2.93
	FROC1.5-015	39.6%	1.065	1.5	98.7	0.970		0.15	180	3.81	0.83	1.33
IIa	FRN100-5-M	39.0%	1.050	1.0	100.0	0.956	0.05	MONOTONIC				N/A
	FRN100-10-M	38.5%	1.036	1.0	101.1	0.955	0.10					N/A
	FRN100-15-M	40.6%	1.091	1.0	101.7	1.009	0.15					N/A
IIb	FRN100-5-12	36.3%	0.976	1.0	102.2	0.907	0.05	0.12	42	3.98	0.92	N/A
	FRN100-5-15	36.5%	0.981	1.0	101.2	0.876		0.15	25	3.82	0.86	N/A
	FRN100-5-20	38.9%	1.047	1.0	102.4	0.988		0.19	3	5.18	0.86	N/A
	FRN100-5-21	38.5%	1.036	1.0	101.3	9.770		0.21	1	10.77	0.91	N/A
	FRN100-10-08	35.4%	0.951	1.0	100.5	0.895	0.10	0.09	N/A	0.84	0.45	N/A
	FRN100-10-12	39.6%	1.066	1.0	100.4	0.990		0.13	9	5.09	0.77	N/A
	FRN100-10-13	39.1%	1.053	1.0	102.3	0.985		0.12	10	10.24	0.92	N/A
	FRN100-10-18	38.2%	1.027	1.0	101.0	0.969		0.17	5	10.42	0.97	N/A
	FRN100-10-20	41.0%	1.103	1.0	99.7	1.011		0.19	1	8.31	0.82	N/A
	FRN100-10-22	36.4%	0.979	1.0	104.8	0.908		0.20	0	10.75	0.93	N/A
	FRN100-15-12	37.0%	0.995	1.0	100.8	0.910	0.15	0.12	8	5.11	0.65	N/A
	FRN100-15-15	38.8%	1.045	1.0	103.6	0.973		0.15	3	4.18	0.68	N/A
	FRN100-15-20	37.1%	0.999	1.0	102.9	0.929		0.19	0	6.50	0.79	N/A
	FRN100-15-16	39.7%	1.067	1.0	101.9	0.986		0.16	1	11.37	0.88	N/A
	FRN100-15-10	36.2%	0.973	1.0	101.7	0.909		0.11	32	9.35	0.80	N/A

Table 4.1 Test parameters and summary results

Test series	Test ID	$(w_i)_{ave}$	e_i	OCR	σ'_{vc} (kPa)	e_c	Cyclic tests					PCC* ε_{v-pc} (%)
							$\alpha = \tau_o/\sigma'_{vc}$	τ_{cy}/σ'_{vc}	$N_{(\gamma=3.75\%)}$	γ_{max} (%)	r_{u-max}	
IIIa	FRR-100-M	47.4%	1.275	1.0	104.6	0.842	0.00	MONOTONIC				N/A
	FRR-200-M	51.2%	1.377	1.0	199.0	0.809						N/A
	FRR-100-M	44.9%	1.208	1.0	300.6	0.761						N/A
	FRR-200-M	65.6%	1.765	1.0	398.5	0.741						N/A
IIIb	FRR100-015	50.9%	1.492	1.0	97.3	0.853	0.00	0.14	3	8.37	0.79	3.26
	FRR100-010	51.9%	1.470	1.0	103.4	0.866		0.10	29	5.87	0.92	2.80
	FRR100-0125	48.9%	1.251	1.0	96.8	0.852		0.12	9	7.99	0.94	3.04
	FRR100-0125-7day	51.5%	1.375	1.0	101.3	0.845		0.12	18	7.91	0.86	2.76
	FRR100-0125-24hr	56.0%	1.505	1.0	101.0	0.843		0.12	14	10.76	0.93	3.75
IVa	QRP100-009		1.022	1.0	97.9	0.787	0.00	0.10	21	4.70	0.90	N/A
	QRP100-013		1.084	1.0	103.7	0.789		0.12	17	5.16	0.91	N/A
	QRP100-015		1.245	1.0	99.8	0.788		0.14	6	4.41	0.87	N/A
	QRPV100-1		1.141	1.0	95.9	0.790	0.00	0.12	17	4.68	0.95	2.22
	QRPV100-2		1.345	1.0	96.8	0.799		0.12	8	2.13	0.83	1.14
	QRPV100-3		1.345	1.0	99.7	0.787		0.12	6	0.41	0.53	0.49
	QRPV100-6		1.345	1.0	98.8	0.788		0.12	8	0.63	0.66	0.85
IVb	KIN080-003	37.5%	1.013	1.0	80.0	0.958	0.00	0.24	10	4.70	0.90	N/A
	KIN080-001	36.1%	0.974	1.0	80.0	0.896		0.26	3	4.52	0.75	N/A
	KIN080-002	35.8%	0.967	1.0	81.0	0.888		0.17	90	3.85	0.81	N/A
IVc	KCR080-025	31.0%	0.837	1.0	82.4	0.793	0.00	0.24	2	5.84	0.74	N/A
	KCR080-020	31.0%	0.837	1.0	80.6	0.795		0.19	8	5.85	0.74	N/A
	KCR080-017	31.6%	0.852	1.0	80.5	0.795		0.16	23	3.89	0.73	N/A

4.1 Monotonic shear loading response

Constant volume monotonic direct simple shear tests were performed on undisturbed specimens of Fraser River silt as described in Chapter 3 of this Thesis. Herein, the investigation was mainly focused on testing specimens initially consolidated to: (i) different vertical consolidation stress levels to study the influence of initial effective confining stress; and (ii) different initial static shear loading (static bias) levels.

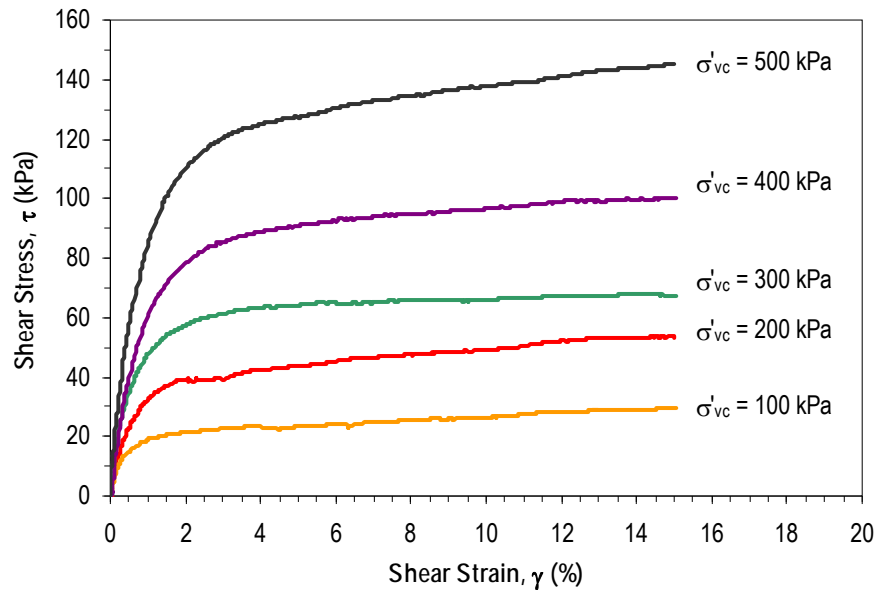
4.1.1 Effect of initial effective confining stress

The tests conducted on specimens initially consolidated to different effective vertical confining stress (σ'_{vc}) levels, between 100 to 500 kPa, are examined herein; in Test Series Ia (Table 3.3), all the tests were conducted with no initial static shear bias. Based on data from one-dimensional oedometer testing conducted as an initial part of the overall testing program, the preconsolidation pressure (yield stress) of the natural silt was estimated to be between 85 kPa and 95 kPa (Sanin 2005). Therefore, it is reasonable to state that consolidation of DSS specimens to σ'_{vc} levels above 100 kPa represents a condition where all the shear tests in Series Ia commenced from a normally consolidated stress state.

Typical stress-strain and the stress-path response obtained from the constant-volume monotonic tests conducted on specimens consolidated to $\sigma'_{vc} \sim 100$ kPa through ~ 500 kPa are presented in Figure 4.1 and 4.2 respectively. As may be noted from the stress paths (Figure 4.2) the specimens have deformed initially in a contractive manner followed by a

dilative response. The points at which phase transformation (from contractive to dilative) occurs are indicated by a “dot” symbol in Figure 4.2. Phase transformation seems to have occurred at the same mobilized shear stress ratio (τ/σ'_v). In terms of the stress-strain characteristics (Figure 4.1), all the samples can be considered to have exhibited behaviour of no “strain-softening”.

Figure 4.1 Constant volume monotonic DSS test on undisturbed specimens of Fraser River Delta silt at varying confining stress levels: Stress-strain curves; $\sigma'_{vc} = 100, 200, 300, 400$ and 500 kPa.



The stress paths were normalized to the initial effective confining stress, σ'_{vc} , and Figure 4.3 shows that the stress paths from all tests follow a consistent pattern. Clearly, the normalized stress paths for all the tests appears to be almost coincident (or fall within a narrow range) indicating that the response of normally consolidated silt is similar to that typically observed for normally consolidated clays (Atkinson and Bransby, 1978).

Figure 4.2 Constant volume monotonic DSS test on undisturbed specimens of Fraser River Delta silt at varying confining stress levels: Stress path curves; $\sigma'_{vc} = 100, 200, 300, 400$ and 500 kPa.

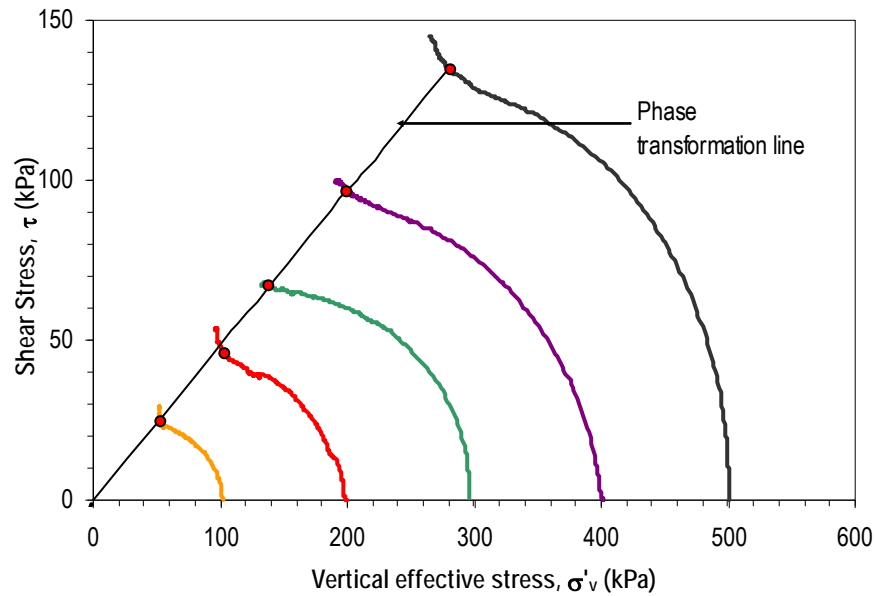
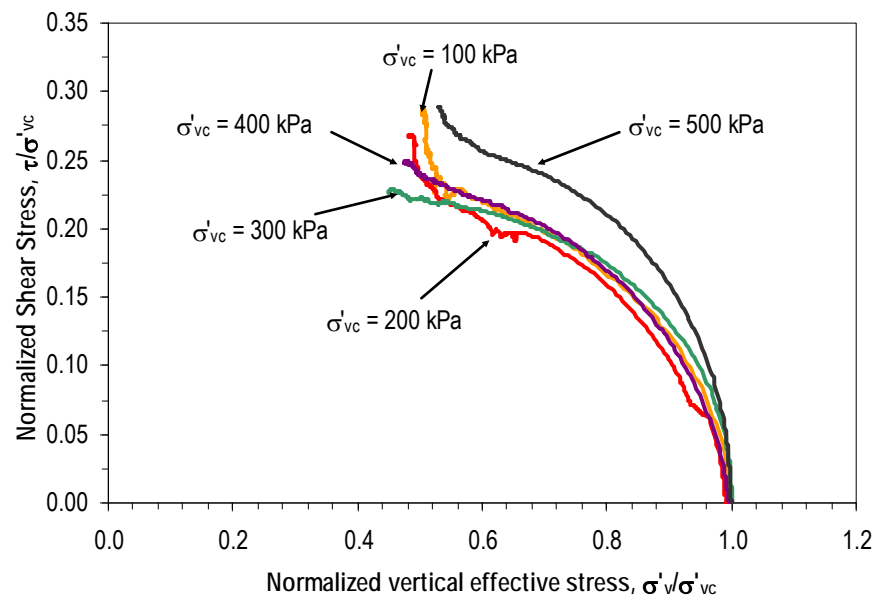


Figure 4.3 Constant volume monotonic DSS test on undisturbed specimens of Fraser River Delta silt at varying confining stress levels: Normalized stress path curves; $\sigma'_{vc} = 100, 200, 300, 400$ and 500 kPa.



4.1.2 Effect of initial static shear stress bias

DSS tests in Test Series IIa was performed on specimens consolidated to the same initial effective confining stress (σ'_{vc}) of ~ 100 kPa and selected values of “initial static shear stress bias ($\alpha = \tau_o/\sigma'_{vc}$)” - i.e., $\alpha = 0.05, 0.10$ and 0.15 .

After initial consolidation under the applied vertical stress, the static shear stress to meet the prescribed “initial static shear stress bias” was applied in an incremental manner while keeping the specimen in a drained condition; the specimen was allowed to reach equilibrium (i.e., stability in vertical and shear strains) under a given shear stress increment, prior to application of the subsequent shear stress increment as appropriate. Figure 4.4 shows the static shear application phase for the three tests with static bias. The slope of the stress-strain curves (Figure 4.4a) displays similarity in the drained shear behaviour in all three specimens. For the first shear increment to $\tau_o = 5$ kPa, all specimens reach a shear strain γ of about 0.05%. Volumetric strain versus shear strain response (Figure 4.4b) also show that all specimens reach a similar volumetric strain for the same applied shear.

Figures 4.5 and 4.6 show the stress strain and stress path response for these tests including the specimen tested with no static shear bias. The stress-strain response shows a slight increase in the shear strength with the increase in initial static bias for the specimens tested at $\tau_o/\sigma'_{vc} = 0.05$ and $\tau_o/\sigma'_{vc} = 0.10$. That trend is not noticeable for the specimen tested at $\tau_o/\sigma'_{vc} = 0.15$ for up to 5% shear strain. The stress paths presented in Figure 4.6 show that the phase transformation point occurs approximately at the same shear stress ratio as those observed from the monotonic tests conducted without static bias. These observations are in agreement with the uniqueness

of phase transformation line observed for sands by Ishihara (1996), Vaid and Chern (1985), and Negussey et al. (1988).

Figure 4.4. Application of static shear prior to monotonic shear in constant volume DSS test on undisturbed specimens of Fraser River Delta silt at varying initial static shear bias (α): $\sigma'_{vc} = 100$; $\alpha = 0.05, 0.10, 0.15$. a) Stress-Strain curve, b) Volumetric strain versus shear strain.

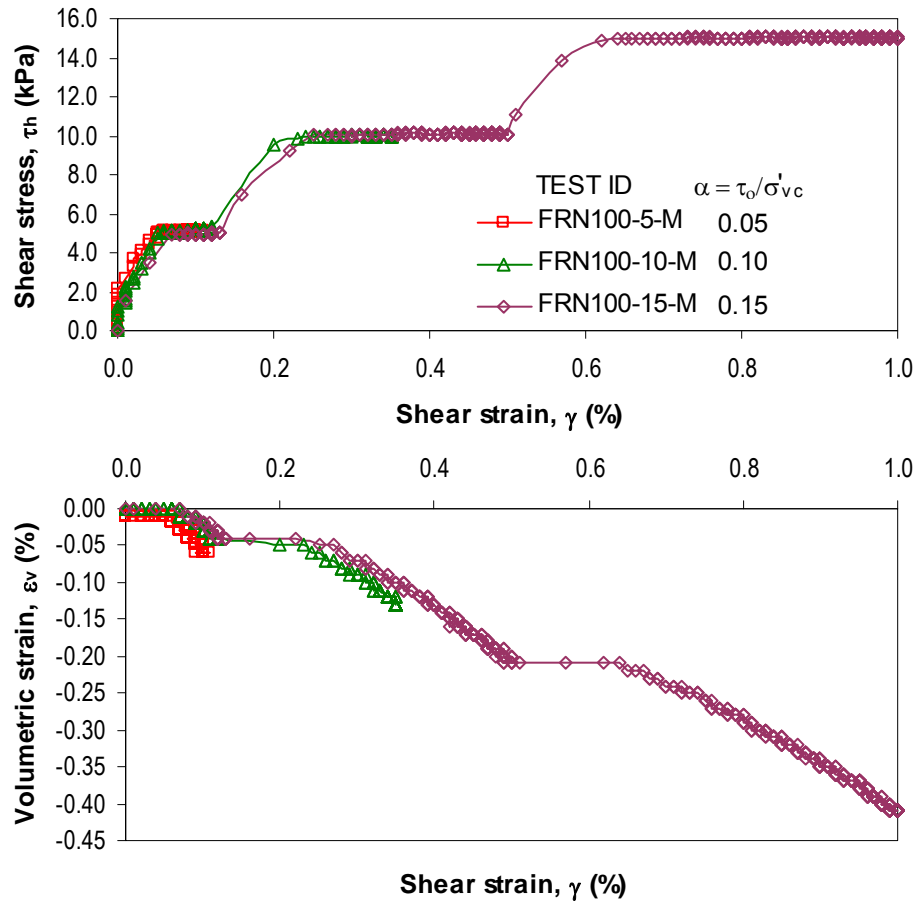


Figure 4.5 Constant volume monotonic DSS test on undisturbed specimens of Fraser River Delta silt at varying initial static shear bias (α): Stress-strain curves; $\sigma'_{vc} = 100$; $\alpha=0.05, 0.10, 0.15$.

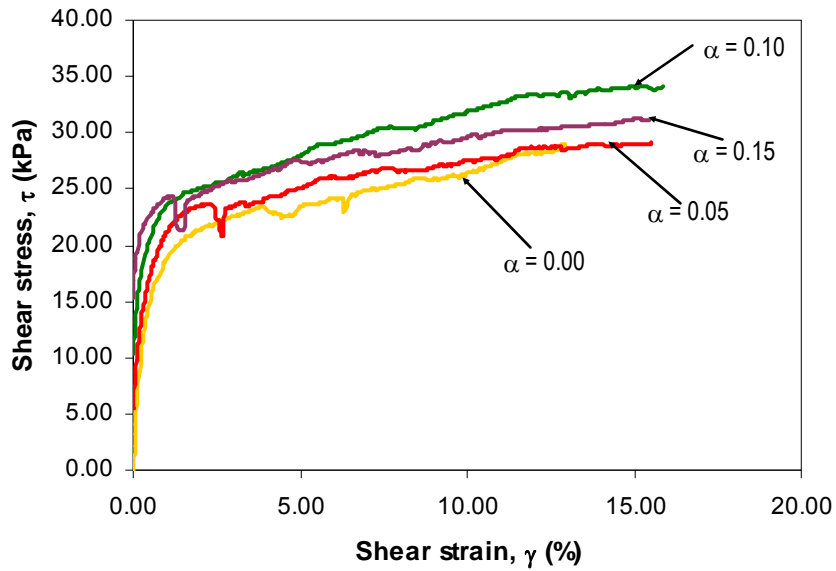
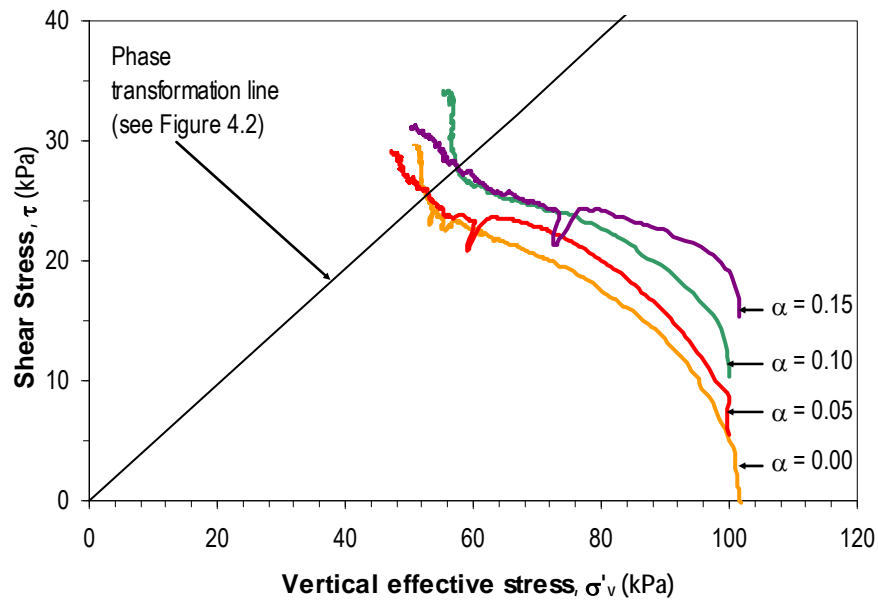


Figure 4.6 Constant volume monotonic DSS test on undisturbed specimens of Fraser River Delta silt at varying initial static shear bias (α): Stress path curves; $\sigma'_{vc} = 100$; $\alpha=0.05, 0.10, 0.15$.



4.2 Cyclic response

The following sections present the results from a detailed investigation to assess the cyclic shear response of Fraser River silt. The effects of the following parameters on the cyclic shear response of this material are investigated: (i) effect of initial confining stress – from tests conducted on specimens consolidated to different vertical effective stress levels with no static shear (Test Series Ib, Table 3.3); (ii) the effect of the initial static shear bias – studied using tests conducted on specimens consolidated under different initial static shear stress conditions vertical effective stress levels (Test IIb, Table 3.3); (iii) the effect of overconsolidation - from tests conducted on specimens overconsolidated in the laboratory to different overconsolidation ratios with no static shear (Test Series Ic, Table 3.3). It is noted that data from some of the tests on Fraser River silt (i.e., same material tested in the present investigation) conducted by the author as a part of her Masters thesis work (Sanin 2005) at the University of British Columbia were also included in the interpretations since such expansion of the database assisted arriving at more robust conclusions.

4.2.1 Effects of initial effective confining stress

4.2.1.1 General stress strain pore water pressure response

Test series Ib investigates the effects of the initial effective confining stress on the cyclic shear loading response of Fraser River Delta silt. Sanin (2005) has already presented the results for normally consolidated specimens of Fraser River Delta silt for values of σ'_{vc} equal to 85 kPa, 100 kPa and 200 kPa. The study indicated that the influence of the effective confining stress

on the cyclic shear response of Fraser River Delta silt was not significant for that range of effective stress; however, it was noted that further work would be necessary to arrive at more robust conclusions. The current study expands the range of initial effective confining stress up to 400 kPa. Results from constant volume cyclic shear tests on Fraser River silt conducted with $\sigma'_{vc} = 100$ kPa under varying cyclic stress ratio levels are presented in Figures 4.7 through 4.10. Figures 4.11 to 4.14 present the results of cyclic tests conducted at $\sigma'_{vc} = 300$ kPa at different cyclic stress ratios. Similarly, Figures 4.15 through 4.17 present the results for different values of CSR at a nominal initial confining stress of 400 kPa.

The details related to any individual tests can be noted directly from the figures. The intent here is to present typical test results and then examine and highlight some of the key observations and findings emerging from these results.

Figure 4.7 Constant volume cyclic simple shear DSS test on undisturbed specimen of normally consolidated Fraser River Delta silt: Stress strain and stress path curves; $\sigma'_{vc} = 100$; CSR = 0.14.

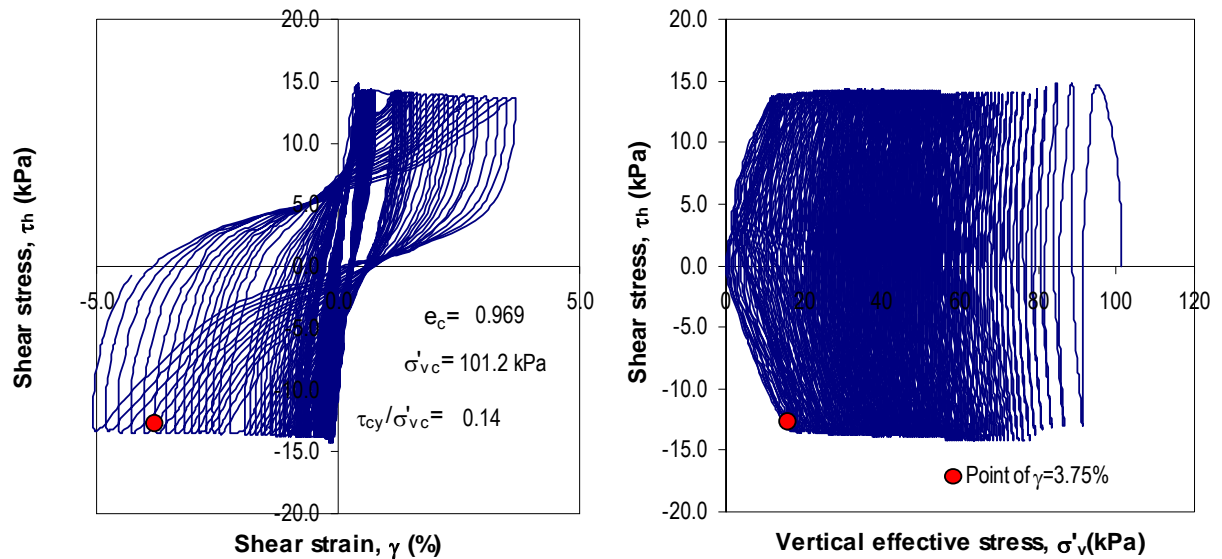


Figure 4.8 Constant volume cyclic simple shear DSS test on undisturbed specimen of normally consolidated Fraser River Delta silt: Stress strain and stress path curves; $\sigma'_{vc} = 100$; CSR = 0.17.

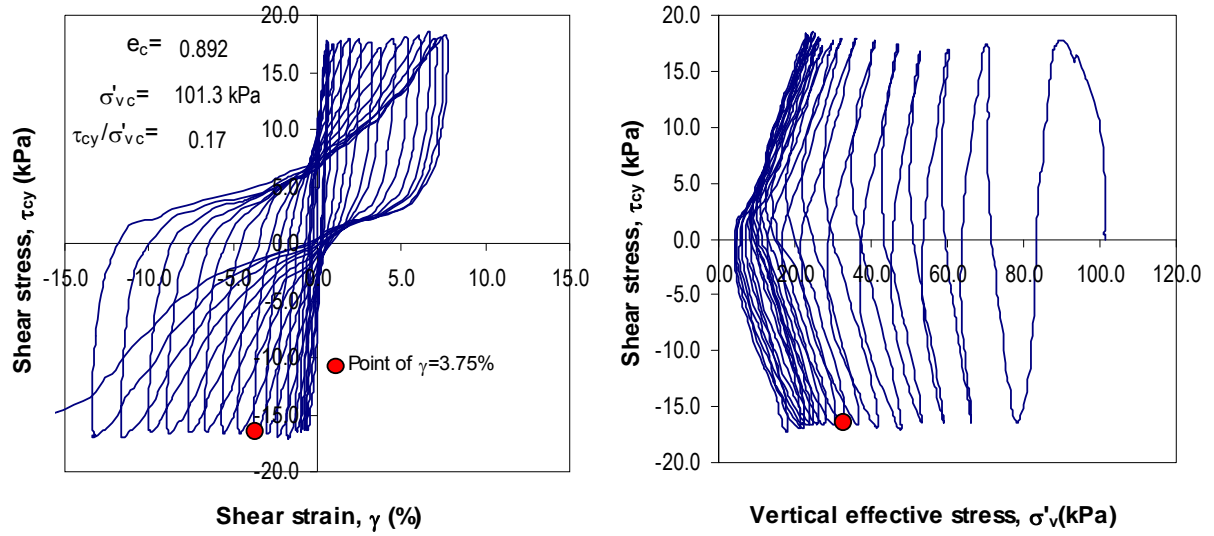


Figure 4.9. Constant volume cyclic simple shear DSS test on undisturbed specimen of normally consolidated Fraser River Delta silt: Stress strain and stress path curves; $\sigma'_{vc} = 100$; CSR = 0.20.

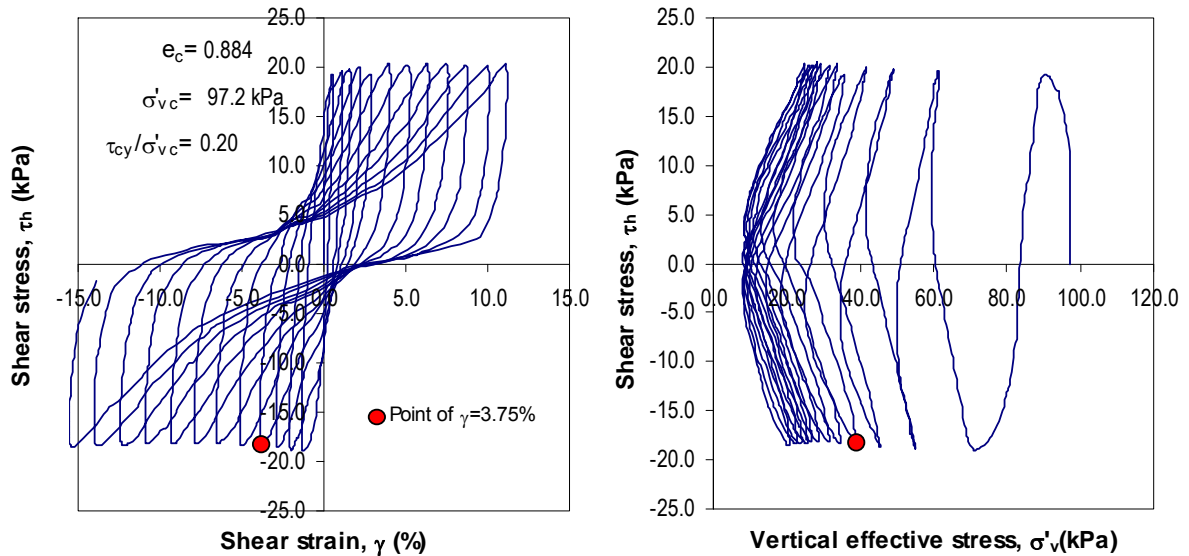


Figure 4.10 Constant volume cyclic simple shear DSS test on undisturbed specimen of normally consolidated Fraser River Delta silt: Stress strain and stress path curves; $\sigma'_{vc} = 100$; CSR = 0.29.

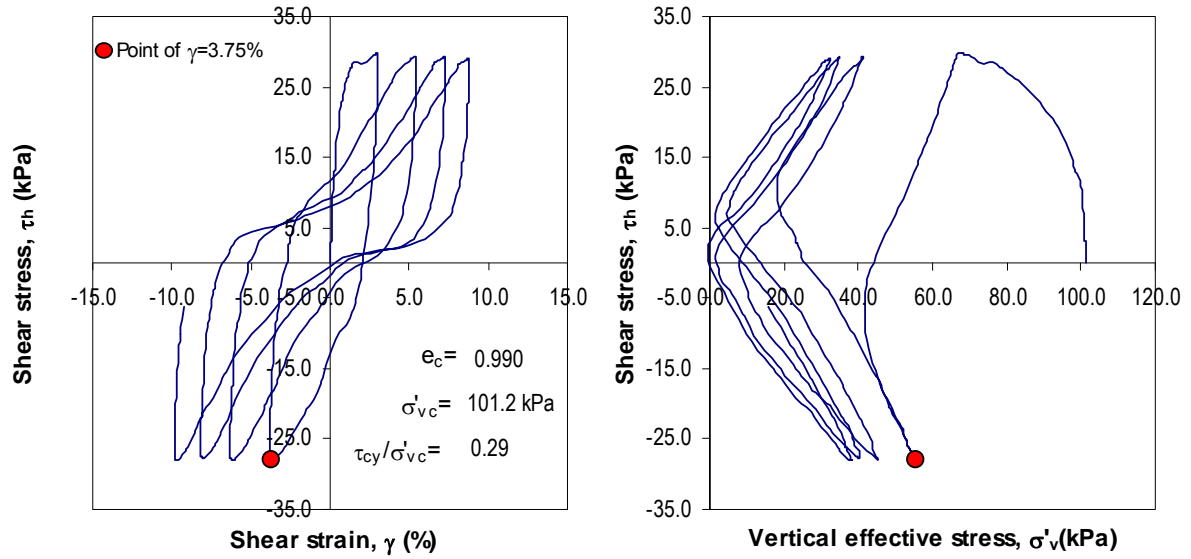


Figure 4.11 Constant volume cyclic simple shear DSS test on undisturbed specimen of normally consolidated Fraser River Delta silt: Stress strain and stress path curves; $\sigma'_{vc} = 300$; CSR = 0.12.

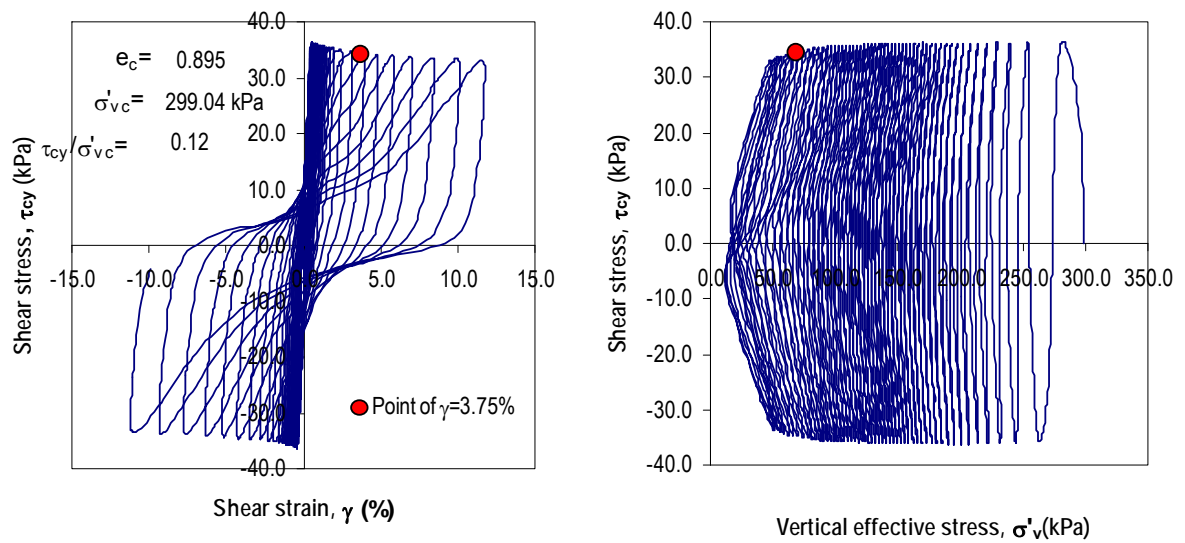


Figure 4.12 Constant volume cyclic simple shear DSS test on undisturbed specimen of normally consolidated Fraser River Delta silt: Stress strain and stress path curves; $\sigma'_{vc} = 300$; CSR = 0.15.

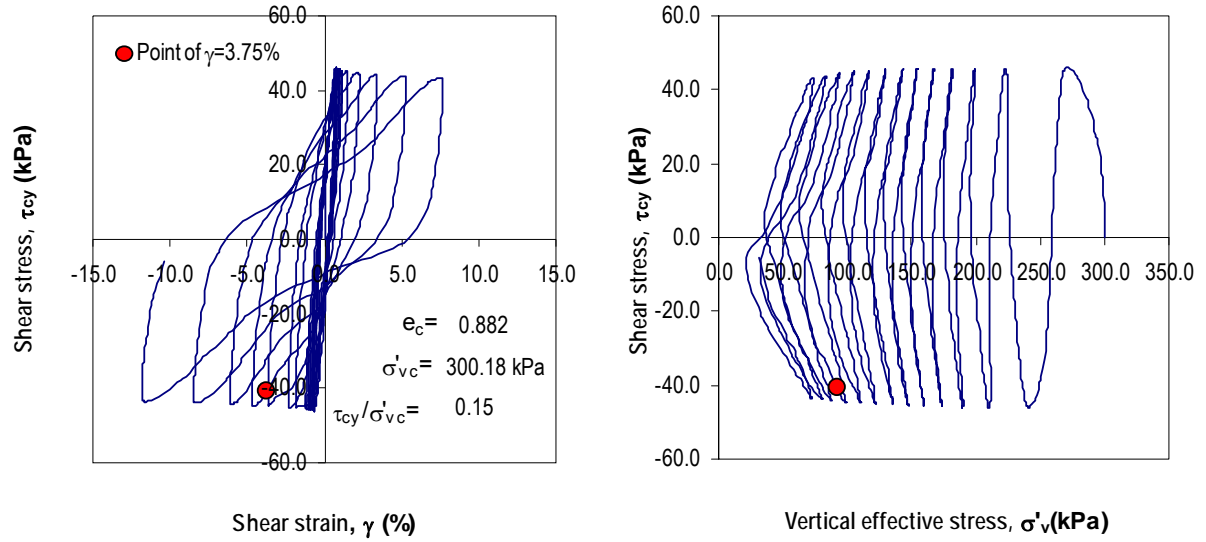


Figure 4.13 Constant volume cyclic simple shear DSS test on undisturbed specimen of normally consolidated Fraser River Delta silt: Stress strain and stress path curves; $\sigma'_{vc} = 300$; CSR = 0.17.

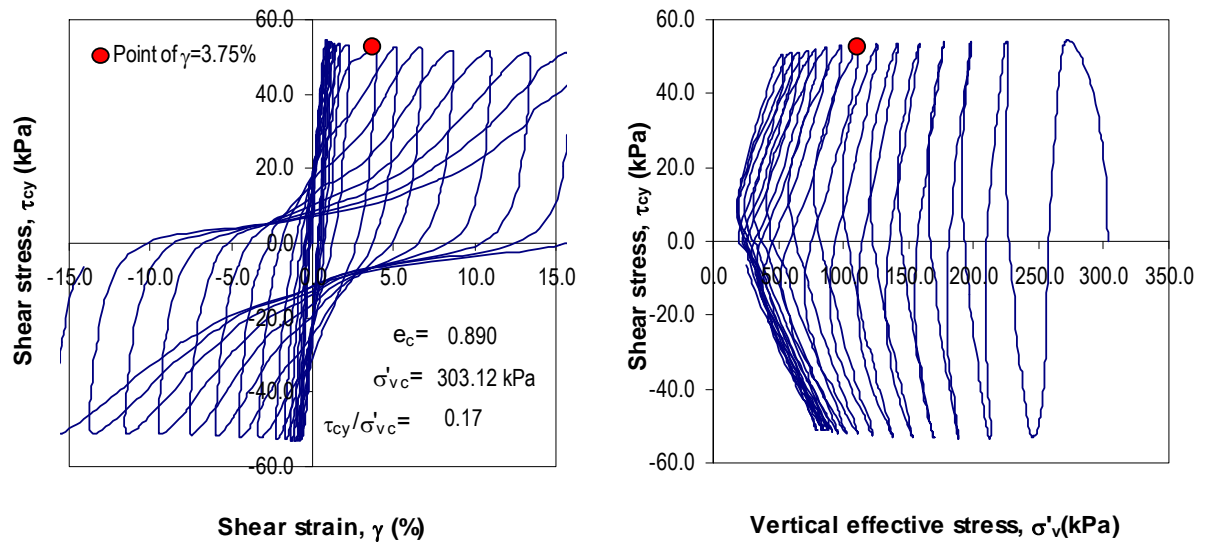


Figure 4.14 Constant volume cyclic simple shear DSS test on undisturbed specimen of normally consolidated Fraser River Delta silt: Stress strain and stress path curves; $\sigma'_{vc} = 300$; CSR = 0.20.

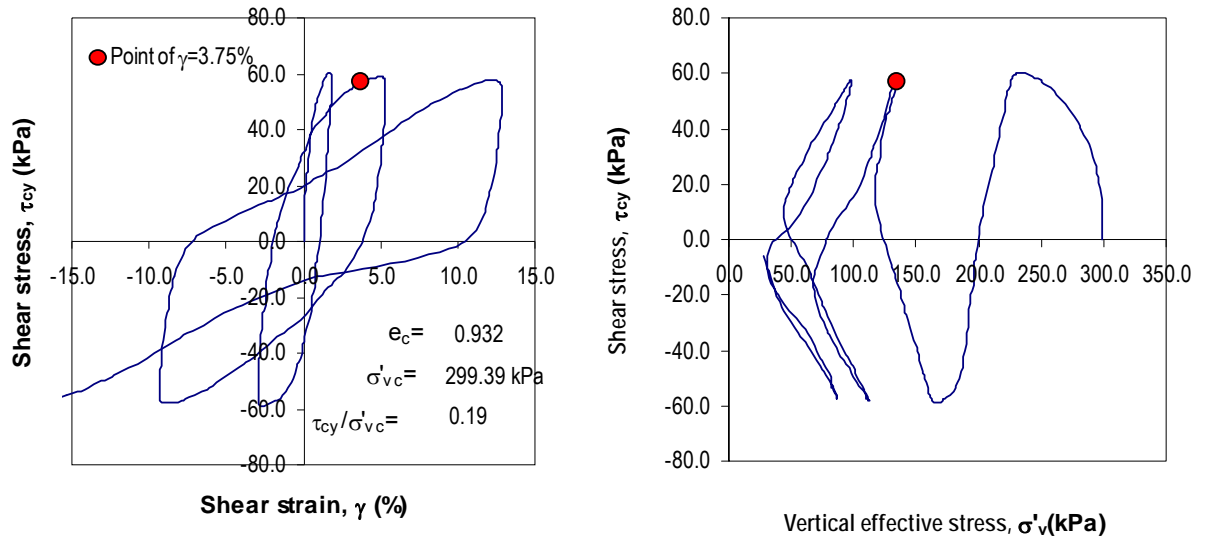


Figure 4.15 Constant volume cyclic simple shear DSS test on undisturbed specimen of normally consolidated Fraser River Delta silt: Stress strain and stress path curves; $\sigma'_{vc} = 400$; CSR = 0.12.

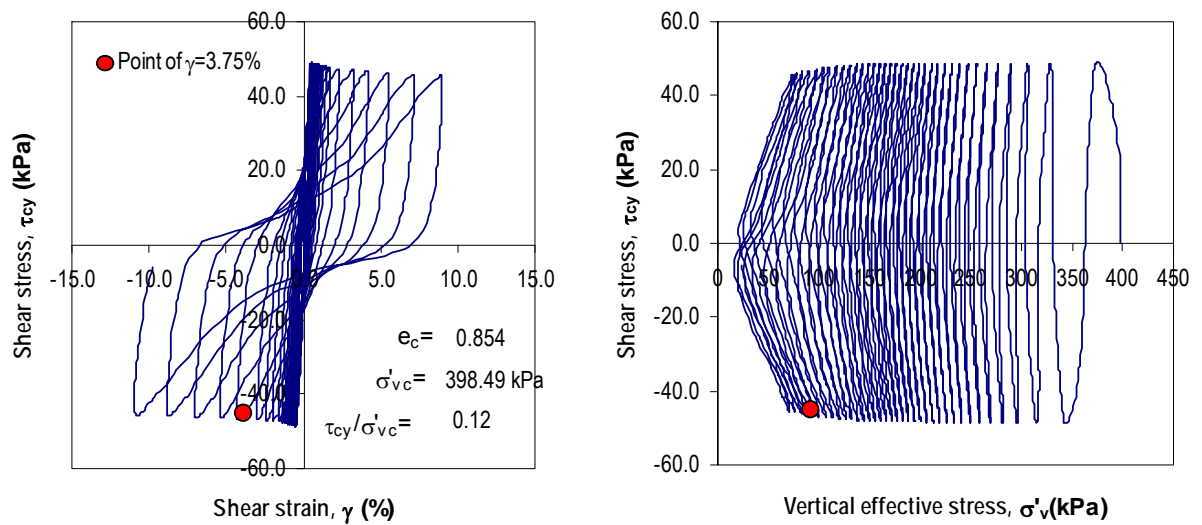


Figure 4.16 Constant volume cyclic simple shear DSS test on undisturbed specimen of normally consolidated Fraser River Delta silt: Stress strain and stress path curves; $\sigma'_{vc} = 400$; CSR = 0.17.

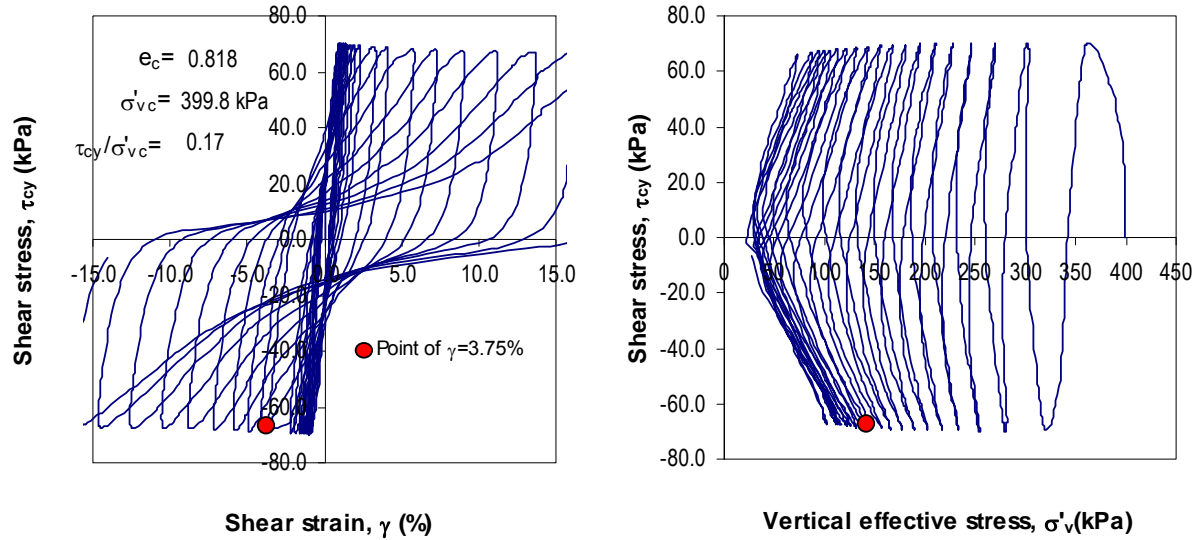
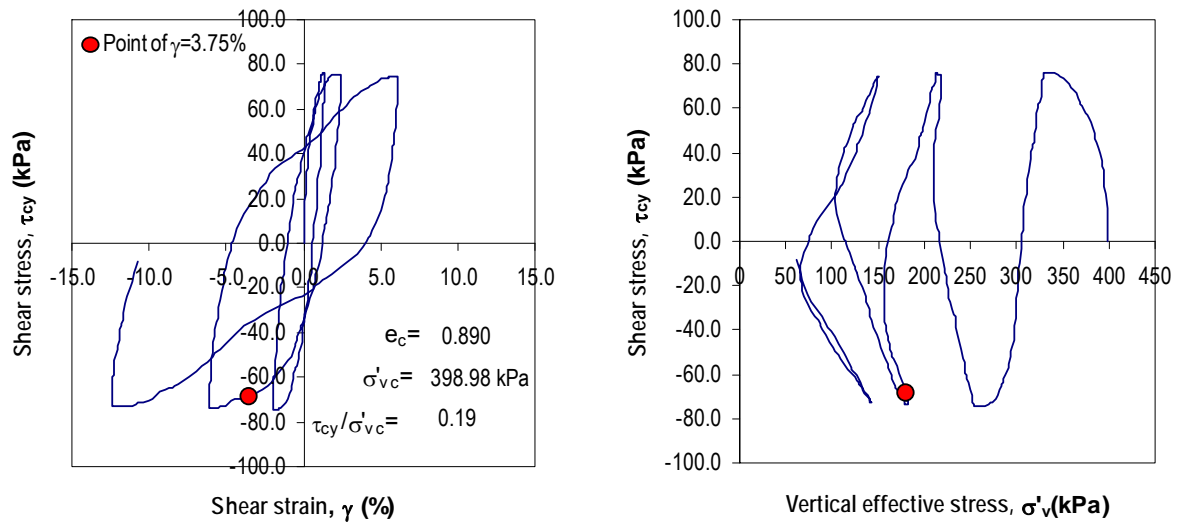


Figure 4.17 Constant volume cyclic simple shear DSS test on undisturbed specimen of normally consolidated Fraser River Delta silt: Stress strain and stress path curves; $\sigma'_{vc} = 400$; CSR = 0.19.



The variation of equivalent excess pore water pressure (Δu) vs. number of loading cycles for the cyclic tests conducted with $\sigma'_{vc} = 100, 300$, and 400 kPa at different cyclic stress ratios are

presented in Figure 4.18 through 4.20, respectively. While all the specimens exhibit gradual increase of Δu with increasing number of loading cycles, the rate of generation of equivalent excess pore water pressure ratio $r_u [=(\Delta u/\sigma'_{vc})]$ with number of cycles increases with increasing applied CSR. For example, the specimen with $\sigma'_{vc} = 100$ kPa that was subjected to $CSR = 0.29$ developed $r_u = 100\%$ in about 4 cycles (see Figure 4.10); whereas, the specimen tested with $\sigma'_{vc} = 100$ kPa but $CSR = 0.10$ only developed $r_u = 50\%$ even after experiencing 140 cycles of loading (see Figure 4.7). It is also of interest to note that the build-up of equivalent excess pore water pressure with the increasing number of cycles results in significant cyclic shear strains even at moderate levels of cyclic loading. For example, with a CSR value of 0.21, shear strains of the order of 12% were reached in about 11 cycles compared to almost no shear strains observed in a specimen that was imparted with 140 load cycles of $CSR = 0.10$.

Figure 4.18 Constant volume cyclic simple shear DSS test on undisturbed specimen of normally consolidated Fraser River Delta silt: Excess pore water pressure vs. number of loading cycles for different CSR values; $\sigma'_{vc} = 100$ kPa.

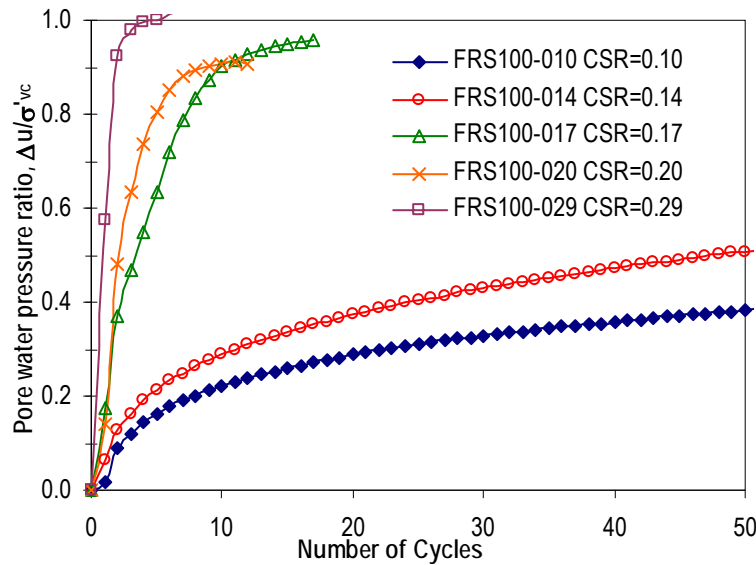


Figure 4.19 Constant volume cyclic simple shear DSS test on undisturbed specimen of normally consolidated Fraser River Delta silt: Excess pore water pressure vs. number of loading cycles for different CSR values; $\sigma'_{vc} = 300$ kPa.

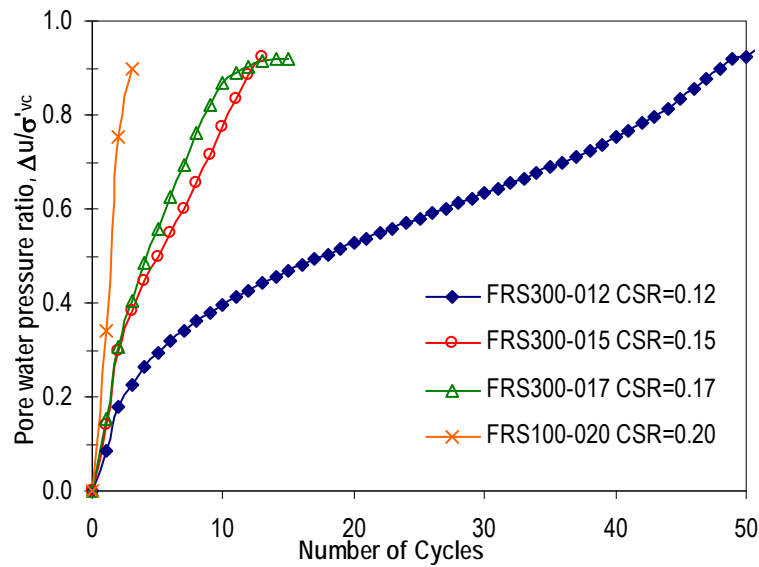
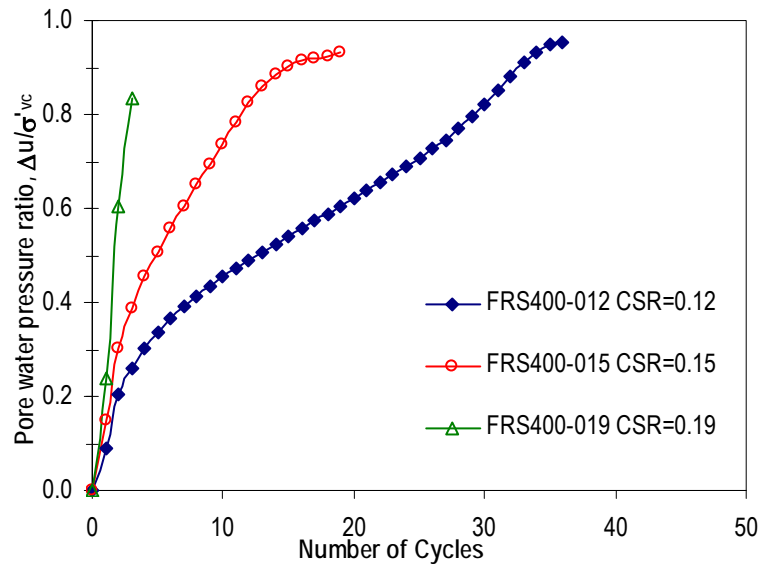


Figure 4.20 Constant volume cyclic simple shear DSS test on undisturbed specimen of normally consolidated Fraser River Delta silt: Excess pore water pressure vs. number of loading cycles for different CSR values; $\sigma'_{vc} = 400$ kPa.



In a general sense, it is reasonable to state that all the specimens initially show cumulatively contractive response, and with increasing number of load cycles, the specimens display cumulative increase in excess pore water pressure with associated progressive degradation of shear stiffness. In a given cycle, the shear stiffness experiences its transient minimum when the applied shear stress is close to zero (when the effective stress is minimum). It is important to note that the shear response gradually changed from contractive to dilative (or experienced phase transformation) during the ‘loading’ (or increasing shear stress) phases. However, significant contractive response was noted during ‘unloading’ (or decreasing shear stress) phases suggesting significant plastic volumetric strains during unloading, particularly in specimens that have experienced phase transformation.

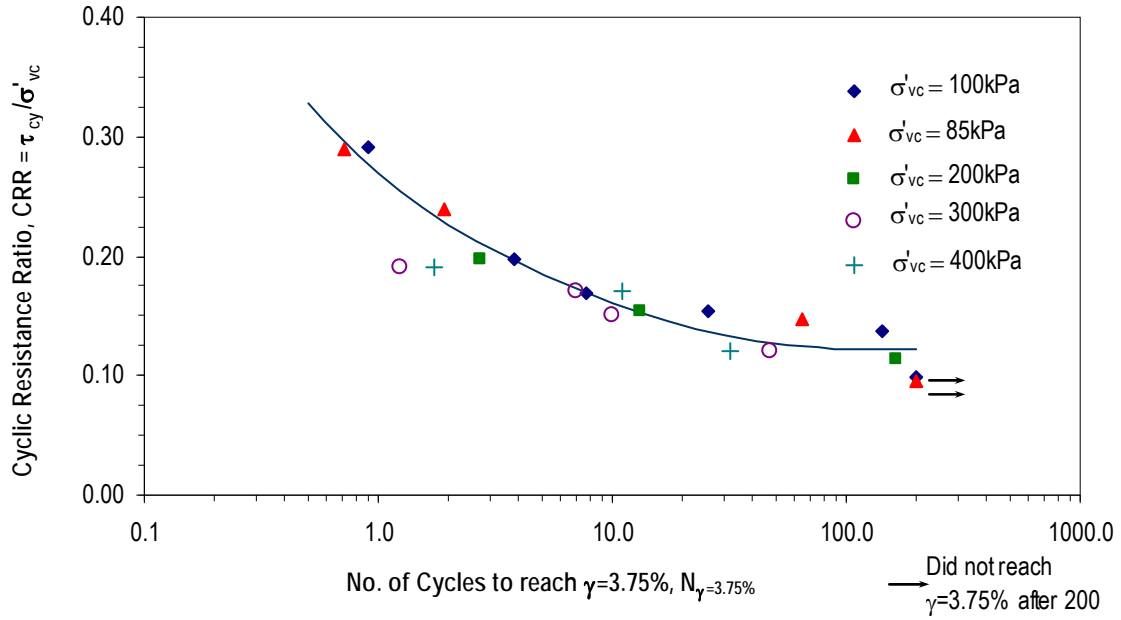
All the specimens eventually experienced zero, close to zero, transient vertical effective stress conditions during cyclic loading. This cyclic mobility type response is generally similar in form to the undrained (constant-volume) cyclic shear responses observed from cyclic shear tests on natural silts, fine-grained mine tailings, and clays (Sanin 2005; Wijewickreme et al. 2005a; Zergoun and Vaid 1994) and compact to dense reconstituted sand (Sriskandakumar 2004; Kammerer et al. 2002). Clearly, it is of importance to note that the observed cyclic mobility type of response is unaffected although the specimens have been consolidated to significantly different initial consolidation confining stress levels (σ'_{vc}).

4.2.1.2 Cyclic shear resistance

It is also of interest to examine the cyclic shear resistance of Fraser River silt by comparing the response observed from DSS testing under different applied cyclic loadings. In order to facilitate this comparison, the number of load cycles required to reach a single-amplitude horizontal shear strain $\gamma = 3.75\%$, in a given constant volume DSS test under a given applied CSR, was defined as $N_{\gamma=3.75\%}$. This $\gamma = 3.75\%$ condition in a DSS specimen is essentially equivalent to reaching a 2.5% single-amplitude axial strain in a triaxial soil specimen. An identical definition has been previously used to assess the cyclic shear resistance of sands by the U.S. National Research Council (NRC 1985), and it also has been adopted in many previous liquefaction studies at UBC.

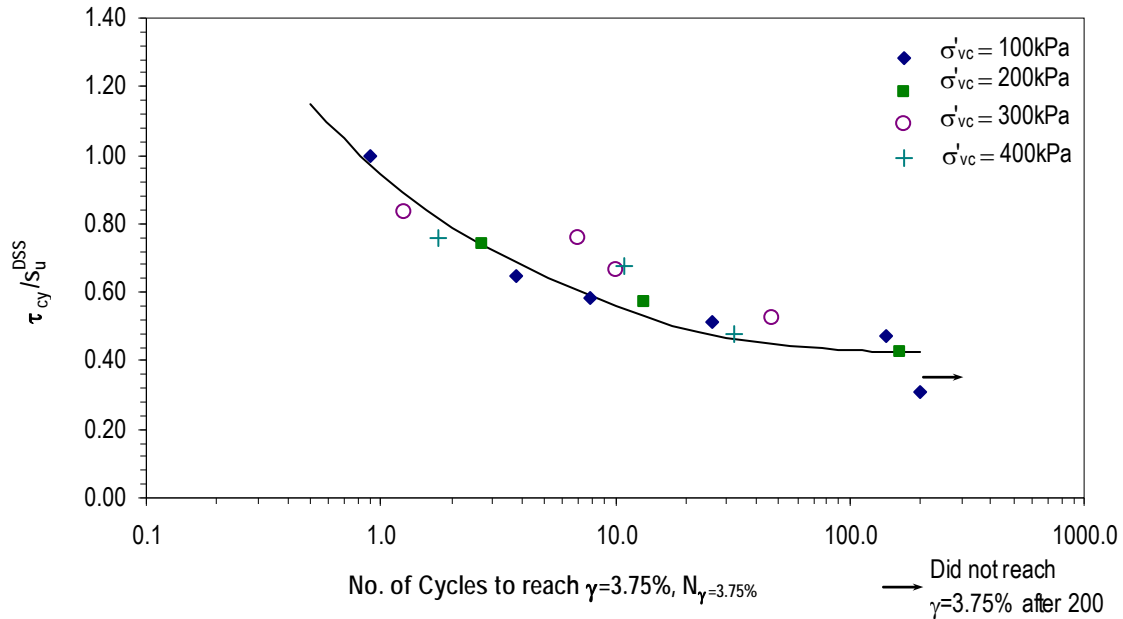
The applied cyclic stress ratio [$CSR = (\tau_{cy}/\sigma'_{vc})$] is plotted against number of cycles to reach single-amplitude $\gamma = 3.75\%$ in Figure 4.21. The data points seem to fall on a single trend-line suggesting that cyclic resistance is relatively insensitive to the confining pressure (and the changed initial void ratio due to consolidation) and that the response is influenced only by the mobilized shear stress ratio. It is important to note that the observation is also in accord with the coincidence of normalized stress paths found from monotonic shear testing work of the same soil, as described in Section 4.1. Similar behaviour has been observed by Zergoun and Vaid (1994) for normally consolidated clay in cyclic triaxial tests, and the findings are in harmony with the typical behavioural frameworks noted for normally consolidated clay (e.g., Atkinson and Bransby 1978).

Figure 4.21 Cyclic resistance ratio (τ_{cy}/σ'_{vc}) from constant volume cyclic DSS tests on undisturbed specimens of normally consolidated Fraser River Delta silt at varying initial confining stress levels.



The results of the cyclic DSS tests performed at initial confining stress levels $\sigma'_{vc} = 100, 200, 300$ and 400 kPa can also be plotted in the form of cyclic strength ratio defined as the ratio of the applied cyclic shear stress, τ_{cy} to the undrained shear strength in the DSS, s_u^{DSS} , as shown in Figure 4.22. This approach has been previously been used to interpret the results of cyclic testing for clays (e.g., Zergoun and Vaid 1994, Andersen 2009, Idriss and Boulanger 2008). The data points seem to fall on a single trend-line also suggesting that the cyclic resistance of Fraser River silt is not sensitive to the initial confining stress. The observations are also in accord with the normalized behaviour observed for the monotonic DSS loading.

Figure 4.22. Cyclic strength ratio (τ_{cy}/s_u^{DSS}) from constant volume cyclic DSS tests on undisturbed specimens of normally consolidated Fraser River Delta silt at varying initial confining stress levels.



It is also of interest to review the above observations with respect to the generally accepted response of relatively clean sands. In sands, the cyclic resistance generally increases with increasing density; for a given relative density, the cyclic resistance in sands has been noted to decrease with increasing confining stress (Seed and Harder 1990). In addition to the effects of density and confining pressure, the differences in particle fabric alone could lead to significant differences in CRR (Wijewickreme et al. 2005b). The observations presented herein suggests that, for the tested Fraser River silt, the dilative tendency arising due to stress densification seems to have overcome the possible contractive tendency due to the increase in confining stress. Park and Byrne (2004) and Wijewickreme et al. (2005b) have noted similar effects due to stress densification in their tests on sands.

4.2.2 Effects of initial static shear loading

4.2.2.1 General stress strain pore water pressure response

As indicated in Table 3.3, the effects of static shear bias were investigated for three different values of $\alpha = (\tau_o/\sigma'_{vc})$: 0.05, 0.10 and 0.15 (Test Series IIb). The cyclic loading stress-strain and stress path responses at different CSR values with initial static bias of 0.05, are presented in Figures 4.23 to 4.26. Similarly, the results test performed with α values of 0.10, are presented in Figures 4.27 to 4.32. Figures 4.33 to 4.37 present the results of tests with initial α values of 0.15.

Figure 4.23 Constant volume cyclic simple shear DSS test on undisturbed specimen of normally consolidated Fraser River Delta silt: Stress strain and stress path curves; $\sigma'_{vc} = 100$ kPa; CSR = 0.12; $\alpha=0.05$.

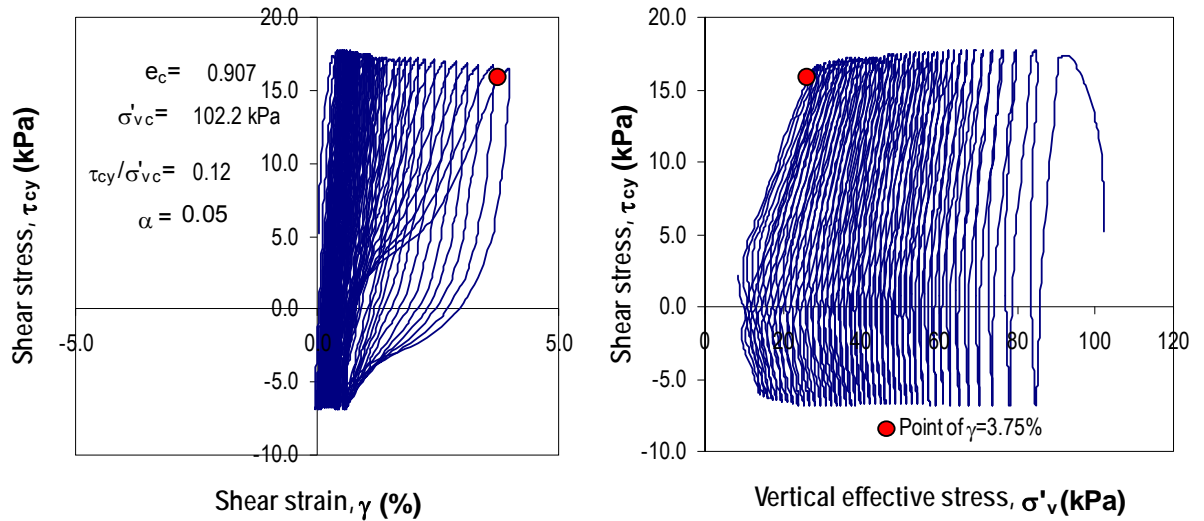


Figure 4.24 Constant volume cyclic simple shear DSS test on undisturbed specimen of normally consolidated Fraser River Delta silt: Stress strain and stress path curves; $\sigma'_{vc} = 100$ kPa; CSR = 0.15; $\alpha=0.05$.

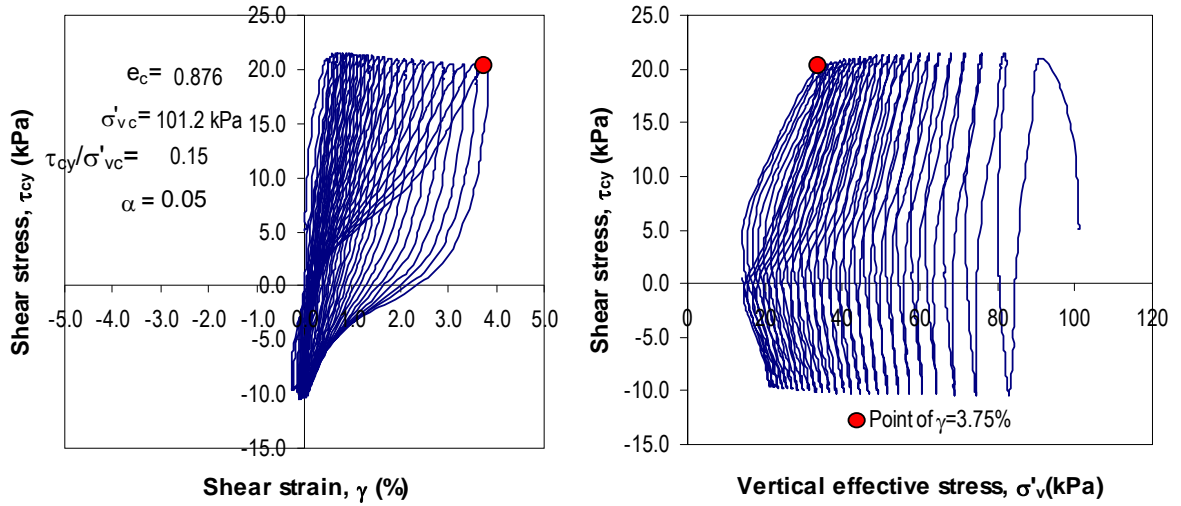


Figure 4.25 Constant volume cyclic simple shear DSS test on undisturbed specimen of normally consolidated Fraser River Delta silt: Stress strain and stress path curves; $\sigma'_{vc} = 100$ kPa; CSR = 0.19; $\alpha=0.05$.

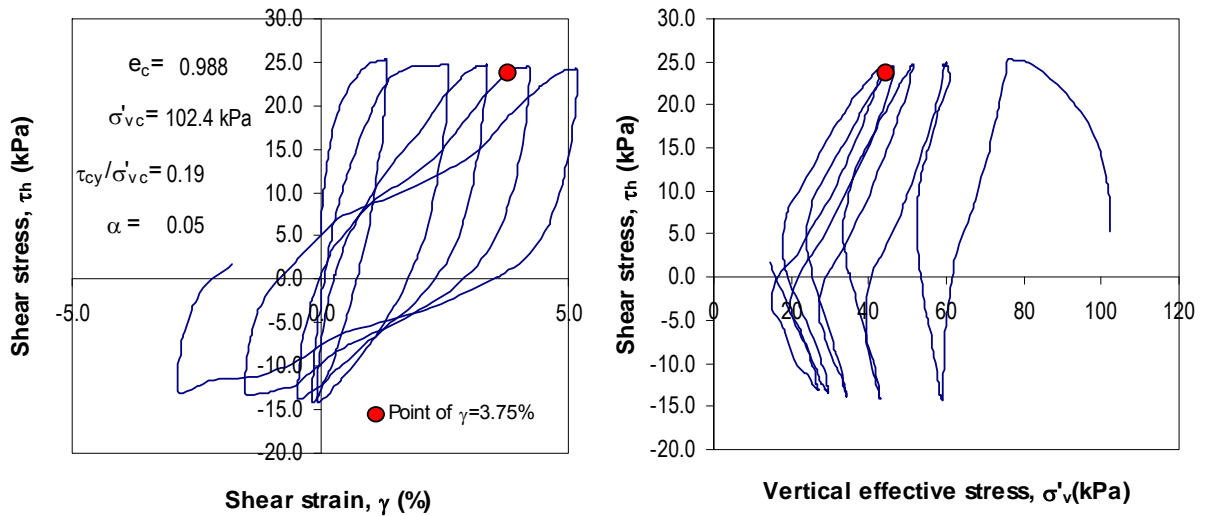


Figure 4.26 Constant volume cyclic simple shear DSS test on undisturbed specimen of normally consolidated Fraser River Delta silt: Stress strain and stress path curves;
 $\sigma'_{vc} = 100 \text{ kPa}$; $\text{CSR} = 0.21$; $\alpha = 0.05$.

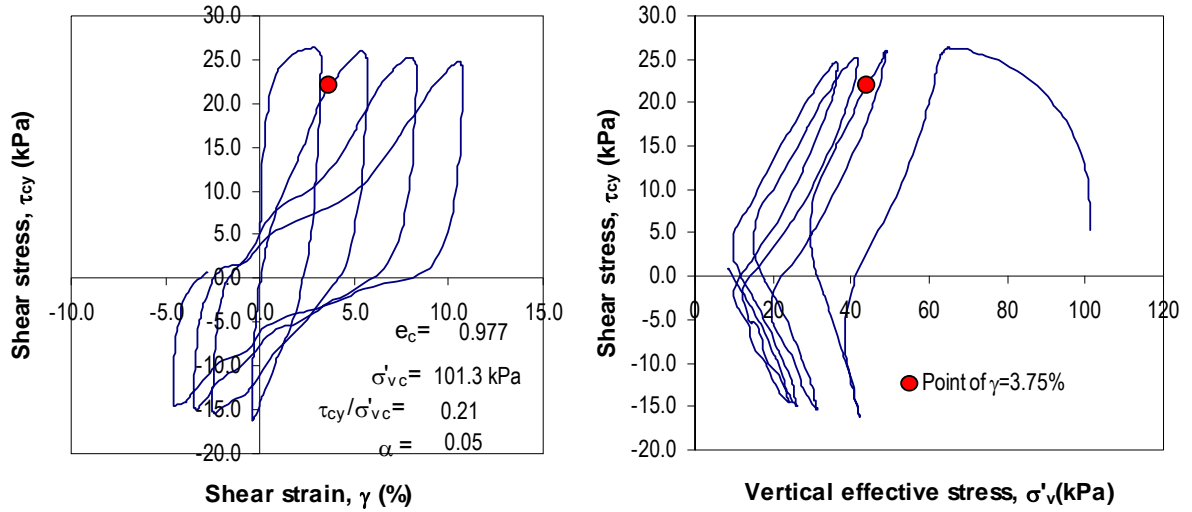


Figure 4.27 Constant volume cyclic simple shear DSS test on undisturbed specimen of normally consolidated Fraser River Delta silt: Stress strain and stress path curves;
 $\sigma'_{vc} = 100 \text{ kPa}$; $\text{CSR} = 0.09$; $\alpha = 0.10$.

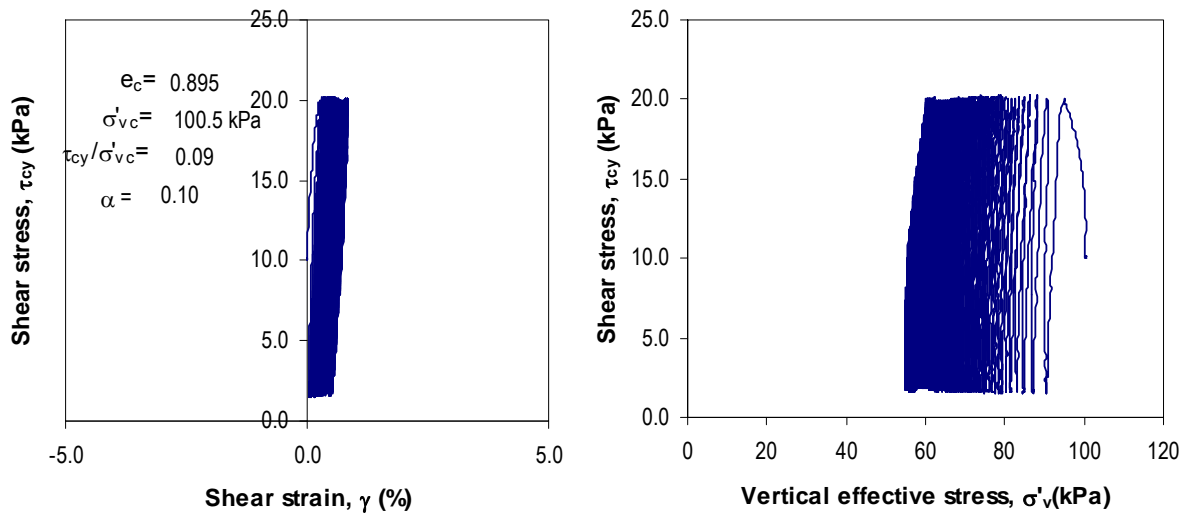


Figure 4.28 Constant volume cyclic simple shear DSS test on undisturbed specimen of normally consolidated Fraser River Delta silt: Stress strain and stress path curves;
 $\sigma'_{vc} = 100 \text{ kPa}$; $\text{CSR} = 0.13$; $\alpha = 0.10$

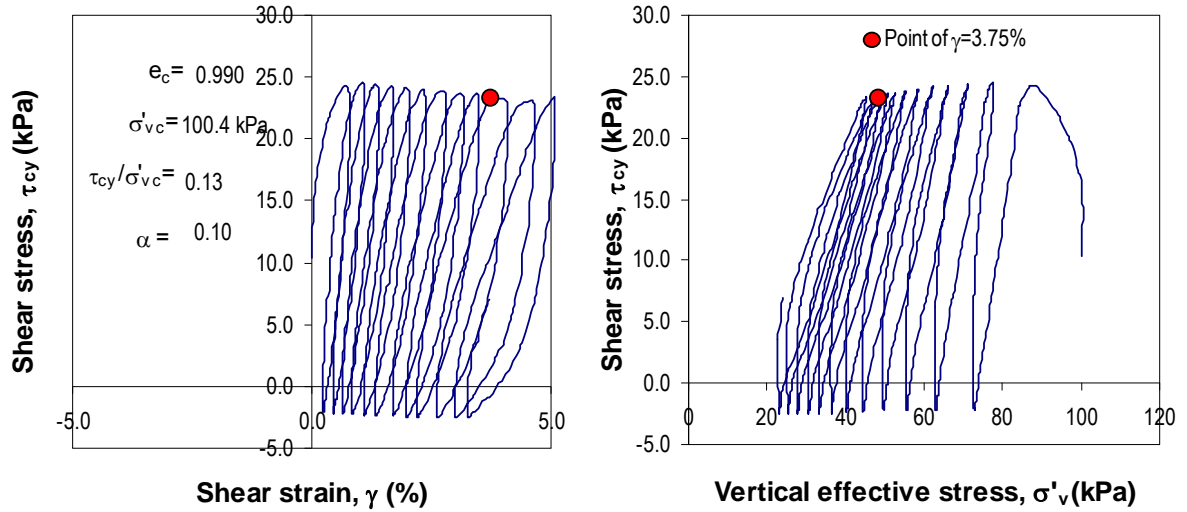


Figure 4.29 Constant volume cyclic simple shear DSS test on undisturbed specimen of normally consolidated Fraser River Delta silt: Stress strain and stress path curves;
 $\sigma'_{vc} = 100 \text{ kPa}$; $\text{CSR} = 0.12$; $\alpha = 0.10$.

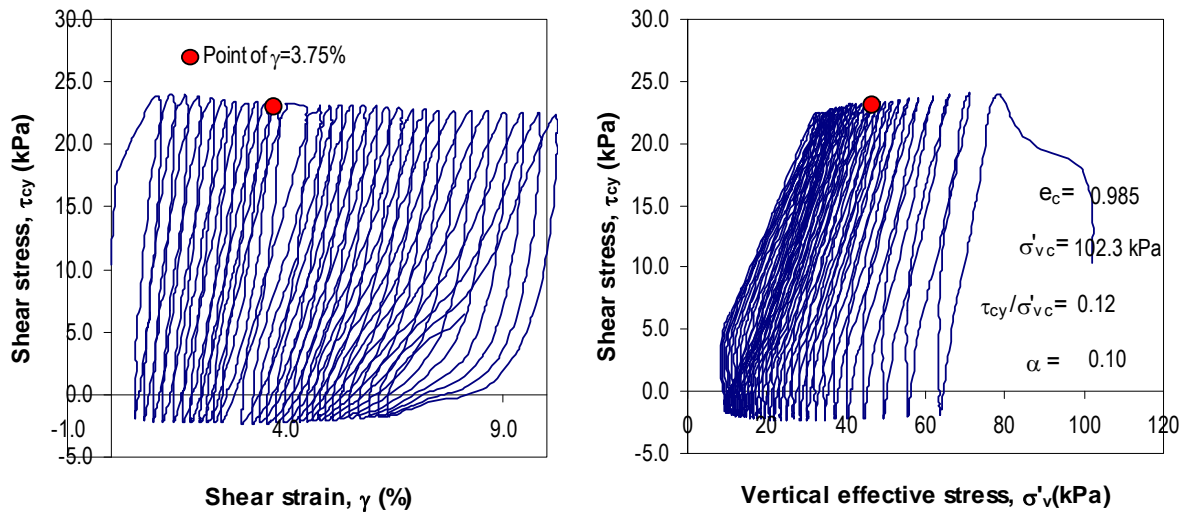


Figure 4.30 Constant volume cyclic simple shear DSS test on undisturbed specimen of normally consolidated Fraser River Delta silt: Stress strain and stress path curves; $\sigma'_{vc} = 100$ kPa; CSR = 0.17; $\alpha=0.10$.

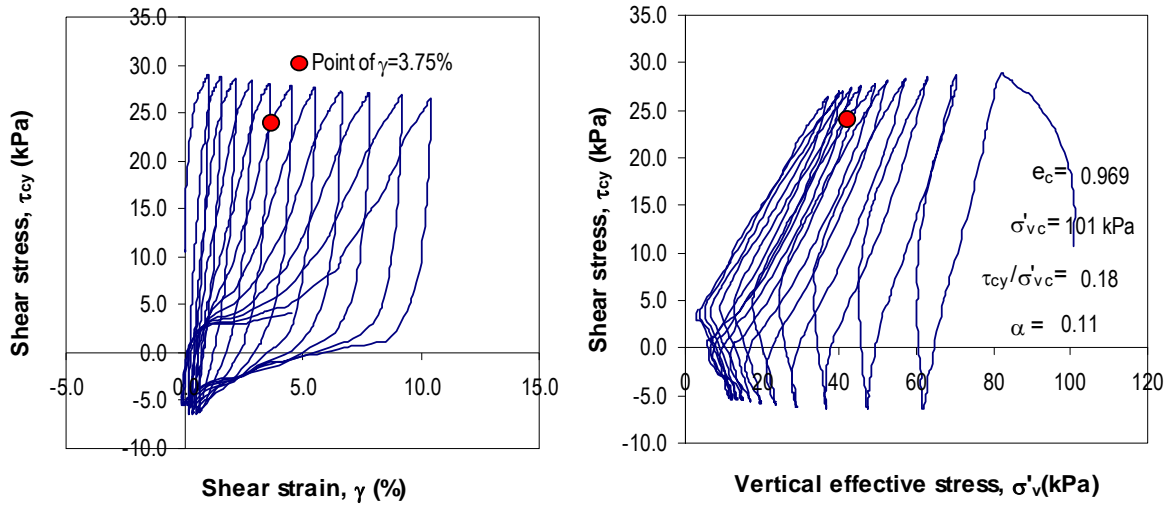


Figure 4.31 Constant volume cyclic simple shear DSS test on undisturbed specimen of normally consolidated Fraser River Delta silt: Stress strain and stress path curves; $\sigma'_{vc} = 100$ kPa; CSR = 0.19; $\alpha=0.10$.

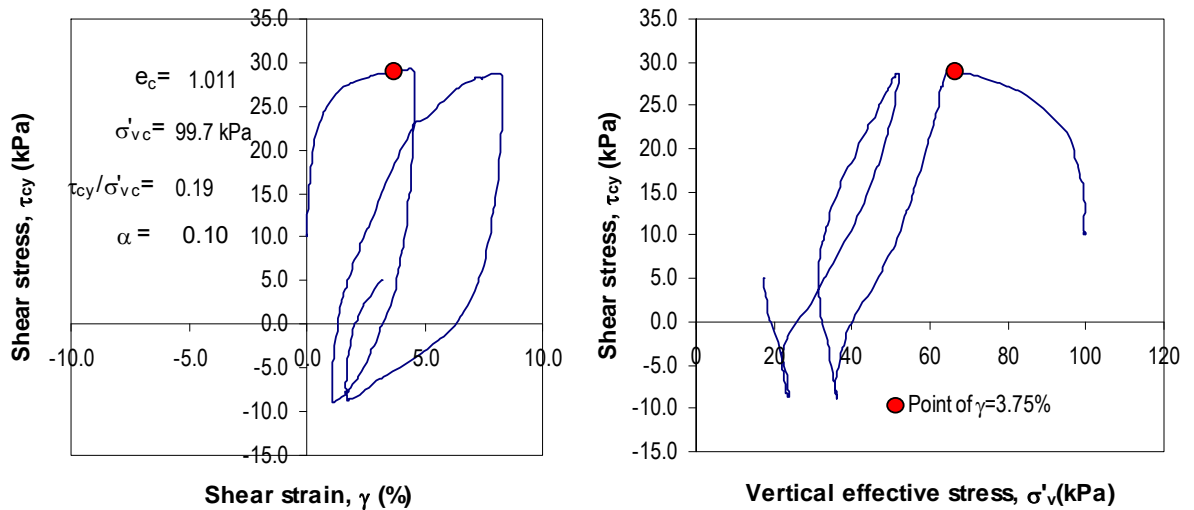


Figure 4.32 Constant volume cyclic simple shear DSS test on undisturbed specimen of normally consolidated Fraser River Delta silt: Stress strain and stress path curves; $\sigma'_{vc} = 100$ kPa; CSR = 0.20; $\alpha = 0.10$.

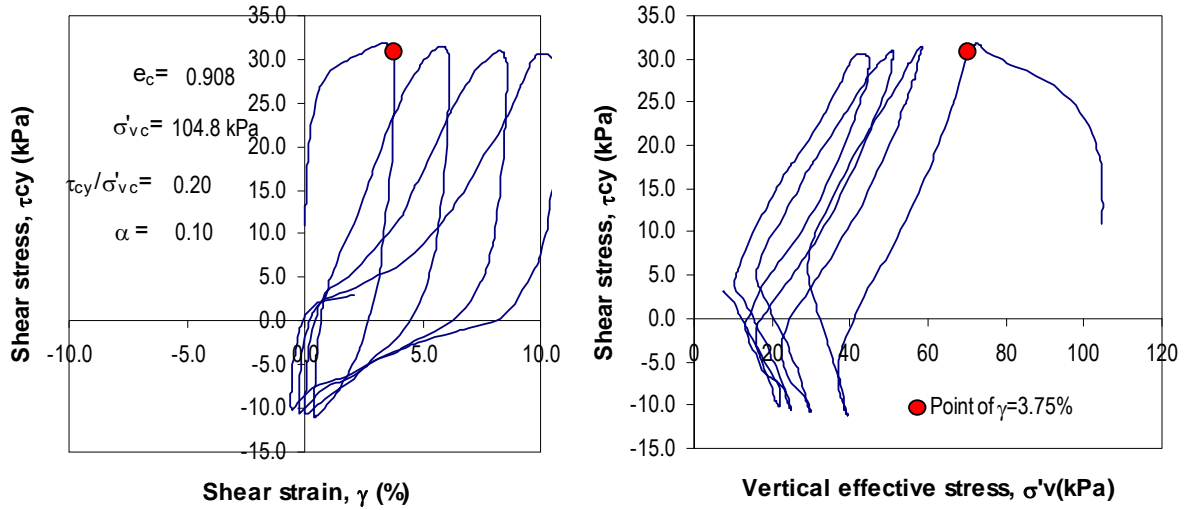


Figure 4.33 Constant volume cyclic simple shear DSS test on undisturbed specimen of normally consolidated Fraser River Delta silt: Stress strain and stress path curves; $\sigma'_{vc} = 100$ kPa; CSR = 0.12; $\alpha = 0.15$.

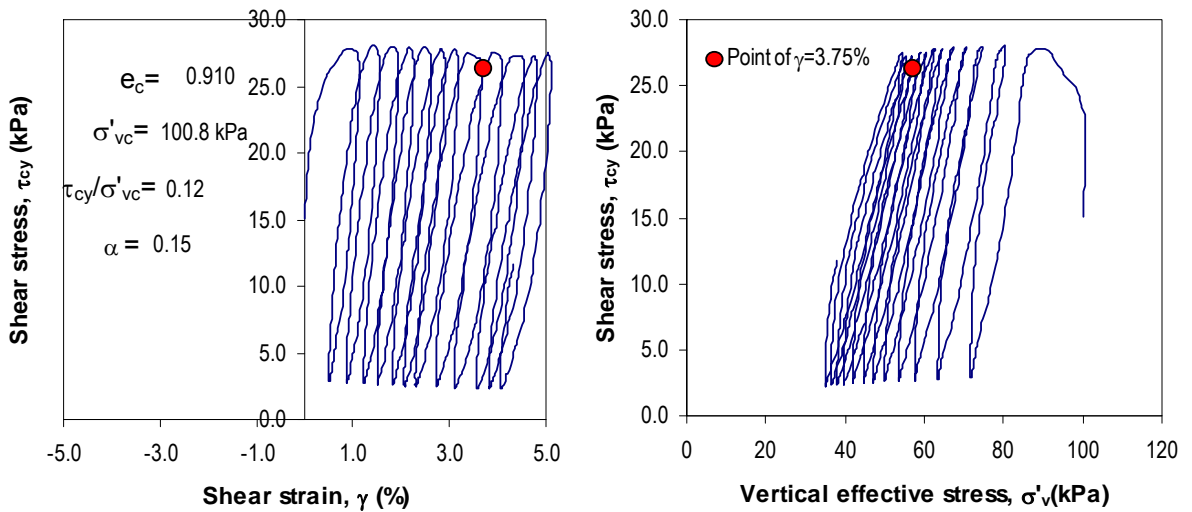


Figure 4.34 Constant volume cyclic simple shear DSS test on undisturbed specimen of normally consolidated Fraser River Delta silt: Stress strain and stress path curves; $\sigma'_{vc} = 100$ kPa; CSR = 0.15; $\alpha = 0.15$.

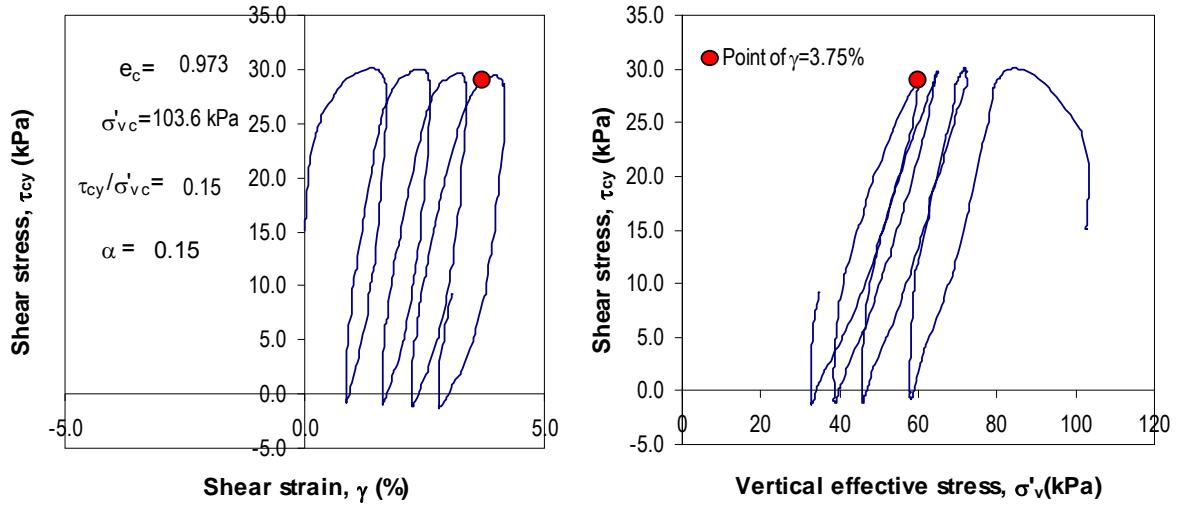


Figure 4.35 Constant volume cyclic simple shear DSS test on undisturbed specimen of normally consolidated Fraser River Delta silt: Stress strain and stress path curves; $\sigma'_{vc} = 100$ kPa; CSR = 0.19; $\alpha = 0.15$.

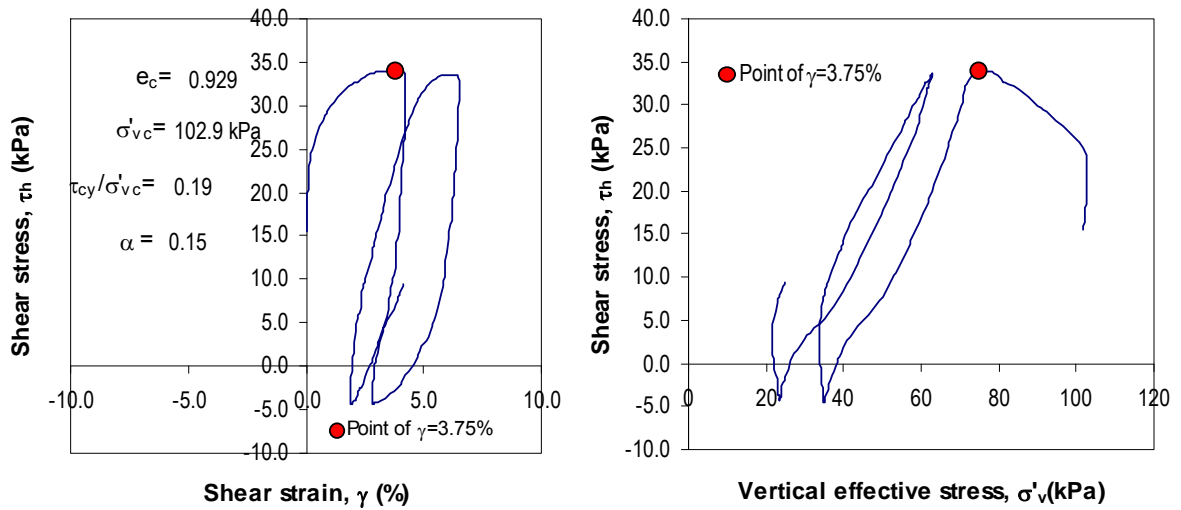


Figure 4.36 Constant volume cyclic simple shear DSS test on undisturbed specimen of normally consolidated Fraser River Delta silt: Stress strain and stress path curves; $\sigma'_{vc} = 100$ kPa; CSR = 0.16; $\alpha=0.15$.

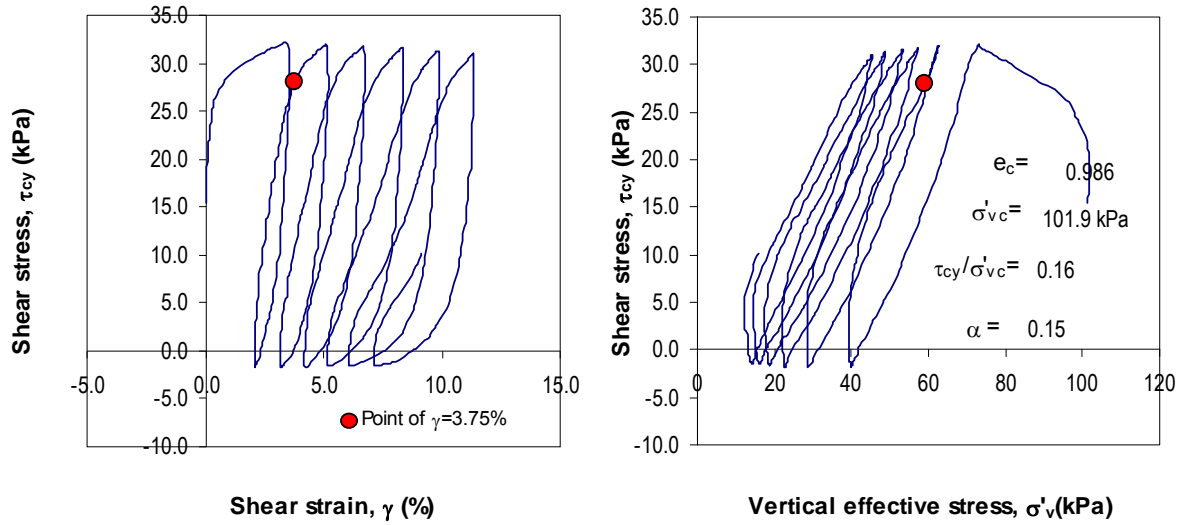
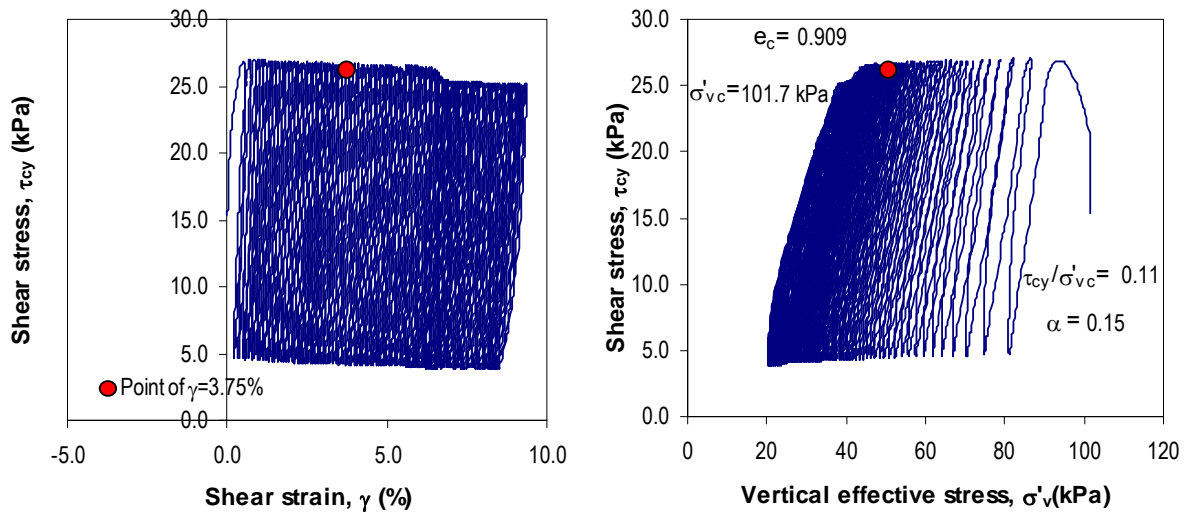


Figure 4.37 Constant volume cyclic simple shear DSS test on undisturbed specimen of normally consolidated Fraser River Delta silt: Stress strain and stress path curves; $\sigma'_{vc} = 100$ kPa; CSR = 0.11; $\alpha=0.15$.



As may be noted, cyclic mobility type strain development was observed in all of the tests throughout the cyclic loading process. Again, liquefaction in the form of strain softening accompanied by loss of shear strength did not manifest itself regardless of the α value and applied CSR level, or the degree of excess pore water pressure developed. In other words, the observed behaviour suggests that the tested silts are unlikely to experience flow failure under undrained cyclic loading, including those specimens subjected to an initial static shear stress bias up to 0.15. However, the build-up of equivalent excess pore water pressure with the increasing number of cycles could result in significant cyclic shear strains even at moderate levels of cyclic loading. As may be noted from the Figures 4.23 to 4.37 (of Test series IIb, IIc and IId), the potential for build-up of excess pore water pressure and the accumulated shear strains seem to increase with increasing initial static shear stress bias level.

The excess pore water pressures ratios ($r_u = \Delta u / \sigma'_{vc}$) developed during cyclic loading are further examined in Figure 4.38 and 4.39 for two selected CSR values, where r_u versus number of load cycles from cyclic shear tests involving three distinct values of α are compared. The results indicate that there is a marked increase of the rate of development excess pore water pressure r_u (with respect to the applied number of CSR cycles) with increasing α level.

Figure 4.38 Constant volume cyclic simple shear DSS test on undisturbed specimen of normally consolidated Fraser River Delta silt: Pore water pressure development at different initial static shear values and constant CSR = 0.15.

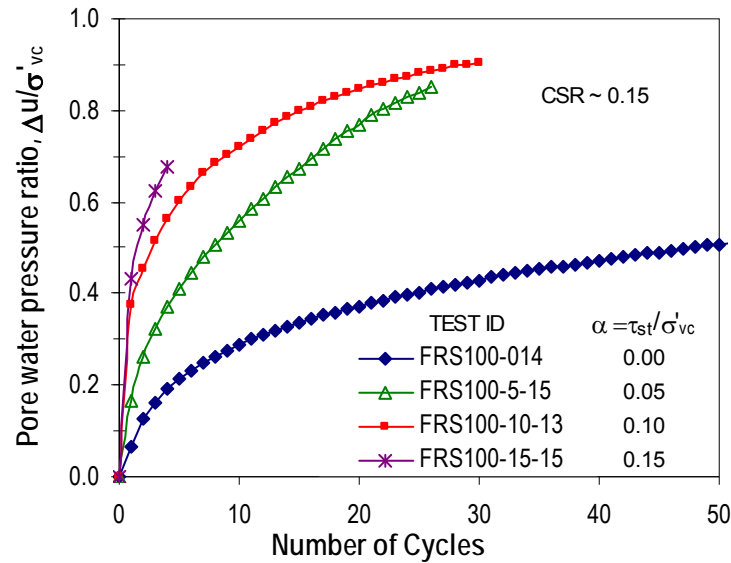
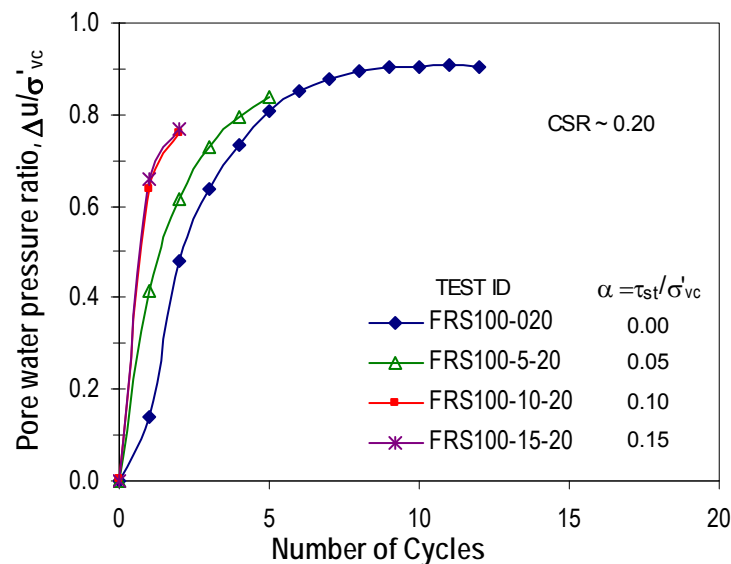


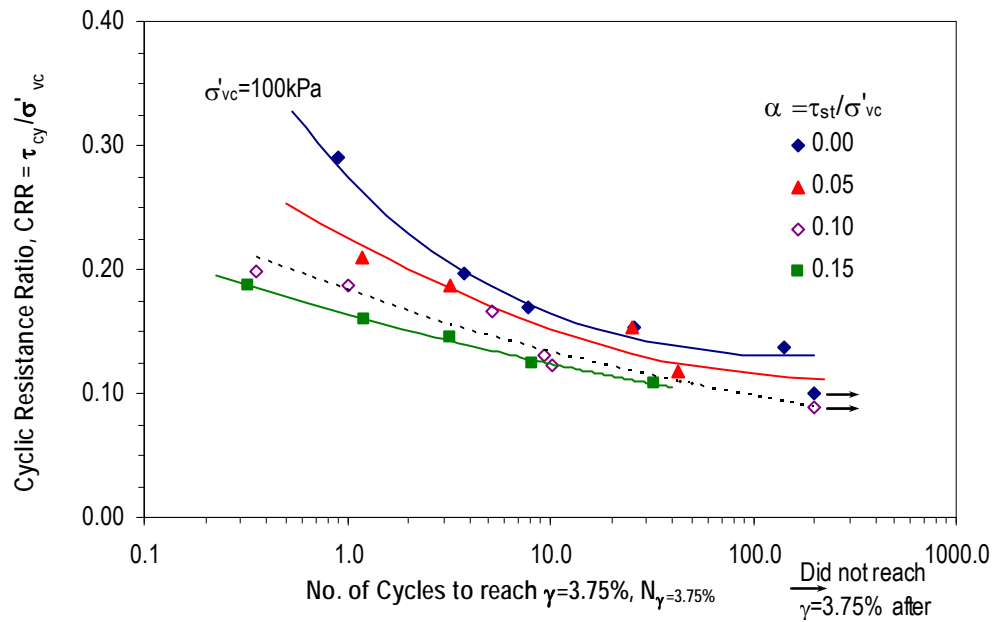
Figure 4.39 Constant volume cyclic simple shear DSS test on undisturbed specimen of normally consolidated Fraser River Delta silt: Pore water pressure development at different initial static shear values and constant CSR = 0.20.



4.2.2.2 Cyclic shear resistance

The number of load cycles ($N_{\gamma=3.75\%}$) required to reach a single-amplitude horizontal shear strain $\gamma = 3.75\%$ under a given applied CSR was plotted in Figure 4.40 to examine the effect of α on cyclic shear resistance. While appreciating that allowance should be made for the expected variability in field samples of soil and experimental scatter, the CRR versus $N_{\gamma=3.75\%}$ relationship for each value of α can be represented by trend-lines as shown in Figure 4.40. Comparison of these trend-lines reveals that the CRR of the tested material would generally decrease with increasing initial static shear stress level.

Figure 4.40 Cyclic resistance ratio from constant volume cyclic DSS tests on undisturbed specimens of normally consolidated Fraser River Delta silt at varying initial static shear bias.



4.2.3 Effects of overconsolidation

4.2.3.1 General stress strain pore water pressure response

Figures 4.41 and 4.42 present the typical stress path and stress-strain relationships obtained for constant volume cyclic tests on laboratory overconsolidated (OC) specimens of silt reproduced from Sanin (2005). The tests were conducted with a cyclic stress ratio (CSR) amplitude of 0.21, commencing from a vertical effective consolidation stress of $\sigma'_{vc} \sim 100$ kPa (Test Series Ic – Table 4.1). Because of the essentially identical σ'_{vc} and CSR, the results can also be directly compared with those from shown in Figure 4.9 for normally consolidated Fraser River silt (undisturbed specimens).

Figure 4.41 Constant volume cyclic simple shear DSS test on undisturbed specimen of overconsolidated Fraser River Delta silt: Stress strain and stress path curves; $\sigma'_{vc} = 100$ kPa; CSR = 0.21; OCR=1.3.

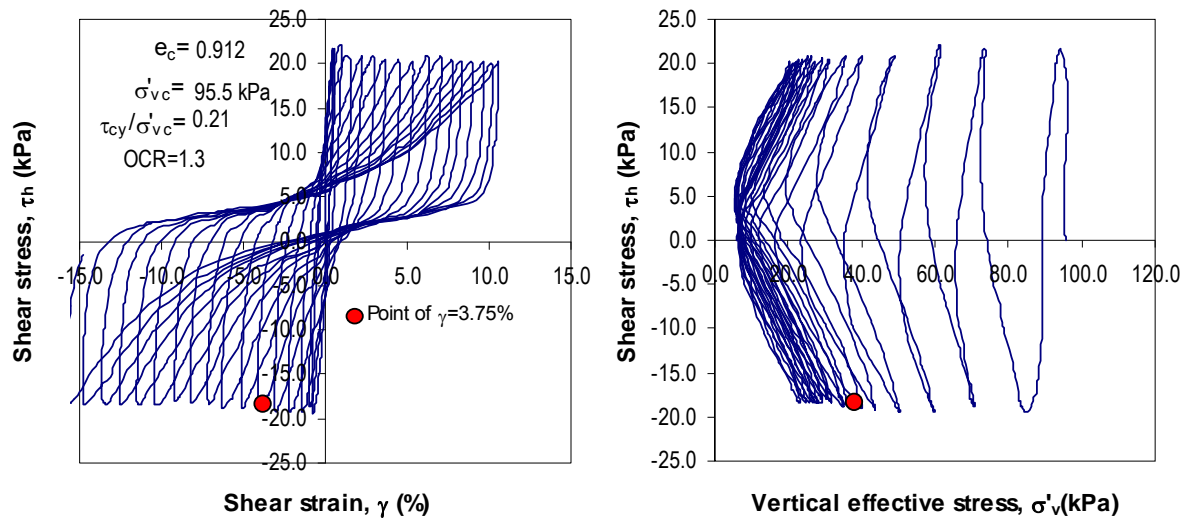
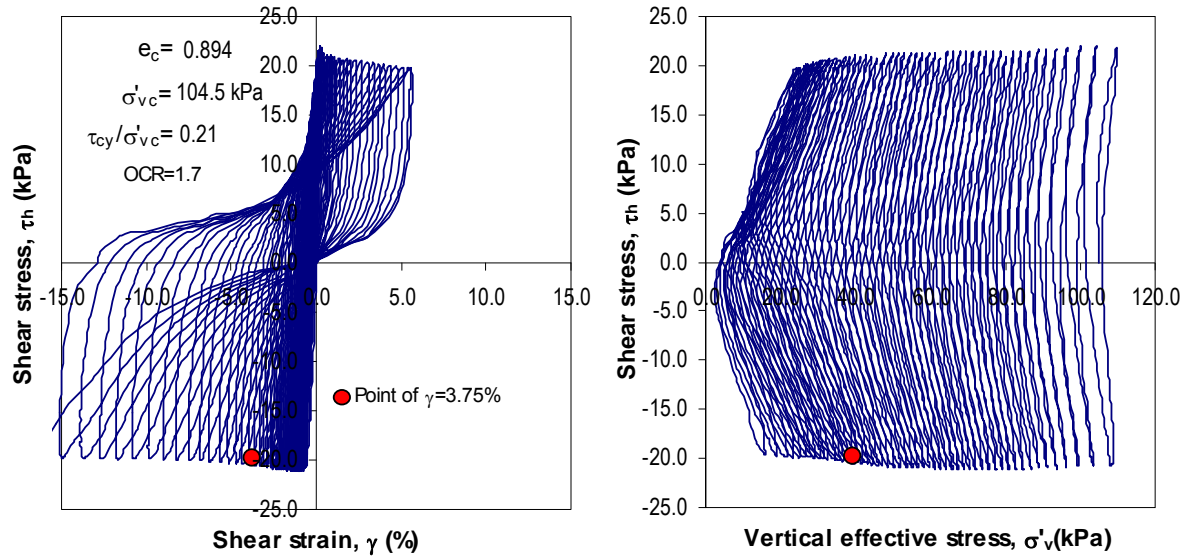


Figure 4.42 Constant volume cyclic simple shear DSS test on undisturbed specimen of overconsolidated Fraser River Delta silt: Stress strain and stress path curves; $\sigma'_{vc} = 100$ kPa; CSR = 0.21; OCR=1.7



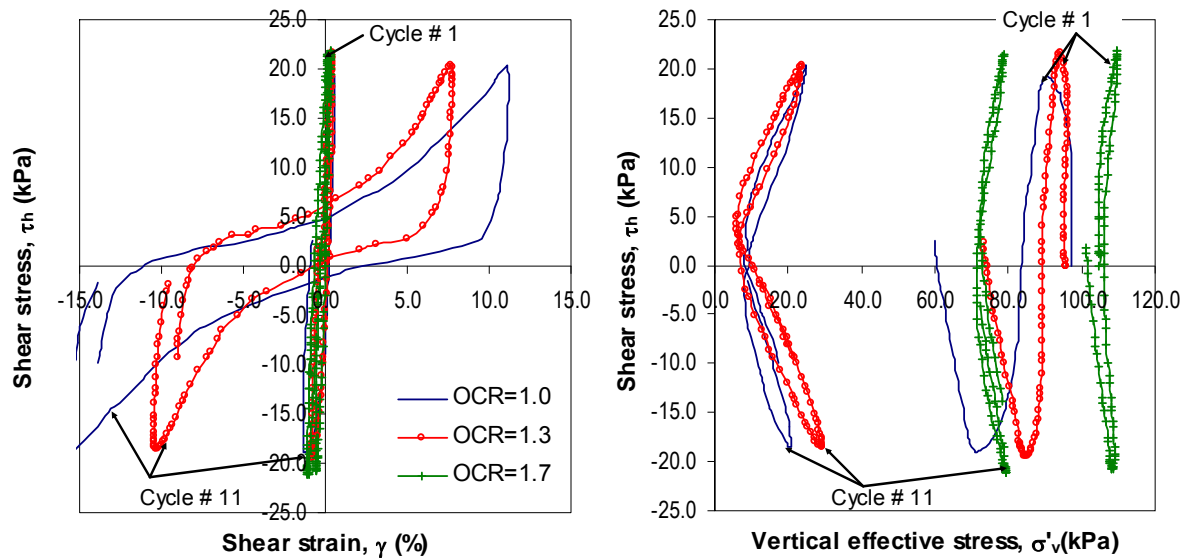
In spite of the overconsolidation effect, the gradual development of equivalent excess pore water pressure with increasing number of cycles along with degradation of shear stiffness is still prevalent. As such, significant permanent cyclic shear strains are still a possibility if the OC silt is subjected to sufficient number of load cycles applied under elevated stress levels. For example, a specimen with an OCR ~ 1.8 when subjected to CSR ~ 0.3 reached $\gamma = 3.75\%$ shear strain criteria in about 7 cycles of loading (Sanin, 2005).

In a general sense, the mechanism of strain development for the tests conducted on OC specimens is via cyclic mobility and, again, similar in form to those observed for the counterpart tests that were conducted on normally consolidated specimens. However, in contrast to the response of the normally consolidated specimen in Figure 4.9 that showed a completely contractive response during both loading and unloading parts of the 1st cycle of

loading, the OC specimens seem to manifest phase transformation from contractive to dilative almost in the first loading cycle itself.

Figure 4.43 presents the comparison of the first and eleventh loading cycles for specimens of Fraser River silt tested at different OCR values. Clearly, the specimens with $OCR > 1.0$ exhibited phase transformation from contractive to dilative behaviour in the first loading cycle. Also, the overconsolidated specimens, for the same number of cycles, developed less shear strain and pore water pressure.

Figure 4.43. Comparison of constant volume cyclic simple shear DSS test on specimens of Fraser River Delta silt at different overconsolidation ratios. First and eleventh loading cycles: Stress strain and stress path curves; $\sigma'_{vc} = 100$ kPa; $CSR = 0.21$.

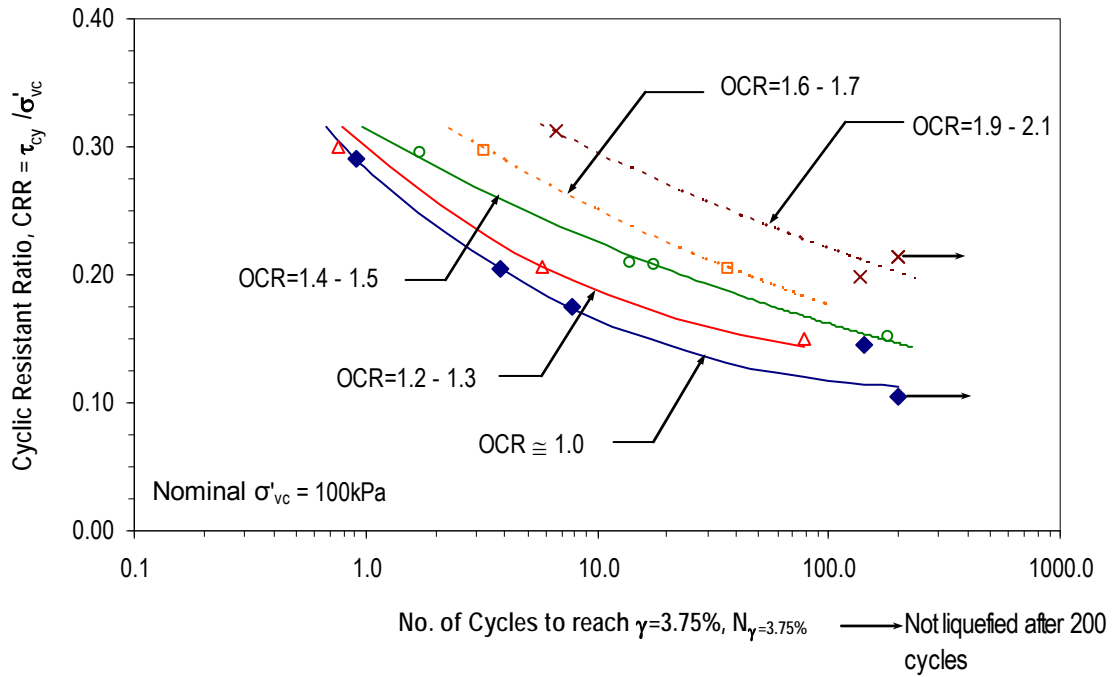


4.2.3.2 Cyclic shear resistance

The variation of CRR versus $N_{\gamma=3.75\%}$ obtained using the results from the tests on overconsolidated Fraser River silt is depicted in Figure 4.44. The graphs clearly show that the CRR generally increases with increasing level of overconsolidation. This effect only becomes

noticeable when the material is overconsolidated to a level above $OCR \sim 1.3$. Similar findings have been reported by Andersen (2009) after analyzing data from different types of soils that included clays, silts and sands.

Figure 4.44 Cyclic resistance ratio from constant volume cyclic DSS tests on undisturbed specimens of Fraser River Delta silt at varying overconsolidation ratios.



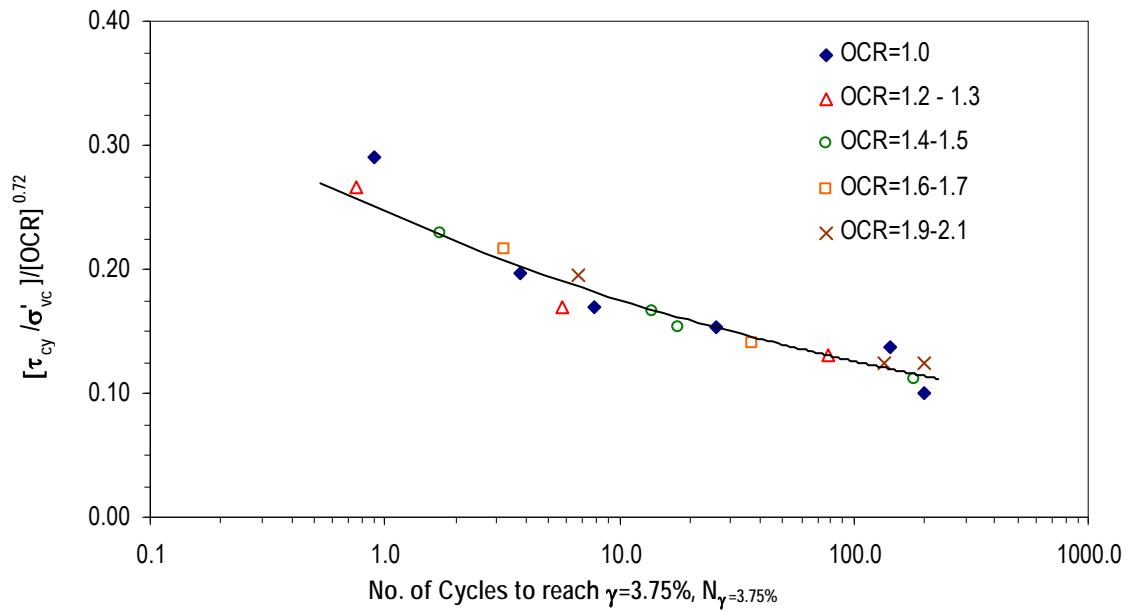
As shown in Figure 4.21, the cyclic resistance ratio of Fraser River Delta silt seems to be independent from the initial confining stress in the virgin compression range (for σ'_{vc} greater than the in situ vertical effective stress). The data from the overconsolidated tests on Fraser River silt can also be represented by a relatively unique curve in the form of:

$$CRR = \left[\tau_{cy} / \sigma'_{vc} \right] / [OCR]^{0.72}$$

Equation. 2

as shown in Figure 4.45. The uniqueness of the curve in the recompression range has also been observed in sands [Terzaghi et al. (page 201) 1996; Mesri 2009 personal communication].

Figure 4.45 Cyclic resistance ratio from constant volume cyclic DSS tests on undisturbed specimens of Fraser River Delta: Effect of overconsolidation ratio.



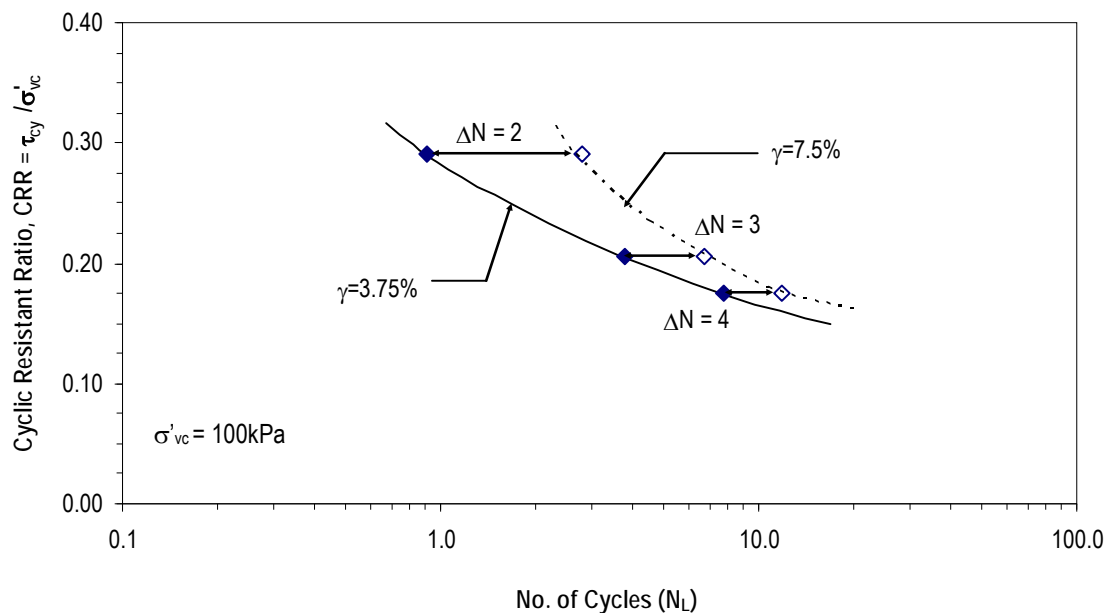
4.3 Other considerations and discussion

4.3.1 Sensitivity of cyclic shear resistance to strain criteria

In order to assess the sensitivity to the strain criterion, the CRR values for the Test Series I(b) were determined considering an alternate strain criterion of $\gamma = 7.5\%$, and these alternate CRR values are compared in Figure 4.46 with the counterpart values obtained using $\gamma = 3.75\%$. In Figure 4.46, based on the observed cyclic stress strain response, the additional number of load cycles required to increase γ from 3.75% to 7.5% for a given test has been denoted by ΔN . As

may be noted, at higher cyclic stress ratio levels, only a small number of additional load cycles ($\Delta N = 2$) are required to cause this doubling of shear strain amplitude. The required ΔN appears to increase with reducing shaking intensity. Clearly, the data presented demonstrate the potential disadvantages in the definition of cyclic shear resistance using a specific strain criterion. In earthquake engineering problems, deformations during seismic loading mostly govern the design, for example, the determination of required remedial ground improvements. The above observations suggest that, if laboratory testing is undertaken to characterize earthquake response, the strain criterion used in the definition of CRR should be carefully reviewed to ensure that it is commensurate with the acceptable strain levels with respect to the specific problem under study.

Figure 4.46 Cyclic resistance ratio from constant volume cyclic DSS tests on undisturbed specimens of Fraser River Delta: Effect of overconsolidation ratio.



4.3.2 Comparison with cyclic shear response of sand

It is useful to make a comparison between the stress-strain and excess pore water pressure response observed for Fraser River silt and those observed from tests on sands. Previous observations by Wijewickreme et al. (2005b) and Sriskandakumar (2004) on the behaviour of Fraser River sand (originating from the same Fraser River deltaic deposit as the tested silt) using the UBC DSS device provides an opportunity make this comparison. This work has shown that relatively loose Fraser River sand ($D_{rc} = 40\%$, $e_c = 0.812$; $\sigma'_{vc} \sim 100$ kPa) under constant volume cyclic shear loading could experience change in shear stiffness from stiff to very soft in an abrupt manner over the duration of one load cycle - this abrupt loss of shear stiffness is clearly in accord with the idea of liquefaction “triggering” as noted previously during other research work on sands (Castro 1975; Ishihara et al. 1975; Vaid and Chern 1985). On the other hand, when the same Fraser River sand was tested under dense conditions ($D_{rc} = 80\%$, $e_c = 0.685$; $\sigma'_{vc} \sim 100$ kPa), it has been observed that the material would exhibit gradual excess pore water pressure development with progressive degradation of shear stiffness with increasing cyclic loading (Sriskandakumar 2004). As noted in GVLTF (2007), these observations suggest that the shear behaviour Fraser River silt, which exhibited gradual excess pore water pressure development with progressive degradation of shear stiffness in constant volume cyclic shear loading, is more similar to dense sand in behavioural pattern than to relatively loose sand.

4.4 Observations on the cyclic shear response of other fine-grained soils

A limited number of tests were performed on other fine-grained materials such as quartz rock powder and Kitimat clay (Test series IV) to observe the type of response of different fine-grained soils to cyclic shear loading. Kitimat clay is a naturally occurring material of low to medium sensitivity, and it is understood to have been deposited in a marine environment. Herein, quartz rock powder and Kitimat clay were selected to generate some limited, but useful, observations on the behavioural patterns for materials having different characteristics for comparison with the response of Fraser River silt.

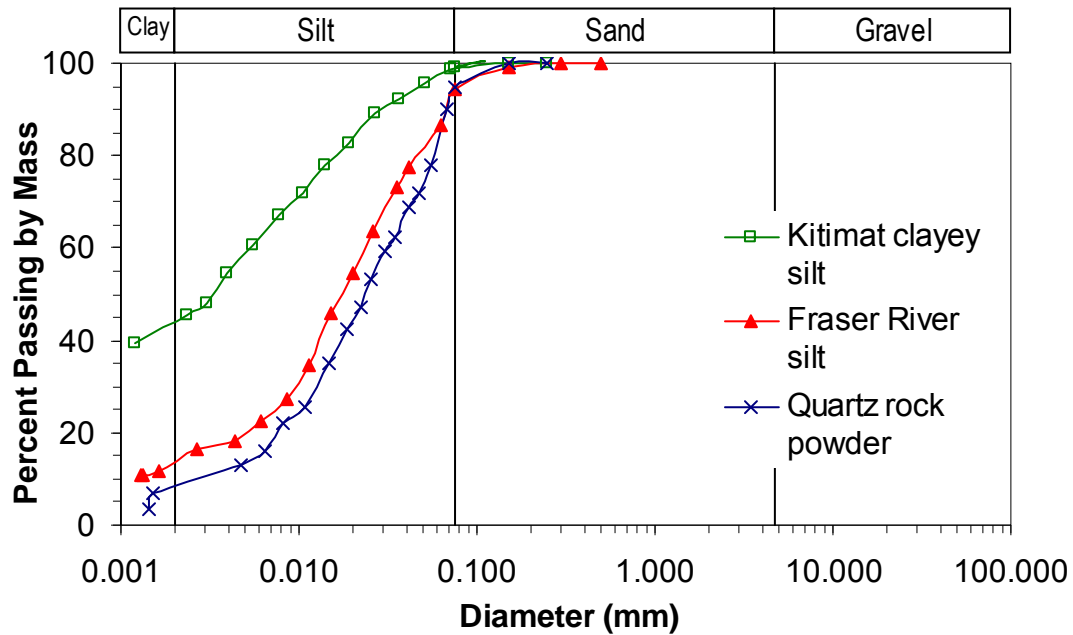
In addition to the tests performed on these two materials, comparisons on the effects of plasticity were made with already available data on other fine-grained soils. Characteristics of the materials used for comparison are shown in Table 4.2. Gradation curves of these two materials compared to the one for Fraser River silt are presented in Figure 4.47.

Table 4.2 Summary of index properties of the materials used for observations of effects of plasticity on the cyclic response of fine-grained materials

	G_s	Sand %	Silt %	Clay %	LL	PI	S_u/σ'_{vc} #	S_u/σ'_{vc} *	Nominal σ'_{vc} (kPa)	e_i (range)	e_c (range)
Quartz rock powder	2.64	5	92	3	-	NP	n.a	n.a	100	1.345	0.79 – 0.80
Kitimat Clay	2.70	1	54	45	37	17	0.31	0.26	80	0.97 – 1.01	0.89 - 0.96
Laterite Tailings	4.10	0	65	35	34	12	n.a.	n.a	100	1.46 – 1.59	1.32 - 1.45
Copper-Gold-Zinc Tailings	3.4 – 4.4	0 - 43	57 – 100	0	19	2	n.a.	n.a	115 – 460	0.59 – 1.72	0.49 - 1.43

n.a.= Not available; # and * = Values of S_u/σ'_{vc} at the peak and 15% shear strain, respectively, from monotonic tests on undisturbed samples

Figure 4.47 Grain size analyses of fine-grained soils analyzed in this study



As described by Wijewickreme et al. (2005a), the copper-gold-zinc tailings were obtained using traditional ore processing methods, and the laterite tailings had been obtained from the processing of limonite ore by a pressure acid leach process. This process involves the solution of nickel and cobalt by sulphuric acid at high temperature and pressure, as described by Chalkley and Toirac (1997). As may be noted from Table 4.2, the plasticity index (PI) of the four materials considered herein span between non-plastic material for the quartz rock powder and $PI = 17$ for the Kitimat clay, in turn, providing reasonable coverage of materials within the region of relatively low plasticity.

4.4.1 Cyclic shear response

Figures 4.48 through 4.50 show the stress-strain and stress path response of natural Kitimat clay subjected to constant volume cyclic direct simple shear at different cyclic stress ratios. All

the specimens show predominantly contractive response during the first quarter to half cycles of loading. In subsequent cyclic loadings, the response gradually changed from contractive to dilative (or experienced phase transformation) during the “loading” (or increasing shear stress) phases. The observed contractive response during “unloading” (or decreasing shear stress) phases suggests significant “plastic deformations” especially after phase transformation. With increasing number of load cycles, the specimens experienced a cumulative increase in excess pore water pressure with associated progressive degradation of shear stiffness. Compared to Fraser River silt, Kitimat clay experienced relatively increased level of degradation of shear stiffness; this is not unexpected since the shearing was conducted at a cyclic stress ratio ($CSR=\tau_{cy}/\sigma'_{vc}$) very close to its monotonic undrained shear strength ratio (S_u/σ'_{vc}) of 0.31. In a given cycle, the shear stiffness experiences its transient minimum when the applied shear stress is close to zero. The observed cyclic mobility type stress-strain response is similar to the undrained (constant volume) cyclic shear responses previously observed from triaxial tests on natural clayey soils (e.g., Zergoun and Vaid 1994).

Figure 4.48 Constant volume cyclic simple shear DSS test on undisturbed specimen of natural Kitimat clay: Stress strain and stress path curves; $\sigma'_{vc} = 80$ kPa; $CSR = 0.24$.

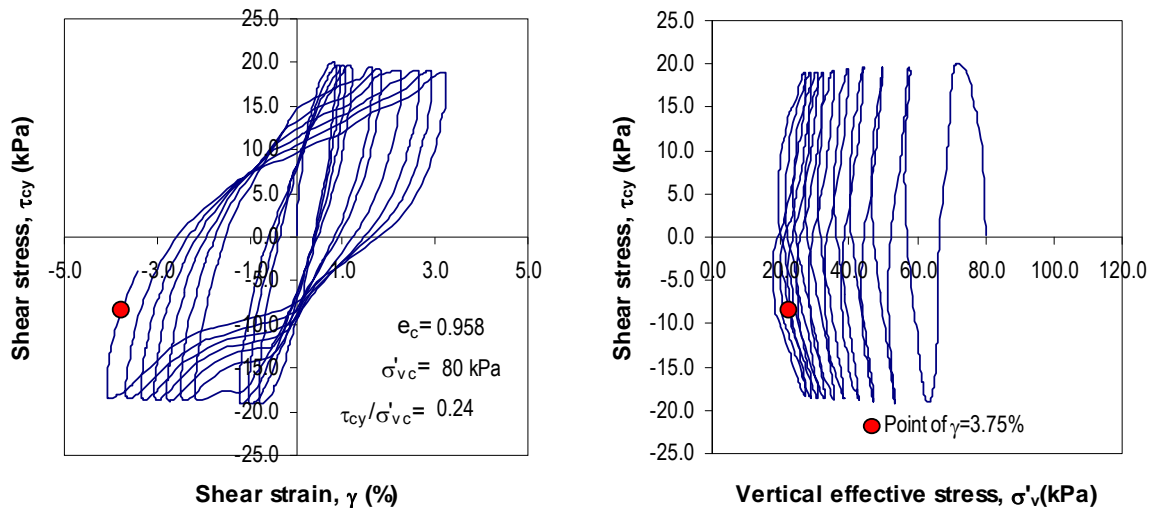


Figure 4.49 Constant volume cyclic simple shear DSS test on undisturbed specimen of natural Kitimat clay: Stress strain and stress path curves; $\sigma'_{vc} = 80$ kPa; CSR = 0.26.

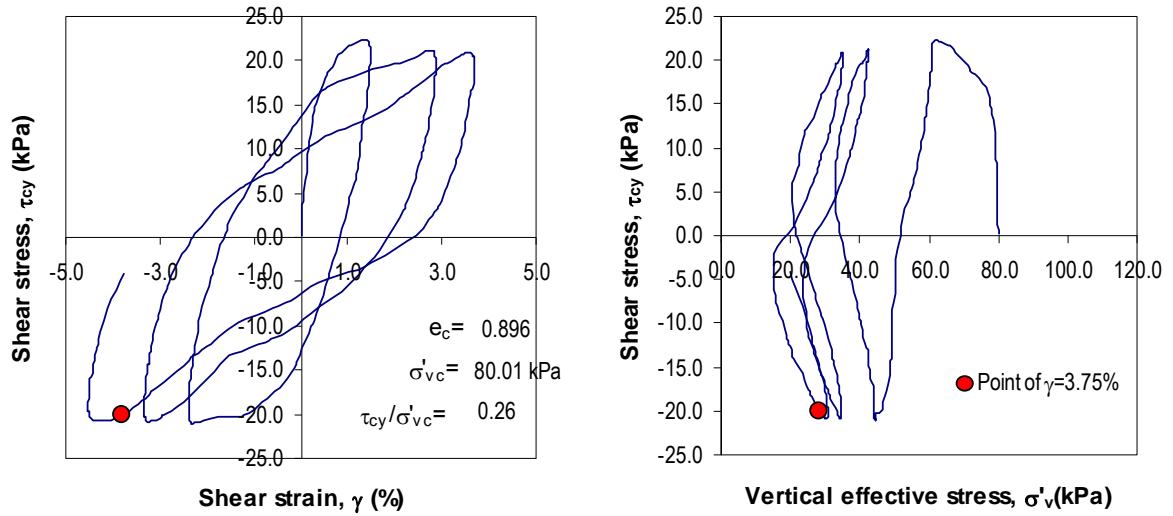
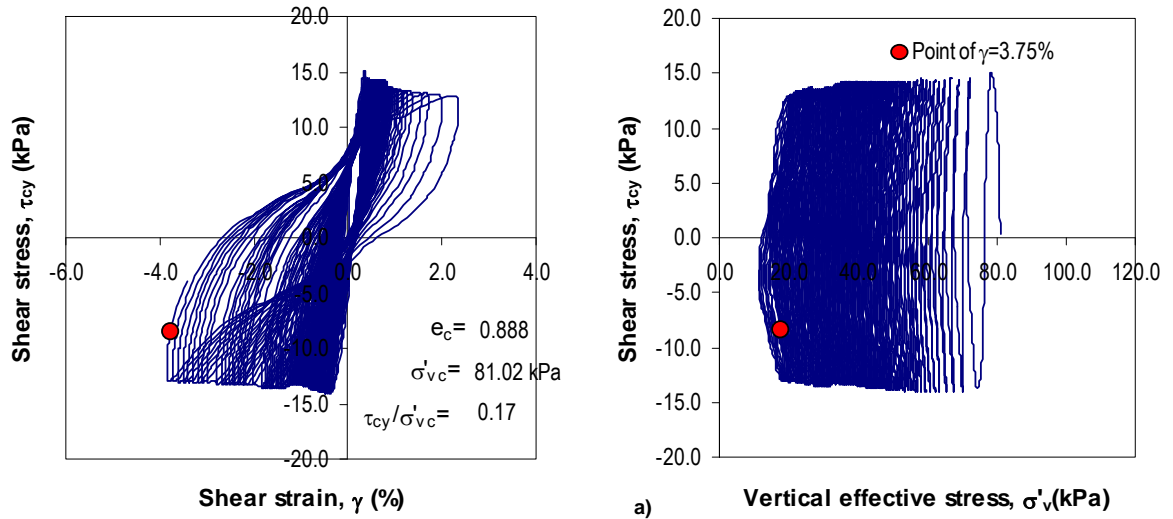


Figure 4.50 Constant volume cyclic simple shear DSS test on undisturbed specimen of natural Kitimat clay: Stress strain and stress path curves; $\sigma'_{vc} = 80$ kPa; CSR = 0.17.



Figures 4.51 through 4.53 show the response of quartz rock powder at different CSR values. Again, a cyclic mobility type response was observed; it is also of interest to note that there is a trend of relatively more abrupt degradation of cyclic shear stiffness, with increasing number of

load cycles, observed for this NC reconstituted quartz powder (with $PI \sim 0$) compared to that of NC undisturbed Fraser River silt under similar CSR amplitudes.

Figure 4.51 Constant volume cyclic simple shear DSS test on specimen of quartz rock powder: Stress strain and stress path curves; $\sigma'_{vc} = 100$ kPa; $CSR = 0.09$.

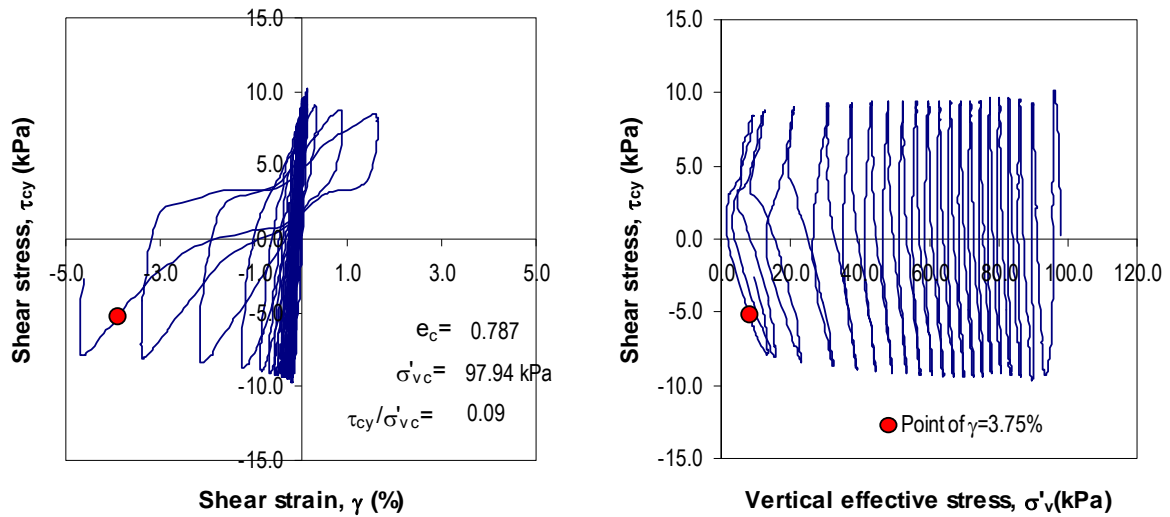


Figure 4.52 Constant volume cyclic simple shear DSS test on specimen of quartz rock powder: Stress strain and stress path curves; $\sigma'_{vc} = 100$ kPa; $CSR = 0.12$.

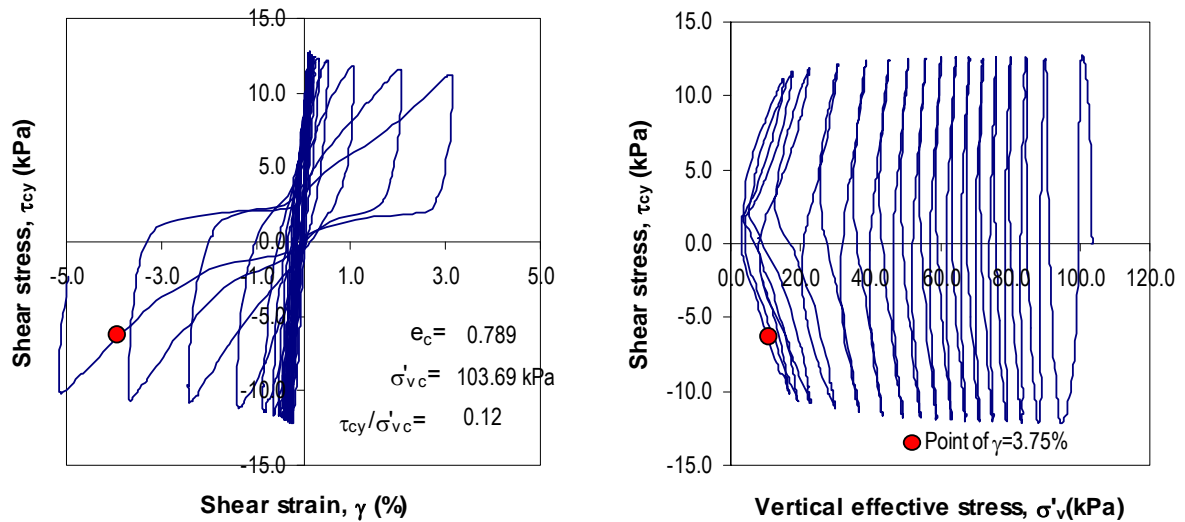
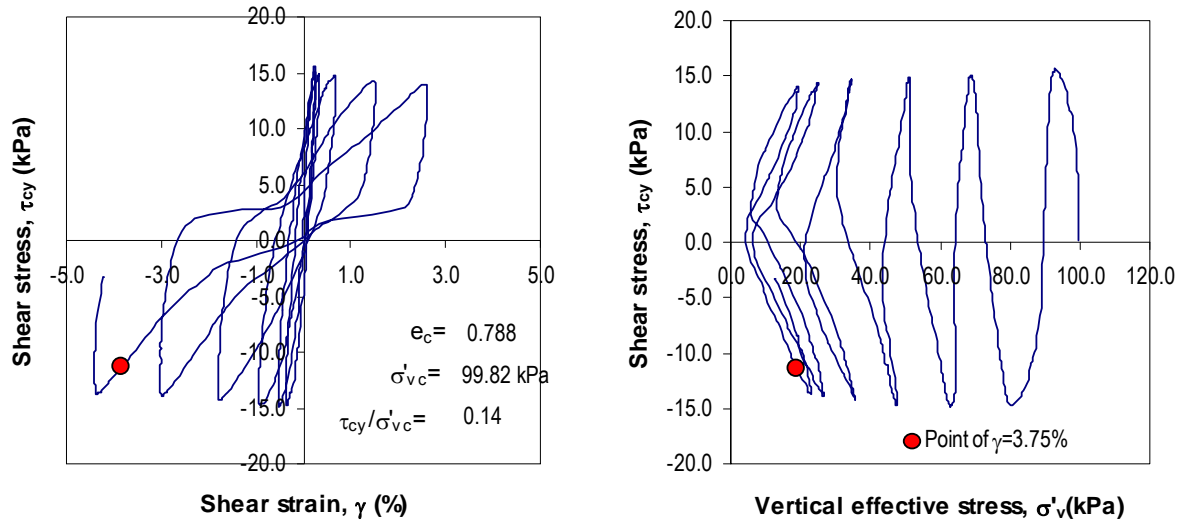


Figure 4.53 Constant volume cyclic simple shear DSS test on specimen of quartz rock powder: Stress strain and stress path curves; $\sigma'_{vc} = 100$ kPa; CSR = 0.14.

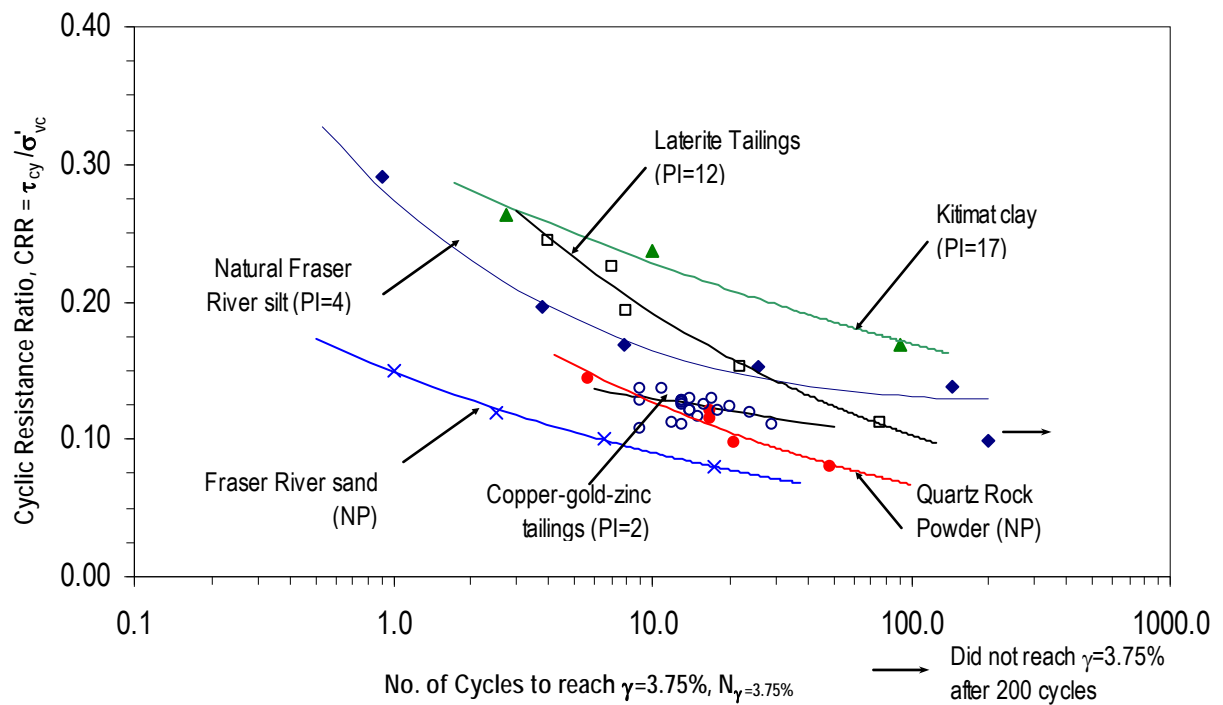


4.4.2 Cyclic shear resistance

The variation of cyclic resistance ratio (CRR) vs. $N_{\gamma=3.75\%}$ related to data from the tests on all the material types considered in this thesis is presented in Figure 4.54. Recognizing that allowance should be made for the expected variability in field samples and experimental scatter, CRR vs. $N_{\gamma=3.75\%}$ relationship for each material can be represented by trend-lines as shown Figure 4.54. Comparison of the trend-lines reveals that the CRR of the materials seem to generally increase with increasing plasticity of the soil. Similar trends have been noted by Guo and Prakash (1999) based on review of cyclic triaxial testing data from a number of sources involving testing of undisturbed as well as re-constituted samples and by Ishihara et al. (1981) based on cyclic triaxial testing on undisturbed fine-grained mine tailings. Andersen (2009) has also observed a similar trend on different clays with a wide range of PI values when tested using direct simple shear and triaxial apparatus. Observation of trends as per Figure

4.54 is significant since the data herein have been derived not only from undisturbed samples, but also using the same direct simple shear device that is judged to simulate field loadings during earthquake shaking.

Figure 4.54 Cyclic resistance ratio from constant volume cyclic DSS tests on undisturbed specimens of fine-grained materials with different plasticity.

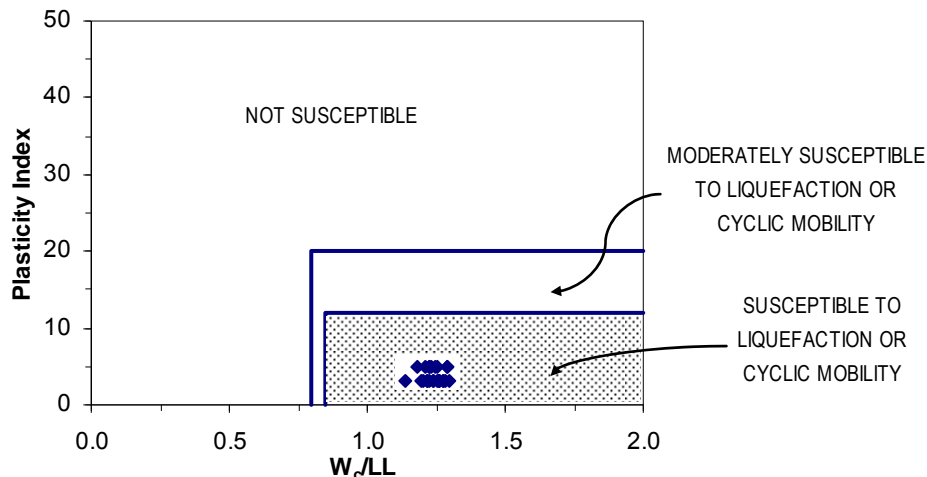


4.5 Comparison of experimental observations with empirical criteria for liquefaction

It is instructive to examine the liquefaction susceptibility of Fraser River silt using some of the commonly used empirical criteria, and compare the findings in relation to the observations from the cyclic DSS testing herein.

The test parameters for Fraser River silt were plotted with respect to Bray et al. (2004) criterion (see Figure 4.55). This criterion, which is based on plasticity index (PI) and (W_c/LL), clearly classify Fraser River silt into the category of susceptible to “liquefaction or cyclic mobility”. This assessment is in conformity with the cyclic mobility observed for Fraser River silt during DSS tests. However, it is important to note that the Bray et al. (2004) criteria do not provide a clear distinction between the “liquefaction associated with strength loss” and “cyclic mobility”.

Figure 4.55 Application to Bray et al (2006) criteria for liquefaction susceptibility to Fraser River Delta silt.



A clear statement of seismic performance becomes a challenge when a material exhibits cyclic mobility, where the level of strain accumulation is directly linked to the applied CSR and the

number of cycles. While empirical criteria are simple and practically attractive as screening tools, the above comparisons demonstrate that the understanding of the shear strain development in cyclic-mobility is fundamental to assessing the performance of the silt under cyclic loading.

Through detailed examination of soil behaviour, Idriss and Boulanger (2008) have suggested that an approximate dividing line between coarse-grained and fine-grained behavioural patterns (from a liquefaction point of view) can be established using soil plasticity index (PI) as a parameter. They have referred to coarse-grained soils as having “sand-like” behaviour, and fine-grained soils as having “clay-like” behaviour and recommended that a PI value of 7 be used as the demarcation between coarse and fine-grained liquefaction response. Bray and Sancio (2006) have also defined criteria to classify the behaviour of fine-grained soils, based primarily on plastic limit, liquid limit and moisture content.

Using the Idriss and Boulanger (2008) approach, the natural Fraser River silt tested herein, with $PI \sim 4$, would be classified as “sand-like” in current practice. As such, it would be of interest to assess the cyclic shear resistance of Fraser River silt using field-based cyclic resistance ratio (CRR) versus penetration resistance charts developed for “sand-like” soils; using available field cone penetration resistance data of $q_c = 1.6$ MPa and $\sigma'_{vc} = 85$ kPa as average field values (see Table 3.1), along with appropriate “silt corrections” applied using this approach, the CRR of Fraser River silt would be estimated as 0.075 (i.e., this implies that liquefaction would “trigger” if the silt was subjected to 15 cycles of loading with $CSR = 0.075$). On the other hand, in the present laboratory study, results from two specimens of NC Fraser River silt (with $\sigma'_{vc} \sim 100$ kPa) subjected to constant CSR cyclic loading indicate

the following: (a) Test No. FRS100-014 with $CSR = 0.14$, experienced $r_u = 35\%$ and single amplitude cyclic shear strain $\gamma_{cyc} = 0.4\%$ in 15 cycles, and $r_u = 45\%$ and $\gamma_{cyc} = 0.45\%$ in 30 cycles (Figure 4.7); (b) Test No. FRS100-010 with $CSR = 0.10$, experienced $r_u = 27\%$ and $\gamma_{cyc} = 0.20\%$ in 15 cycles, and $r_u = 35\%$ and $\gamma_{cyc} = 0.25\%$ in 30 cycles. The above relatively low r_u and γ_{cyc} values observed from tests with $CSR > 0.10$ suggest a laboratory-based CRR value for Fraser River silt that is clearly higher than the $CRR = 0.075$ estimated based on field-based charts assuming “sand-like” behaviour. Idriss and Boulanger (2008) have cautioned that the value of $PI = 7$ suggested as the delineation between sand-like and clay-like behaviour is in fact a transition zone, and the liquefaction assessments may have to be adjusted on a site-specific basis if justified by the results of detailed testing. The current findings from Fraser River silt would serve as an example in this regard, demonstrating how detailed laboratory testing could complement field-based approaches in the assessment of cyclic shear performance of fine-grained low plastic silts.

4.6 Summary and principal findings

Under constant volume cyclic DSS loading, Fraser River silt exhibited cumulative decrease in effective stress with increasing number of load cycles (i.e., cyclic-mobility-type strain development mechanism) regardless of the initial σ'_{vc} , initial static shear stress bias (α), OCR, and applied CSR level. No strain softening and/or loss of shear strength were observed in any of the tests. The cyclic resistance ratio (CRR) of normally consolidated Fraser River silt was not sensitive to the initial σ'_{vc} for the tested stress range of $85 \text{ kPa} < \sigma'_{vc} < 400 \text{ kPa}$. The CRR

of Fraser River silt was noted to increase with increasing overconsolidation ratio (OCR), for $OCR > 1.3$. The test results also indicated that the cyclic resistance would reduce with increase in initial static shear stress bias (α).

In an overall sense, for the tested natural low plastic Fraser River silt, the potential for development of significant deformations under cyclic load appears to be the dominant concern as opposed to strain softening and/or loss of shear strength. This observation suggests that the Fraser River silt is unlikely to experience flow failure under cyclic loading.

Based on the criteria proposed by Bray et al. (2004) for liquefaction assessment, the Fraser River silt tested herein would classify as susceptible to “liquefaction or cyclic mobility”. The observations of the laboratory testing also suggest that this soil is susceptible to cyclic mobility during DSS loading. However, the empirical criteria do not provide a distinction between liquefaction involving loss of shear strength and cyclic mobility. With respect to Idriss and Boulanger (2008) approach, the analyzed Fraser River silt would classify as “sand-like”. The limited cone penetration test data available from testing, conducted at the location of samples obtained for this study, provided an opportunity to apply the field-based approach by Idriss and Boulanger (2008). This exercise suggested that the laboratory-based CRR value for Fraser River silt is clearly higher than the $CRR = 0.075$ estimated based on field-based charts assuming “sand-like” behaviour. These demonstrate the value of detailed laboratory testing in complementing field-based approaches in the assessment of cyclic shear performance of fine-grained low plastic silts.

5 EFFECTS OF PARTICLE STRUCTURE IN THE MECHANICAL RESPONSE OF FINE-GRAINED SOILS

In general, it is fair to state that the behaviour of a given field soil condition is best examined in the laboratory by testing of good quality “undisturbed” soil specimens. The possibility to obtain reasonably undisturbed samples of certain low-plastic silts has been already demonstrated (e.g., Bray et al. 2004, Sanin and Wijewickreme 2006); in spite of this, due to increased costs and difficulties with such undisturbed field sampling, there is a tendency to use reconstituted specimens for assessing the shear response of silts. Moreover, argument has also been made that the testing of reconstituted samples would be suitable if the objective is to determine the material characteristics at critical state (Jefferies and Been, 2006).

With this background, it was considered suitable to compare the shear performance observed in undisturbed specimens of Fraser River silt with that from reconstituted material. This section presents the results of a series of tests performed on reconstituted specimens of Fraser River Delta silt; the results are then compared to those performed with the same testing parameters on undisturbed samples.

The observations made from limited experimental work to study the behavioural characteristics under monotonic shear loading of the reconstituted silt material are initially presented for

comparison with the results from tests on undisturbed Fraser River silt described in Chapter 4. Data from monotonic shear tests are initially presented then followed by data derived from cyclic tests.

5.1 Mechanical response of undisturbed and reconstituted Fraser River silt

The results from a series of tests performed on specimens of reconstituted material from Fraser River Delta silt are presented herein, and then compared to those from tests conducted on undisturbed specimens of the same material. Details related to the preparation of the reconstituted specimens are described in Chapter 3 of this thesis. The range of void ratios obtained for all the specimens are presented in Table 4.1. It is of interest to note that the end-of-consolidation void ratios (e_c) observed for the reconstituted specimens were somewhat lower than those noted for the undisturbed specimens under similar consolidation stress levels (i.e., density of specimens obtained using reconstitution was observed to be higher than that of undisturbed specimens).

5.1.1 Monotonic shear response

The stress-strain and stress path response observed from four constant volume, monotonic, strain-controlled DSS tests on undisturbed specimens of Fraser River silt initially consolidated to $\sigma'_{vc} \sim 100, 200, 300,$ and 400 kPa are presented in Figures 5.1 and 5.2, respectively (Test series Ia). In order to facilitate a direct comparison, corresponding data derived from similar

tests conducted on reconstituted Fraser River silt (Test series IIIa) are also superimposed on the same figures.

Figure 5.1 Constant volume monotonic DSS test on reconstituted and undisturbed specimens of Fraser River Delta silt at varying confining stress levels: Stress-strain curves; $\sigma'_{vc} = 100, 200, 300$ and 400 kPa.

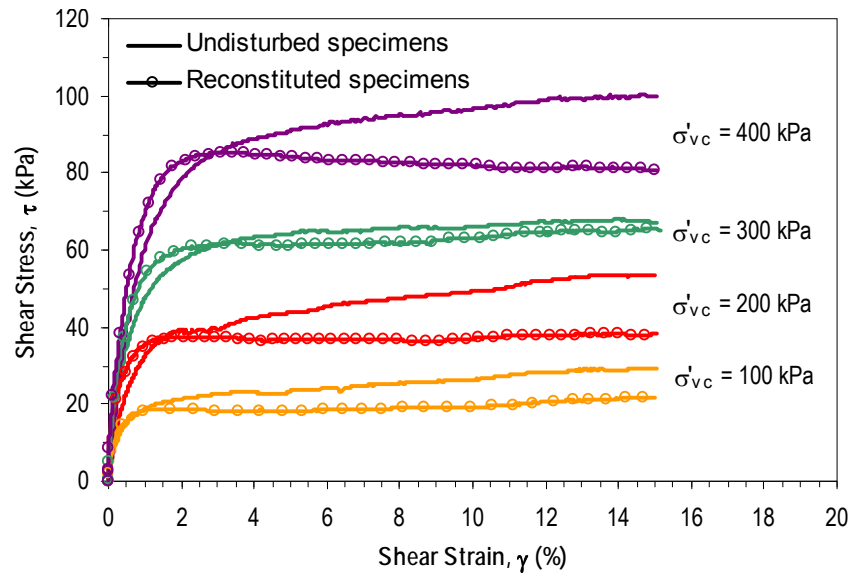
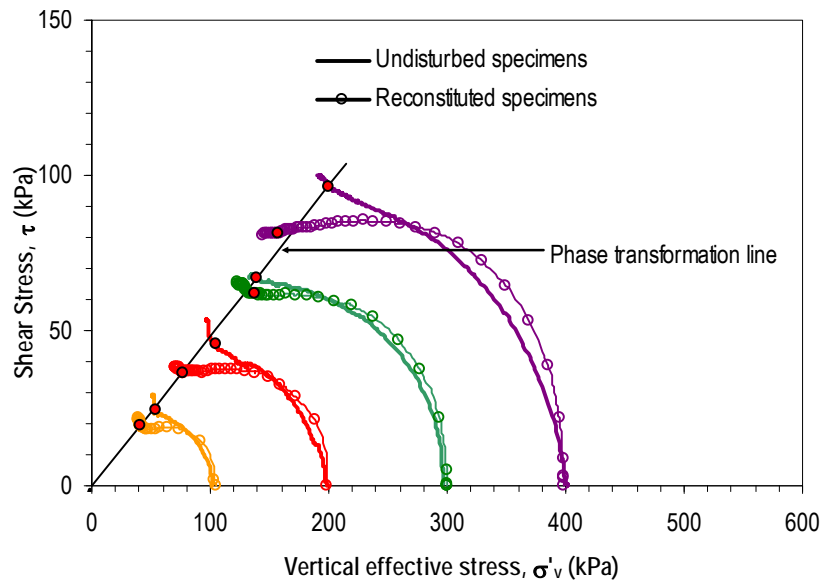


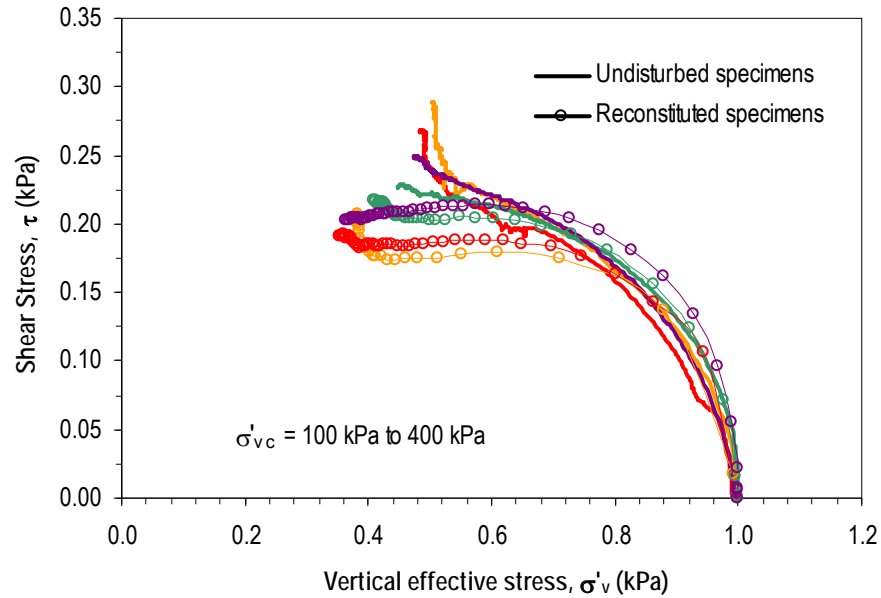
Figure 5.2 Constant volume monotonic DSS test on reconstituted and undisturbed specimens of Fraser River Delta silt at varying confining stress levels: Stress path curves; $\sigma'_{vc} = 100, 200, 300$ and 400 kPa.



The general behaviour of the undisturbed specimens was discussed in Chapter 4 of this thesis. Except for the initial shear strain levels (say up to $\sim 1\%$) where the behaviours were almost identical, reconstituted specimens exhibited a response more contractive than that observed for the undisturbed specimens. Moreover, the reconstituted specimens experienced a mild strain-softening response. In contrast, all the undisturbed specimens exhibited increasing shear resistance with increasing strain. In an overall sense, the reconstituted specimens, despite having a slightly lower void ratio, exhibited a weaker stress-strain response than displayed by the undisturbed specimens. The behavioural contrast between the undisturbed and the reconstituted specimens observable in the specimen initially consolidated to 400 kPa suggest that the original structure of the undisturbed specimens seem to prevail even after consolidating the material to a confining stress level significantly higher than the estimated preconsolidation stress for the natural soil.

The stress paths from the reconstituted specimens were normalized with respect to the initial effective confining stress, σ'_{vc} , and the results are compared with those from undisturbed Fraser River silt in Figure 5.3. The normalized stress paths for both types of specimens fall within a relatively narrow range; however, careful examination would reveal that the reconstituted specimens reach the phase transformation line at a lower normalized shear stress than the reconstituted specimens. In general, the “normalizable” response of normally consolidated silt is similar to that typically observed for normally consolidated clays (Atkinson and Bransby, 1978).

Figure 5.3 Constant volume monotonic DSS test on reconstituted and undisturbed specimens of Fraser River Delta silt at varying confining stress levels: Normalized stress path curves; $\sigma'_{vc} = 100, 200, 300$ and 400 kPa.



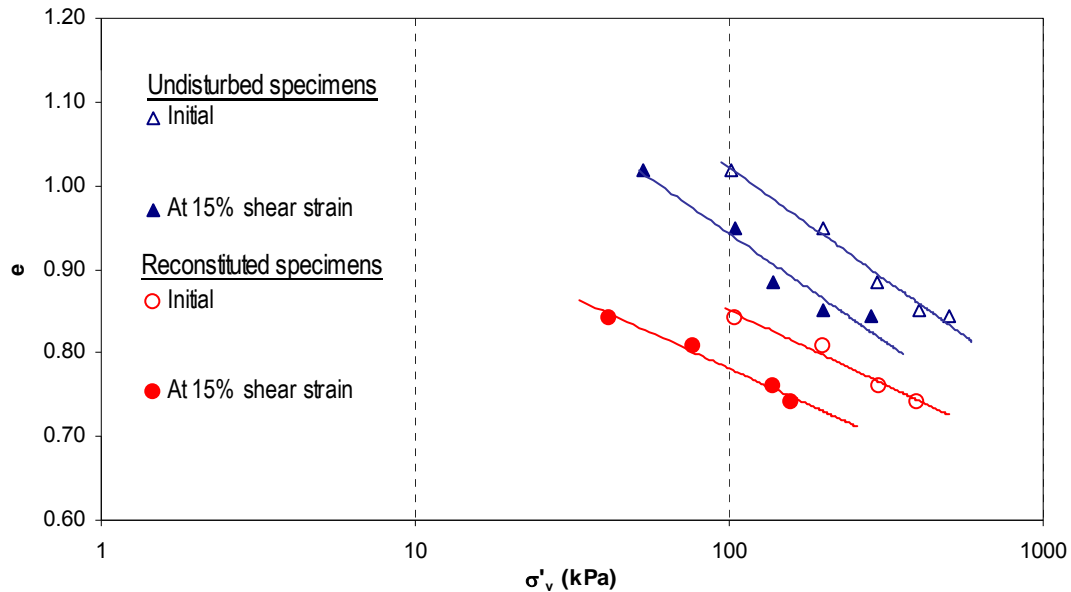
Similar observations have also been made by Høeg et al. (2002) in their comparisons between undisturbed and reconstituted specimens of natural and man-(tailings) made silts. They reported substantial differences in the stress-strain-strength behaviour of undisturbed and reconstituted specimens of natural and man-(tailings) made silts. In their research, all the undisturbed specimens showed dilative behaviour compared to contractive behaviour of the reconstituted specimens. As observed in this study, the densities of the reconstituted specimens analyzed by Høeg et al. (2002) were also higher than the undisturbed specimens, but they all showed lower peak strength and strain softening.

The consolidation stress state in terms of void ratio (e) and corresponding effective stress (σ'_v) are commonly considered as suitable variables to represent the state of a soil. As such, from a fundamental soil behaviour point of view, it is of interest to assess the e - σ'_v state of the

material after consolidation as well as after reaching relatively large strain levels. It is to be noted that, while the vertical effective stress (σ'_v) would change with shear-induced pore water pressure, the void ratio (e) does not change during the shearing process since monotonic DSS tests were conducted at constant volume. With this thinking, the location of $e_c - \log \sigma'_{vc}$ state of the specimens for undisturbed and reconstituted specimens of Fraser River silt immediately after initial consolidation are plotted in Figure 5.4 using two types of open symbols. The $e - \sigma'_v$ states of the same specimens after reaching a shear strain of $\sim 15\%$ are also superimposed in Figure 5.4 using solid symbols. Examination of this figure reveals that initial consolidation state of undisturbed Fraser River silt follow a linear $e - \log \sigma'_v$ relationship. In a similar manner, the initial consolidation state of the reconstituted material also seems to follow a linear $e - \log \sigma'_v$ relationship, but different from that noted for the undisturbed Fraser River silt. The observed linearity is in accord with the well known behaviour for normally consolidated fine-grained soils (Atkinson and Bransby 1978). It is reasonable to state that the difference in particle fabric, aging effects, would be the cause for the difference between the normal consolidation lines for the undisturbed and reconstituted soils.

It is observable that, for each of the undisturbed and reconstituted specimens tested, the $e - \log \sigma'_v$ states of the specimens after reaching a shear strain of about 15% appear to follow a straight line; these straight lines seem to align generally parallel to the counterpart $e_c - \log \sigma'_{vc}$ line depicting the initial consolidation response (i.e., data points with open symbols).

Figure 5.4 e - $\log \sigma'_v$ relationships for undisturbed and reconstituted specimens of Fraser River silt immediately after initial consolidation compared with those after reaching 15% shear strain in monotonic direct simple shear.



The $e - \log \sigma'_v$ states of the specimens after reaching a shear strain of 15%, under identical simple shear loading mode, are distinctly different for the undisturbed and reconstituted silt specimens. It is of relevance to examine these lines drawn at 15% strain level in relation to the well-established critical state concepts (Atkinson and Bransby 1978). If there exists a unique critical state for the tested silt, it would be logical/reasonable to deduce that: (i) the $e - \log \sigma'_v$ state of the undisturbed specimens has clearly not reached the critical state after experiencing shear strains in the order of 15%; and (ii) the $e - \log \sigma'_v$ state of the remoulded specimens after experiencing shear strains in the order of 15% would be more close in location to the existent critical state than the state of the undisturbed specimens after experiencing shear strains in the order of 15%. The large strain $e - \log \sigma'_v$ state reached through monotonic shear testing of remoulded silts has been proposed as a reasonable way to determine the critical state line for silts, which in turn has been argued to be useful for developing the baseline framework

especially for the assessment of static liquefaction (Jefferies and Shuttle 2002). However, the observations presented in Figure 5.4 would suggest that the determination of the “true” critical state line through laboratory monotonic shear testing of undisturbed silt would be extremely difficult, if not impossible. In turn, these observations also suggest that the use of a critical state $e - \log \sigma'_v$ line generated based on reconstituted silt specimens to assess the field performance (i.e., performance of undisturbed soil) may not be suitable for fine-grained soils.

In an overall sense, the experimental observations presented herein, with respect to the $e - \log \sigma'_v$ domain, suggest that the reconstituted and undisturbed silt specimens have exhibited significantly different monotonic loading characteristics, in spite of their identical mineralogical origin and grain size. These differences suggest that the commonly used variables e and σ'_v alone are not sufficient to define/determine the shear behaviour of low plasticity silt; the differences can be reasonably attributed to considerations such as the difference in particle structure (soil fabric) and the age that may not essentially be reflected in the void ratio. For example, the natural fabric and aging effects of the undisturbed silt would not be present in the specimens of reconstituted silt that were prepared from a slurry state; in turn, this seems to have led to a particle structure that is relatively weak in terms of its ability to offer shear resistance. These deductions are in accord with the observations made by Leroueil and Hight (2003) with respect to the performance of several other natural soils.

5.2 Cyclic shear response

Reconstituted specimens of Fraser River delta silt were subjected to cyclic direct simple shear to compare the results with those observed for the undisturbed specimens. All the tests were conducted at nominal initial effective confining stress of 100 kPa to provide a basis for comparison between tests. Stress-strain and stress path curves of the tests conducted at different cyclic stress ratios are presented in Figures 5.5 to 5.7.

Figure 5.5 Constant volume cyclic simple shear DSS test on reconstituted specimen of normally consolidated Fraser River Delta silt: Stress strain and stress path curves; $\sigma'_{vc} = 100$ kPa; CSR = 0.10; consolidation time = 3hrs.

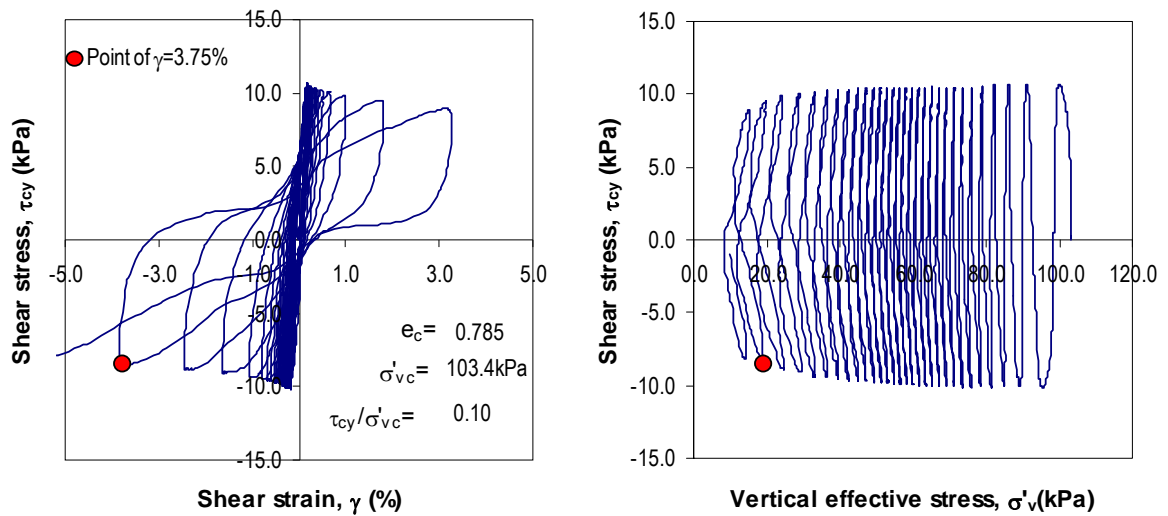


Figure 5.6 Constant volume cyclic simple shear DSS test on reconstituted specimen of normally consolidated Fraser River Delta silt: Stress strain and stress path curves; $\sigma'_{vc} = 100$ kPa CSR = 0.12; consolidation time = 3hrs.

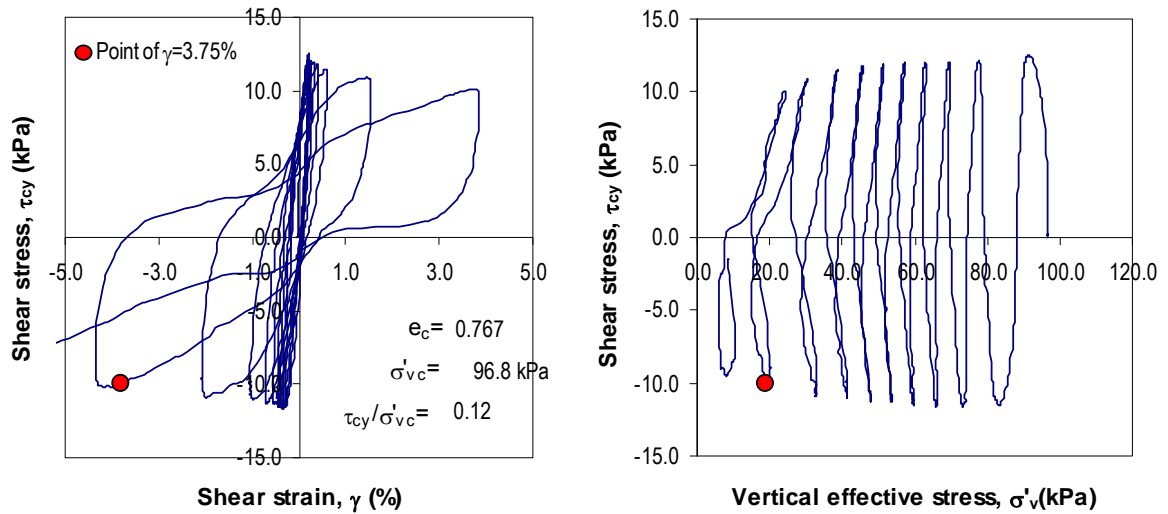
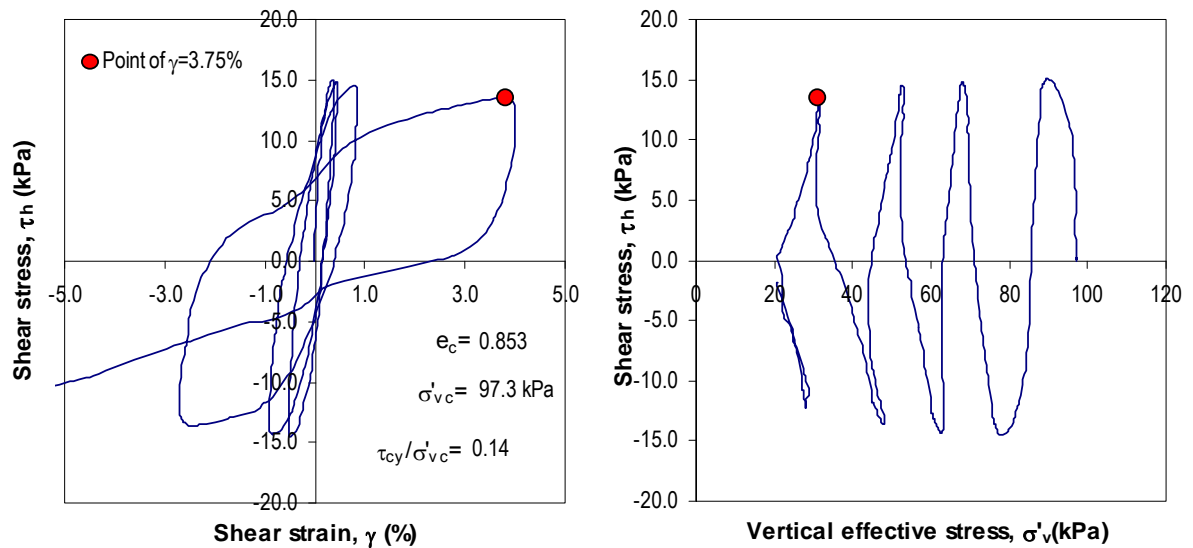


Figure 5.7 Constant volume cyclic simple shear DSS test on reconstituted specimen of normally consolidated Fraser River Delta silt: Stress strain and stress path curves; $\sigma'_{vc} = 100$ kPa; CSR = 0.15; consolidation time = 3hrs.



In a general sense, the reconstituted specimens seem to exhibit gradual increase in excess pore water pressure and degradation of shear stiffness with increasing number of load cycles, similar to the observed response of the undisturbed specimens. Typically, the shear stiffness experienced its transient minimum when the applied shear stress is close to zero. This cyclic mobility type response is generally similar in form to the undrained (constant-volume) cyclic shear responses observed from cyclic shear tests on fine-grained mine tailings, clays, and specimens of dense reconstituted (Wijewickreme et al. 2005a, 2005b). In spite of the observed similarity of the strain development mechanism, there is a dramatic difference in the cyclic shear behaviour between undisturbed and reconstituted specimens under identical CSR amplitudes, and this aspect is discussed below.

5.3 Comparison of cyclic shear response between reconstituted and undisturbed Fraser River silt

The response observed specifically at first and last loading cycles from two selected tests on reconstituted materials are presented in Figures 5.8 and 5.9; in order to make a direct comparison, the observed response from cyclic DSS tests conducted at the essentially identical CSR value on counterpart undisturbed specimens are also superimposed on the same figure. It can be noted that the undisturbed and reconstituted specimens displayed completely contractive response during the 1st half cycle of loading. Beyond that point, the results for the undisturbed specimen shown in Figure 5.8 (CSR=0.10) did not develop significant pore water pressure or cyclic shear strain during cyclic loading and the results for the undisturbed specimen shown in Figure 5.9 (CSR=0.15) exhibited dilative tendency during “loading” (or increasing shear stress

and contractive response during “unloading” (or decreasing shear stress). In contrast, the reconstituted specimens continued to develop excess pore water pressures at a much faster rate (i.e., perform in a contractive manner) leading to a rapid degradation of shear stiffness with increasing number of cycles – particularly, in comparison to those of the undisturbed specimens.

Figure 5.8 Comparison of constant volume cyclic simple shear DSS test on reconstituted and undisturbed specimens of normally consolidated Fraser River Delta silt. First and twenty-ninth loading cycles: Stress strain and stress path curves; $\sigma'_{vc} = 100$ kPa; CSR = 0.10.

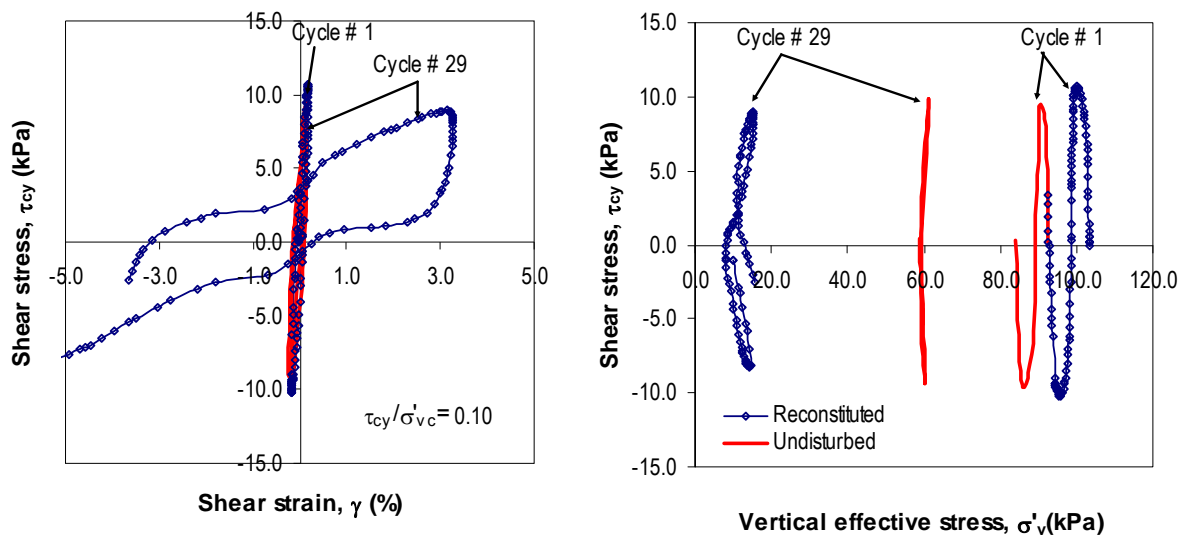
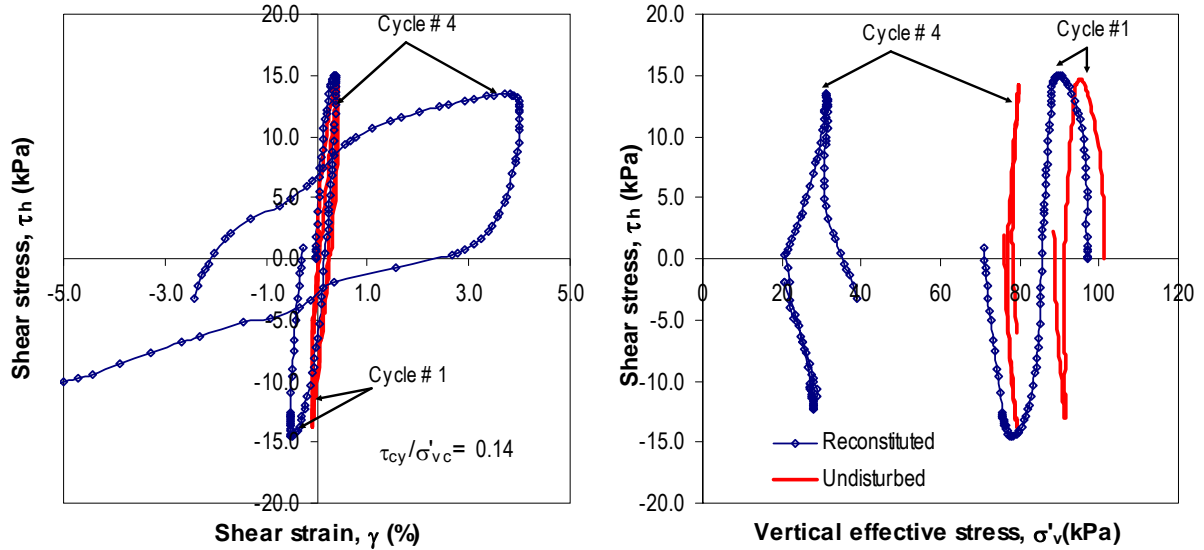
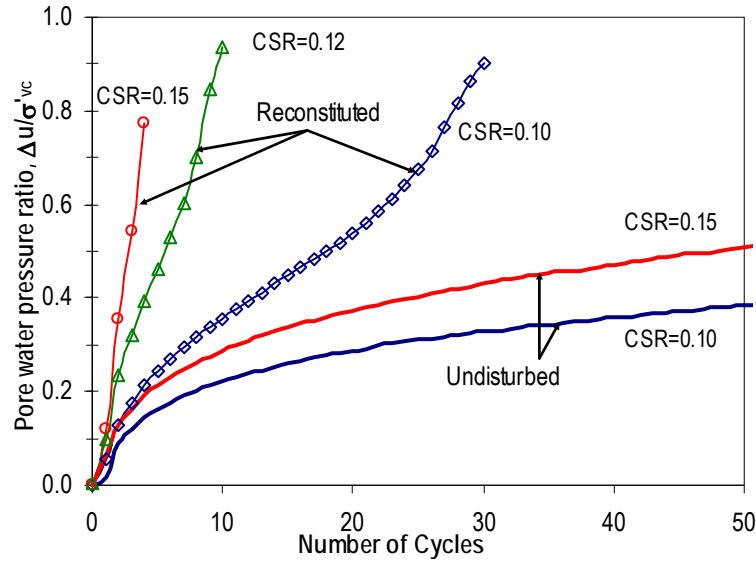


Figure 5.9 Comparison of constant volume cyclic simple shear DSS test on reconstituted and undisturbed specimens of normally consolidated Fraser River Delta silt. First and fourth loading cycles: Stress strain and stress path curves; $\sigma'_{vc} = 100$ kPa; CSR = 0.15.



The generation of excess pore water pressure ratio r_u $[= (\Delta u/\sigma'_{vc})]$ with the number of cycles observed from two undisturbed silt specimens tested with differing CSR amplitudes are presented in Figure 5.10. The response observed from the counterpart tests conducted on reconstituted silt under identical consolidation and CSR loadings are also superimposed in the same figure for direct comparison. As noted in the previously presented stress path plots, the gradual increase of r_u with increasing number of load cycles can be noted from all the tests, and the rate of generation of r_u with number of load cycles increases with increasing CSR. From the point of view of this study, again, it is important to note that there is a remarkably high contractive tendency in reconstituted silt specimens in comparison to undisturbed silt specimens under identical initial consolidation stress and subsequent cyclic shear loading conditions.

Figure 5.10 Constant volume cyclic simple shear DSS test on undisturbed and reconstituted specimens of normally consolidated Fraser River Delta silt: Pore water pressure development at different CSR; $\sigma'_{vc} = 100$ kPa.



In summary, after being subjected to the same number of cycles at the same CSR, the reconstituted specimens seem to clearly experience shear strain, accumulation of excess pore water pressure, and degradation of shear stiffness in a more rapid manner (with respect to increasing number of cycles) compared to those observed from tests conducted on undisturbed specimens. It is important to highlight that these observations are in accord with those findings for the undisturbed and reconstituted specimens from monotonic shear tests; once again, the observations reinforce the significant influence of natural fabric and aging effects on the shear response of silt.

5.3.1 Effects of “ageing” of reconstituted soils on the cyclic shear resistance

The results for the reconstituted silt specimens presented in the previous section were generated from tests conducted on specimens that had been allowed to consolidate for about 3 hours prior to cyclic loading. In order to evaluate the effects of time of consolidation in the cyclic shear resistance (“ageing” effects), two cyclic DSS tests were performed on reconstituted silt specimens that had been left to consolidate for more than three hours. One of the reconstituted specimens was left for consolidation for about 24 hours prior to cyclic loading, and the second test was conducted on a reconstituted specimen left for 7 days prior to cyclic loading. It is of relevance to note that the two specimens were tested at the same cyclic shear loading ($CSR = 0.12$) in order to facilitate direct comparison with those results from the reconstituted specimen tested after 3 hours of consolidation. Figures 5.11 and 5.12 present the results of these two tests in terms of the stress-strain and stress-path behaviour. When compared with the results of Figure 5.6, it can be noted that both “aged” specimens exhibited a slightly less contractive response, requiring a larger number of cycles to reach a given strain level.

Figure 5.11 Constant volume cyclic simple shear DSS test on reconstituted specimen of normally consolidated Fraser River Delta silt, aged specimen: Stress strain and stress path curves; $\sigma'_{vc} = 100$ kPa CSR = 0.12, consolidation time=24hours.

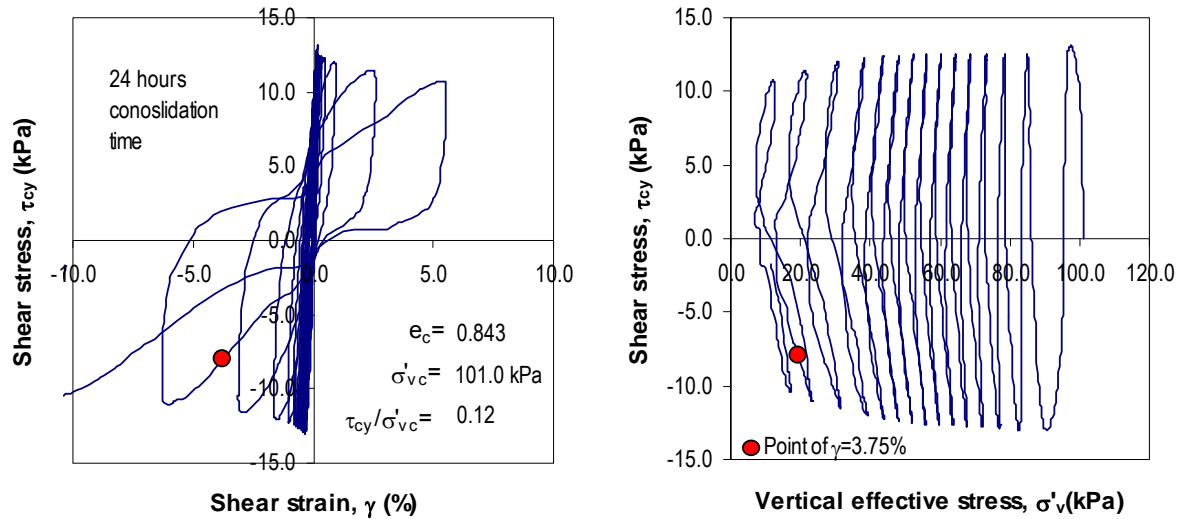
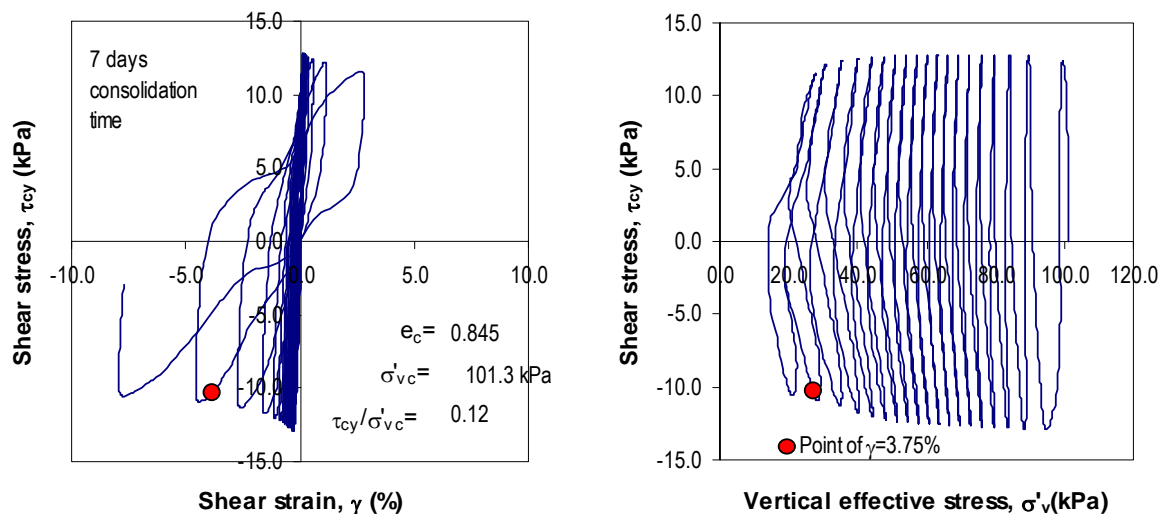


Figure 5.12 Constant volume cyclic simple shear DSS test on reconstituted specimen of normally consolidated Fraser River Delta silt, aged specimen: Stress strain and stress path curves; $\sigma'_{vc} = 100$ kPa CSR = 0.12, consolidation time=7 days.



5.3.2 Cyclic shear resistance

The cyclic resistance ratio (CRR) derived from the above testing process on reconstituted silt specimens can be examined by comparing the response observed from DSS testing under different applied cyclic loadings. The cyclic resistance ratio [$CRR = (\tau_{cy}/\sigma'_{vc})$] versus number of cycles to reach single-amplitude $\gamma = 3.75\%$ derived from the tests conducted on undisturbed and reconstituted specimens of Fraser River silt, with different cyclic load amplitudes, are plotted in Figure 5.13. Despite having a comparatively higher density (see Table 4.1), again, it is evident that all reconstituted specimens consistently exhibited a significantly lower CRR vs. number of cycles characteristic in comparison to the undisturbed specimens. Figure 5.13 also presents the 2 points of CRR vs. No. of cycles obtained for the two “aged” specimens. It is clear that CRR increases with “aging”. Nevertheless, if by doing a simple linear extrapolation to 10,000 years (maximum age of the deposit of Fraser River Delta silt), the number of cycles to reach $\gamma = 3.75\%$ with a $CSR=0.12$ is approximately 30 cycles, which is still low in comparison to the curve obtained for the undisturbed specimens.

5.3.3 Observations on the cyclic shear response between undisturbed and reconstituted specimens on different materials

A limited number of cyclic DSS tests were performed also on Kitimat clay on undisturbed and reconstituted specimens (Test series IVb and IVc respectively) to compare with the observations on Fraser River silt. The response of natural Kitimat clay presented in Figures 4.48 through Figure 4.50 (as discussed in Section 4.4.1) can be compared with Figures 5.14 through 5.16 presenting the counterpart results from tests on reconstituted specimens of the

same material. Figures 5.17 and 5.18 compare the stress-strain and stress paths curves, from two tests, corresponding to the first and last cycles of loading on undisturbed and reconstituted specimens of Kitimat clay.

The type of response is the typical cyclic mobility type observed for the undisturbed specimens. As observed for Fraser River silt, again despite having a comparatively higher density (see Table 4.1), it is evident that all reconstituted specimens consistently required a lower number of cycles to reach a given shear strain level, and the increase in shear strain and gradual increase of pore water pressure ratio occurred at a higher rate. The reconstituted specimens developed significantly higher pore water pressures and accumulated more shear strain in the same number of cycles than the counterpart undisturbed specimens.

Figure 5.13 Cyclic resistance ratio from constant volume cyclic DSS tests on undisturbed and reconstituted specimens of normally consolidated Fraser River Delta silt: Nominal initial effective confining stress $\sigma'_{vc} = 100\text{kPa}$.

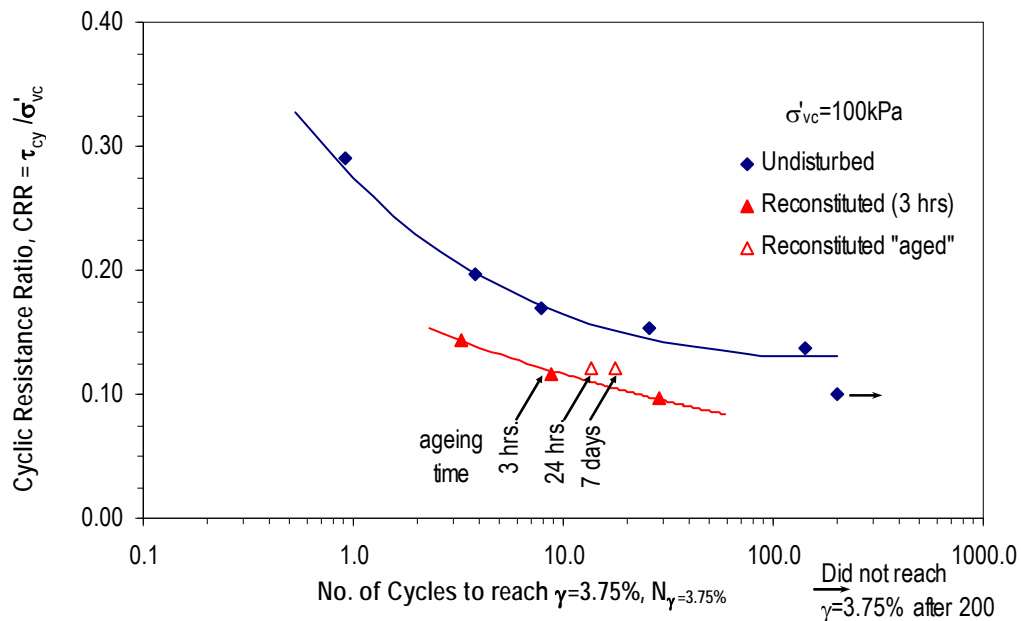


Figure 5.14 Constant volume cyclic simple shear DSS test on reconstituted specimen of Kitimat clay: Stress strain and stress path curves; $\sigma'_{vc} = 80$ kPa CSR = 0.25.

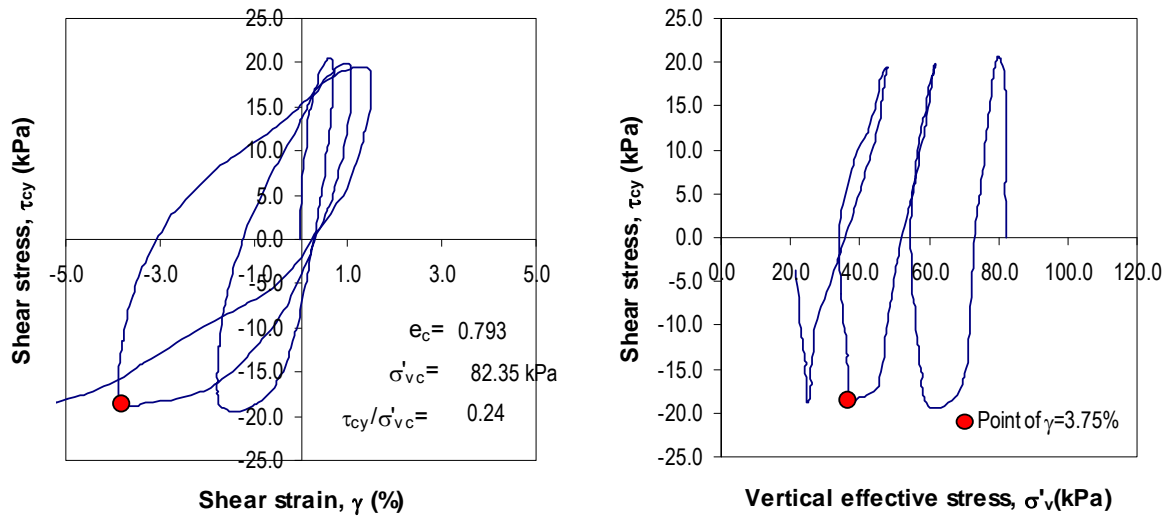


Figure 5.15 Constant volume cyclic simple shear DSS test on reconstituted specimen of Kitimat clay: Stress strain and stress path curves; $\sigma'_{vc} = 80$ kPa CSR = 0.20.

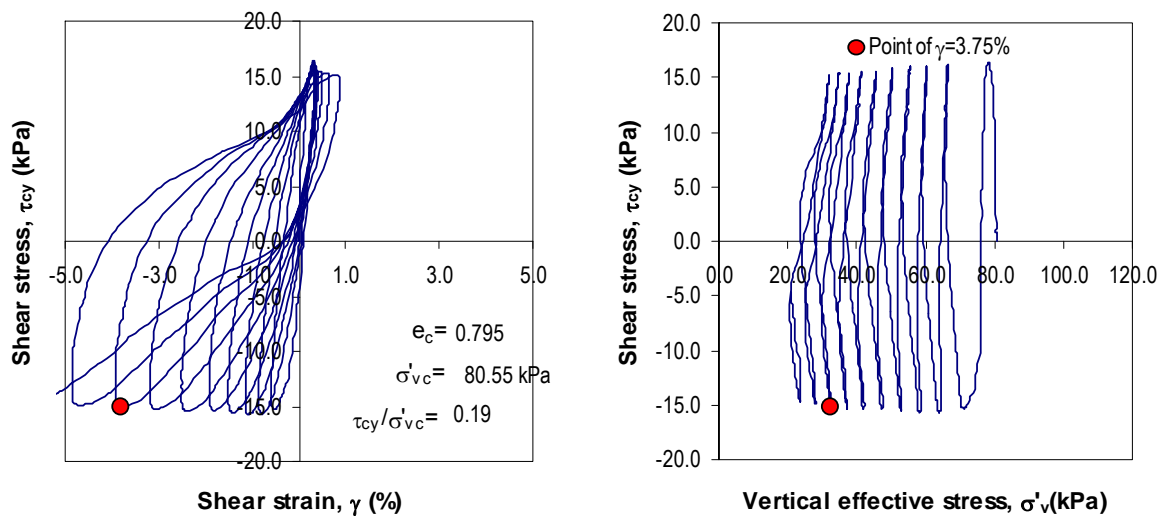


Figure 5.16 Constant volume cyclic simple shear DSS test on reconstituted specimen of Kitimat clay: Stress strain and stress path curves; $\sigma'_{vc} = 80 \text{ kPa}$ CSR = 0.17.

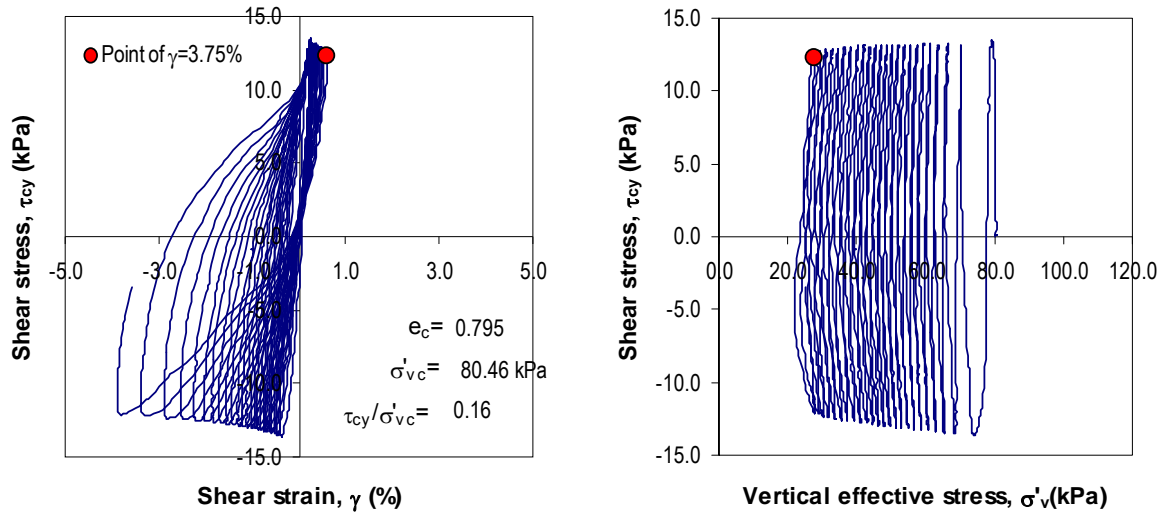


Figure 5.17. Comparison of constant volume cyclic simple shear DSS test on reconstituted and undisturbed specimens of normally consolidated Kitimat clay. First and third loading cycles: Stress strain and stress path curves; $\sigma'_{vc} = 80 \text{ kPa}$; CSR = 0.24.

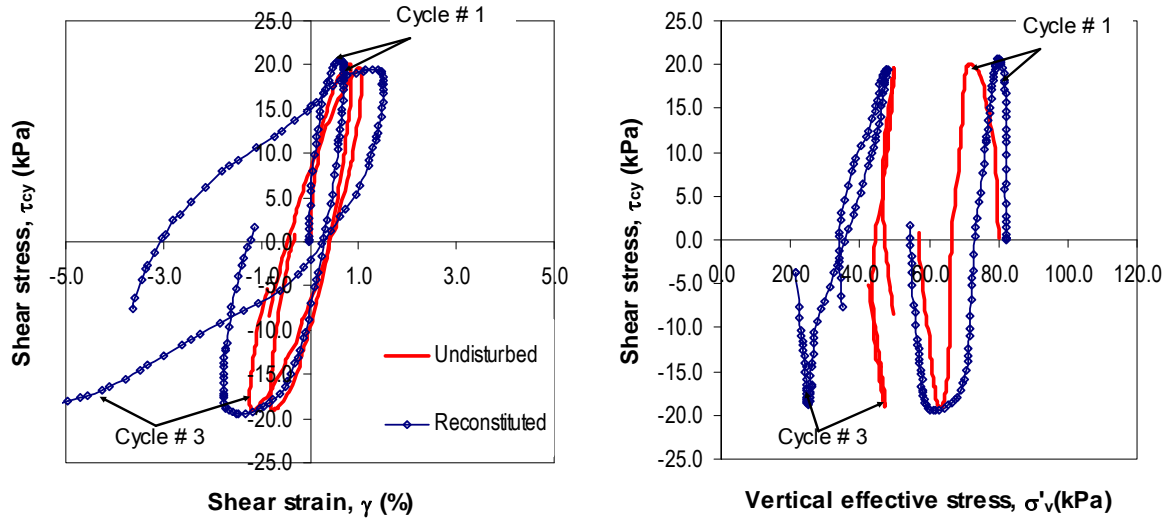


Figure 5.18. Comparison of constant volume cyclic simple shear DSS test on reconstituted and undisturbed specimens of normally consolidated Kitimat clay. First and 24th loading cycles: Stress strain and stress path curves; $\sigma'_{vc} = 80$ kPa; CSR = 0.17.

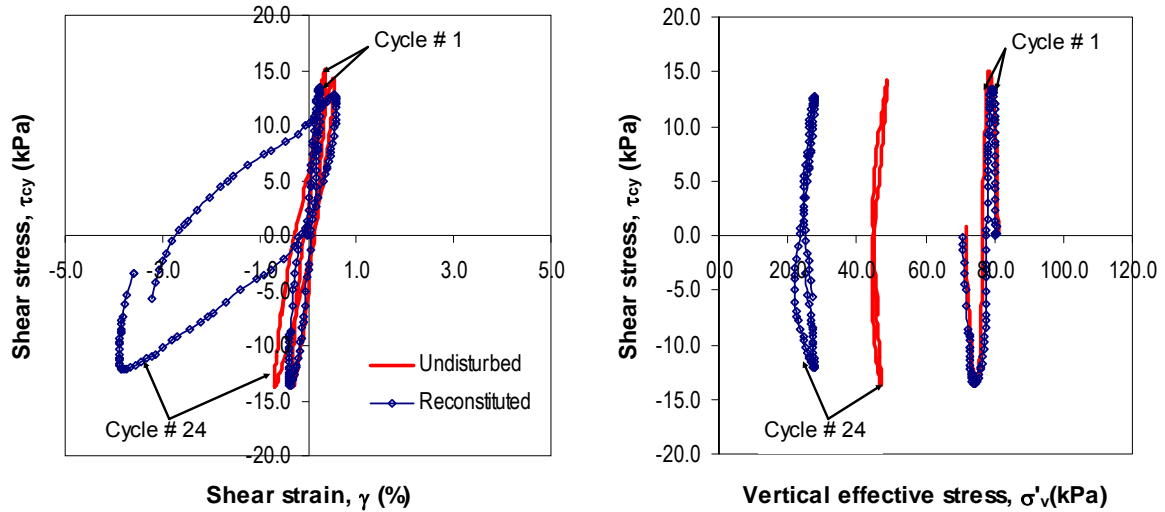
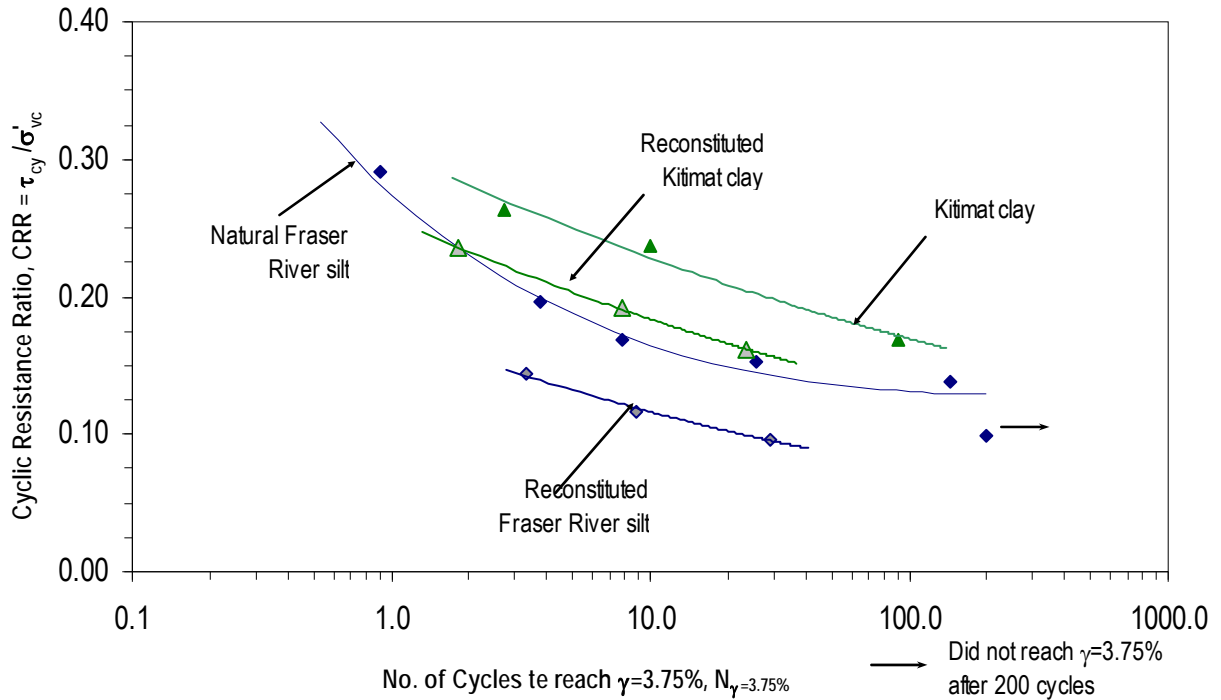


Figure 5.19 presents the cyclic resistance ratio curves for both Fraser River silt and Kitimat clay. Curves for the undisturbed and reconstituted test data are provided in the plot. A significantly lower CRR vs. number of cycles in the reconstituted specimens in comparison to the undisturbed soil can be noted for both materials.

5.4 Summary and principal findings

The constant-volume monotonic and cyclic shear response of low-plastic, normally consolidated fine-grained reconstituted silt (mainly Fraser River silt) was examined using data from monotonic and cyclic direct simple shear DSS tests. The intent was to compare the shear response of the reconstituted specimens with those obtained from undisturbed specimens of the same material under similar consolidation stress conditions.

Figure 5.19 Cyclic resistance ratio from constant volume cyclic DSS tests on undisturbed and reconstituted specimens of normally consolidated Fraser River Delta silt and Kitimat clay.



For the initial vertical effective confining pressure range of 100 to 400 kPa investigated using monotonic shear tests, the specimens of reconstituted low plastic Fraser River silt (despite having a lower density under identical consolidation stress conditions) exhibited a consistently more contractive volume change tendency compared to that observed from the specimens of undisturbed material consolidated to the same stress level. In an overall sense, it can be concluded that the reconstituted specimens exhibited a generally weaker stress-strain response than those displayed by the undisturbed specimens.

The consolidation stress state in terms of void ratio (e) and corresponding effective stress (σ'_v) are commonly considered as suitable variables to represent the state of a soil. However, the experimental observations presented herein, with respect to the $e - \log \sigma'_v$ domain, suggest that

the reconstituted and undisturbed silt specimens have exhibited significantly different monotonic shear characteristics, in spite of their identical mineralogical origin and grain size. The observations also reveal that the use of a critical state $e - \log \sigma'_v$ line generated based on reconstituted silt specimens to assess the field performance (i.e., performance of undisturbed soil) may not be suitable for fine-grained soil.

Under cyclic loading, although cyclic mobility type response similar to undisturbed silts was noted, the reconstituted specimens seem to exhibit a more rapid excess pore water pressure generation and shear stiffness degradation with respect to increasing number of cycles. These observations are in accord with those findings for the undisturbed and reconstituted specimens from monotonic shear tests, thus, emphasizing the significant influence of natural fabric and aging effects on the shear response of silt.

These observed differences between the undisturbed and reconstituted materials suggest that commonly used variables such as e and σ'_v alone are not sufficient to define/determine the shear behaviour of low plasticity silt; the differences can be reasonably attributed to considerations such as the difference in particle structure (soil fabric) and the age which may not be reflected in the void ratio. For example, the natural fabric and aging effects of the undisturbed silt would not be present in the specimens of reconstituted silt that were prepared from a slurry state; in turn, this seems to have led to a particle structure that is relatively weak in terms of its ability to offer shear resistance.

6 POST-CYCLIC RECONSOLIDATION STRAINS IN LOW PLASTIC FRASER RIVER SILT

As noted in Chapter 2. In addition to the shear deformations associated with loss of stiffness and/or strength in some situations, another key mechanism of earthquake-induced deformations is the overall volume change in the soil mass that takes place due to the dissipation of shear-induced excess pore water pressures.

In consideration of the current lack of understanding on this subject, it was considered of importance to study the post-cyclic consolidation characteristics of Fraser River silt in the laboratory as part of the overall research on the earthquake response of low plastic silt. This chapter presents the findings from this experimental research along with new laboratory-based recommendations for estimating post-cyclic settlements of low plastic silts. Section 3.3 describes the testing procedure of the post-cyclic reconsolidation.

In addition to Fraser River silt (test series Ib, Ic, and IIIb), DSS testing was also undertaken on specimens of reconstituted quartz rock powder (test series IVa) to expand the database and to observe the results of post-cyclic reconsolidation. Herein, quartz rock powder was selected to generate some limited, but useful, observations on the behavioural patterns of materials with

different plasticity and grain size distribution for comparison with the response of Fraser River silt.

6.1 Experimental observations

Table 4.1 presents a summary of the testing results of Fraser River silt carried out during this research program. The results include the observed maximum pore water pressure ratio developed during cyclic loading ($\Delta u_{\max}/\sigma'_{vc}$) and the post cyclic volumetric strain (ϵ_{v-ps}) recorded following cyclic loading.

6.1.1 Post-cyclic reconsolidation response

Typical post-cyclic reconsolidation volumetric strain (ϵ_{v-ps}) versus time responses of undisturbed normally consolidated Fraser River silt, overconsolidated Fraser River silt, and reconstituted quartz rock powder are shown in Figures 6.1 through 6.3, respectively. The three curves shown in each figure correspond to post-cyclic consolidation tests conducted on soil specimens that have reached different levels of maximum excess cyclic pore water pressure ratio [$r_{u-\max} = (\Delta u)_{\max}/\sigma'_{vc}$]. The information in Figure 6.1 suggests that the level of $r_{u-\max}$ has a significant influence on the post-cyclic volumetric strains (i.e., post-cyclic consolidation settlements) where there seems to be a trend of increasing ϵ_{v-ps} with increasing level of $r_{u-\max}$. This trend is also observed for overconsolidated Fraser River silt and reconstituted quartz rock powder, as presented in Figures 6.2 and 6.3, respectively.

Figure 6.1 Typical volumetric strain (ε_{v-ps}) versus square-root-time characteristics of normally consolidated natural Fraser River silt during post-cyclic consolidation (Test Series Ib).

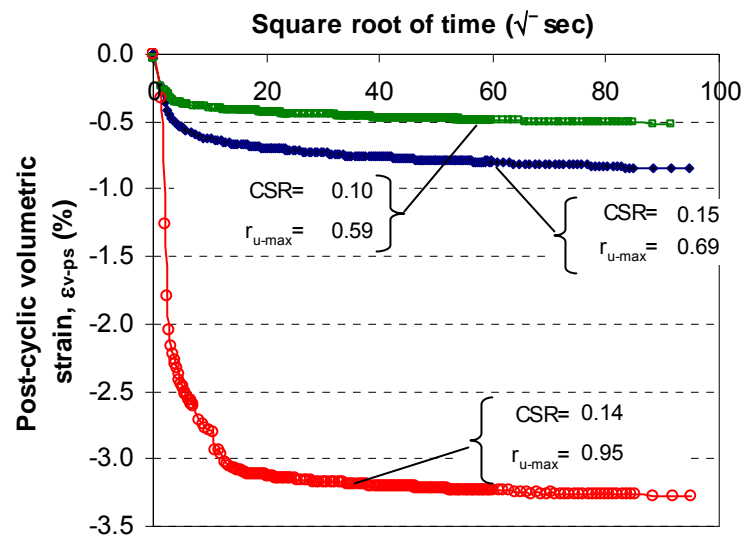


Figure 6.2 Typical volumetric strain (ε_{v-ps}) versus square-root-time characteristics of overconsolidated natural Fraser River silt during post-cyclic consolidation (Test Series Ic).

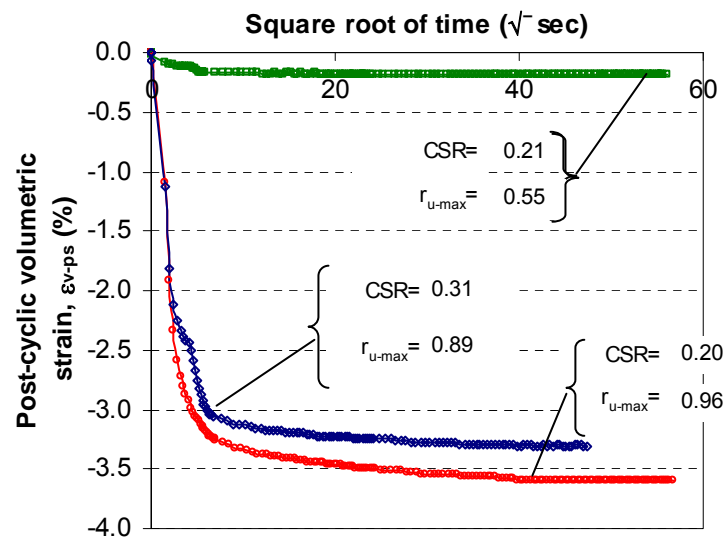
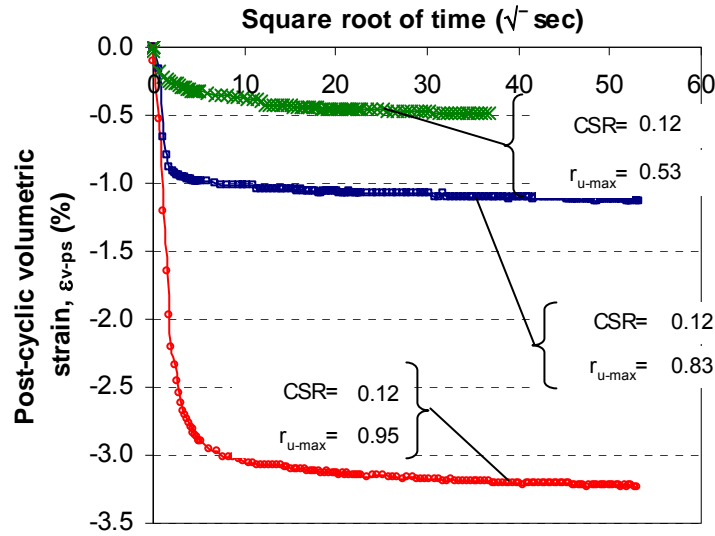
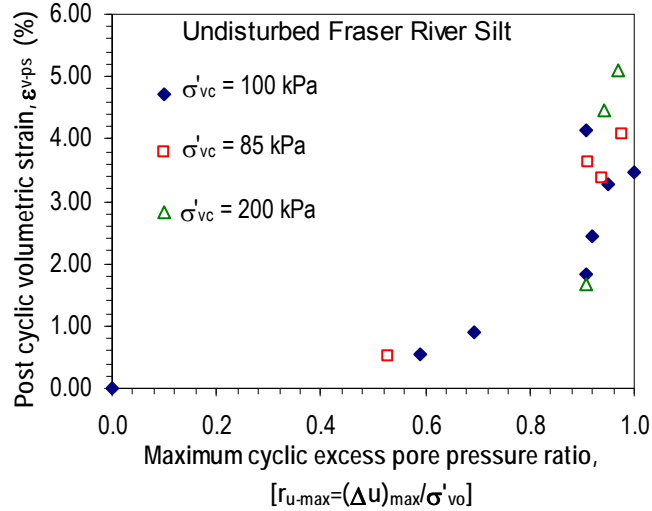


Figure 6.3 Typical volumetric strain (ϵ_{v-ps}) versus square-root-time characteristics of quartz rock powder during post-cyclic consolidation (Test Series IVa).



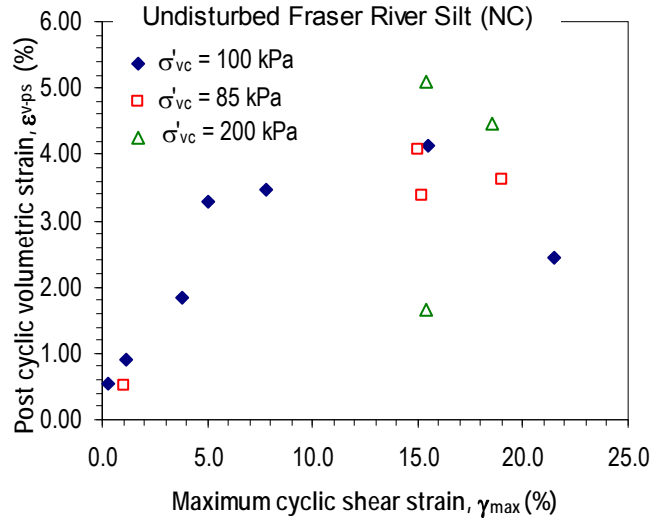
The correspondence between post cyclic volumetric strain and maximum excess pore water pressure ratio obtained from all the tests conducted on normally consolidated undisturbed Fraser River silt specimens (i.e., Series Ib, Table 4.1) are presented in Figure 6.4. The value of ϵ_{v-ps} seems to gradually increase with increasing r_{u-max} during cyclic loading up to an r_{u-max} value of about 0.8; the observed post-cyclic volumetric strains were only in the order of $\sim 0.5\%$ in the specimens that developed relatively small r_{u-max} (< 0.5). Beyond r_{u-max} levels of 0.8, ϵ_{v-ps} values increase rapidly where ϵ_{v-ps} can reach values anywhere between 1.5 to 5%. In general, it can be said that those specimens that generated high maximum excess pore water pressure ratios suffered significantly higher post-cyclic consolidation strains.

Figure 6.4 Post-cyclic volumetric strain (ϵ_{v-ps}) versus maximum cyclic excess pore water pressure ratio (r_{u-max}) during cyclic loading for Fraser River Silt (Test Series Ib).



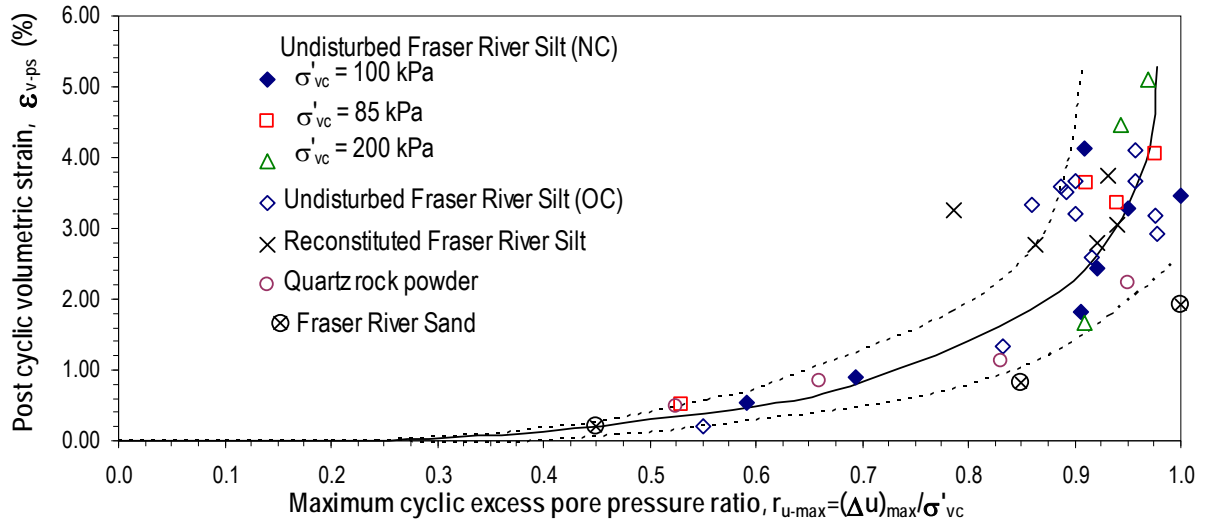
These volume changes appear to be a reflection of significant changes in the particle fabric associated with large shear strains experienced by the specimens under relatively low effective stress conditions during previous cyclic loading. With this consideration in mind, the correspondence between ϵ_{v-ps} and maximum shear strain (γ_{max}) observed during cyclic loading from Test Series I are examined in Figure 6.5. In general, high post-cyclic volumetric strains are associated with high shear strain levels; there appears to be less opportunity to develop a meaningful trendline for this ϵ_{v-ps} versus γ_{max} plot in comparison to that noted in Figure 6.4 for the ϵ_{v-ps} versus r_{u-max} plot.

Figure 6.5 Post-cyclic volumetric strain versus (ε_{v-ps}) versus maximum cyclic shear strain (γ_{max}) during cyclic loading for Fraser River Silt (Test Series Ib).



The values of ε_{v-ps} versus r_{u-max} derived from tests on specimens of overconsolidated Fraser River silt from undisturbed samples (Test Series Ic), reconstituted Fraser River silt (Test Series III), and reconstituted specimens of quartz rock powder (Test Series IV) were superimposed on data in Figure 6.4 for normally consolidated Fraser River silt from undisturbed samples (Test Series Ib); this combined data plot is given in Figure 6.6. The initially gradual, and then rapidly increasing, trend of ε_{v-ps} with increasing r_{u-max} noted for normally consolidated Fraser River silt is also exhibited in the soils of Test Series Ic, III, and IV.

Figure 6.6 Post-cyclic volumetric strain (ε_{v-ps}) versus maximum cyclic excess pore water pressure ratio (r_{u-max}) during cyclic loading using data from all tested soils in this program forming the proposed curve to estimate post cyclic volumetric strain based on maximum pore water pressure during cyclic loading.



Despite the increased scatter of data noted at larger r_{u-max} in Figure 6.6, it can be observed that the values of ε_{v-ps} seem to fall within a common and reasonably coherent trend with respect to r_{u-max} , notwithstanding that these data points arise from specimens of Fraser River silt with different overconsolidation history, particle fabric, initial void ratio, and quartz powder (which is a different low plastic material). Clearly, the value of ε_{v-ps} seems to have a wide range when r_{u-max} exceeds about 0.9 as indicated by the marked bounds for the trend line.

Specifically with respect to Test Series Ic, it is also of interest to note that there appears to be no detectable effect of OCR on the trend observed between ε_{v-ps} and r_{u-max} . It is difficult to provide a direct reasoning for this insensitivity of ε_{v-ps} (to OCR) simply based on measurements made on the stresses and strains and or effective stress changes during cyclic loading alone. However, a possible explanation for this may reside in the fact that the void

ratio of the tested OC materials is still on the order of 0.8 or more; it may be possible that, with such void ratios, the particulate structure/fabric still has ample “void space” to rearrange under high strains and low effective stress conditions prevalent during cyclic loading even though the material is in an OC state.

It would also be of use to compare post-cyclic consolidation strains reported above for Fraser River silts with similar available data from sand. Data obtained from post-cyclic consolidation of Fraser River sand initially subjected to cyclic loading (with initial relative density $D_{rc} = 41\%$; $e_c = 0.81$; initial vertical confining stress $\sigma'_{vc} = 100$ kPa) using the UBC-DSS test device as reported by Sriskandakumar (2004) are superimposed in Figure 6.6 for this purpose. As may be noted, for a given r_{u-max} , the results from the tested Fraser River sand indicate somewhat lower levels of ϵ_{v-ps} in comparison to those observed for Fraser River silts. If recently proposed relationships for volumetric reconsolidation strains as a function of cyclic stress ratio and normalized-clean-sand penetration resistance by Wu (2002) are considered, volumetric reconsolidation strains can range between about 10% for very loose sand to 1% for very dense sands. Therefore, the observed post-cyclic consolidation strains for silts from the present study fall within the domain recommended by Wu (2002) for the sands. It is important to recognize that Fraser River sand and Fraser River silt are two distinctly different materials with different void ratio, particle size distribution, and particle fabric, etc.; as such, other than a superficial comparison as per above, it is not possible to establish a fundamental linkage between the anticipated ϵ_{v-ps} values for the two materials.

6.1.2 An approach for estimation of post-cyclic volumetric strains

The above experimentally observed coherent correlation between ε_{v-ps} versus r_{u-max} provided an opportunity to propose a methodology to estimate the post-cyclic volumetric strains (ε_{v-ps}) under general seismic loading conditions. The method would employ information from laboratory tests as presented herein and ideas commonly used in seismic ground response analysis and liquefaction assessment. The approach, in principle, has already been adopted as a part of current practice by the geotechnical profession in the Greater Vancouver area of the Province of British Columbia, Canada (GVLTF 2007).

The method relies on the following experimentally observed relationships: (i) in a given element of soil, at a given initial effective consolidation stress level, the excess pore water pressure development (or r_u) is primarily dependent on the CSR and the number of applied load cycles (e.g., Figure 4.18); and (ii) the post-cyclic volumetric strains (ε_{v-ps}) are exclusively dependent on r_{u-max} (i.e., as derived from this study, Figure 6.6). With this premise, the following step-wise approach would allow estimation of ε_{v-ps} during seismic loading: (i) assess the anticipated cyclic stress ratio (CSR) for a given design earthquake. The CSR may be obtained using the well-known “simplified method” as described by Idriss and Boulanger (2008), or using a ground response analysis program such as SHAKE (Schnabel et al. 1972); (ii) estimate the number of equivalent load cycles (N_{eq}) of the above CSR considering the design magnitude of the earthquake. For example, the equivalent number of cycles for a design earthquake of magnitude $M=7.0$ is 10 for sands (as recommended by Youd et al. (2001)), and it would be about 25 for clay-like soils as recommended by Idriss and Boulanger (2008).; (iii) knowing the CSR value and N_{eq} , estimate the anticipated r_u using the excess pore

water pressure development characteristics in Figure 4.18 (interpolation of laboratory data may be required between tests conducted at different cyclic loading levels as shown in Figure 4.18); (iv) knowing the r_u value, estimate the expected range of post-cyclic volumetric strain (ϵ_{v-ps}) using the trendline bounds shown in Figure 6.6. As per Figure 4.18, there appears to be a threshold CSR of about 0.15 below which Fraser River silt will not generate large pore pressures and hence will not experience large settlements (unlikely to exceed $\epsilon_{v-ps} \sim 0.5\%$).

It is important to note that the above approach has been proposed based on data from a relatively limited number of tests conducted mainly on low plastic Fraser River silt from a specific location, consolidated to vertical effective stress level in the order of 100 kPa. The approach does not specifically provide for the estimation of the excess pore water pressures (i.e., r_{u-max}) for a general silt material. As such, laboratory post-cyclic consolidation testing of good quality soil samples may be considered to obtain site-specific excess pore water pressure development characteristics. As noted earlier, it is recommended that the quality of the samples be assessed using an approach such as that proposed by Lunne et al. (1999). Alternatively, in the absence of material-specific data, pore pressure generation models that have been shown to provide good estimates of cyclic pore pressure generation in silts (e.g., Green et al. 2000; Polito et al. 2008) may be considered for the estimation of r_{u-max} .

It is also important to exercise caution should this proposed approach be considered for estimating post-cyclic consolidation strains (ϵ_{v-ps}) in other fine-grained soils and under different stress levels. Additional research is needed to confirm the validity of the approach particularly with respect to real-life field earthquake performance data and using the proposed methodology for general practice situations.

6.2 Summary and principal findings

The post-cyclic consolidation response of low-plastic silt was examined using constant volume cyclic direct simple shear (DSS) testing followed by post-cyclic consolidation tests. The intent was to evaluate the post-cyclic consolidation volume changes experienced by silt specimens subjected to cyclic loading at different cyclic stress ratios (CSRs) and different values of cyclic shear strain. The tests were mainly conducted using undisturbed (normally consolidated and overconsolidated) and reconstituted specimens of low plastic natural Fraser River silt from the Fraser River Delta of British Columbia, Canada. Some limited tests were also conducted on reconstituted specimens of quartz rock powder, which essentially represented a non-plastic silt, for comparison purposes.

Consolidation tests conducted on tests initially subjected to constant volume cyclic loading indicate that post-cyclic volumetric strains (ε_{v-ps}) increase with the maximum pore water pressure generated during cyclic loading as well as with the maximum cyclic shear strain to which the specimens were subjected during cyclic loading. The values of ε_{v-ps} arising from the specimens of Fraser River silt with different overconsolidation history, particle fabric, pre-cyclic void ratio, as well as those arising from the quartz powder correlated well with the maximum excess pore water pressure ratio (r_{u-max}). The resulting ε_{v-ps} versus r_{u-max} trend in combination with the relationship of r_u versus number of cycles and cyclic stress ratio (CSR) seems to provide an opportunity to estimate ε_{v-ps} using experimental data. Considering that the present data base is limited to Fraser River silt for one location, additional research to generate laboratory data on other silty materials and to collect and synthesize field data from past

earthquakes would be required to confirm the applicability of the above observations and proposed approaches for general geotechnical engineering design.

7 SUMMARY AND CONCLUSIONS

The constant-volume shear response of low-plastic, fine-grained natural silt (Fraser River silt) was examined using data from constant volume monotonic and cyclic DSS tests. The intent was to advance the present limited knowledge on the response of fine-grained natural soil deposits subjected to earthquake-induced loading. The research was focused on understanding the effects of the following factors on the monotonic and cyclic loading response of low plastic Fraser River silt : initial vertical effective stress, initial static shear bias, and overconsolidation. The work also included a comparison between responses of undisturbed and reconstituted specimens under the same loading conditions and post-cyclic response. This chapter summarizes the key contributions, and presents conclusions and recommendations originating from the research.

For the purpose of clarity, this information is presented as separate sections for each of the following areas of work: (i) Cyclic shear response of Fraser River silt; (ii) Cyclic shear response of other fine-grained soils; (iii) Comparison of the response of undisturbed versus reconstituted Fraser River silt; (iv) Post-cyclic reconsolidation response of low-plastic silt; and (v) Recommendations for future research.

7.1 Cyclic shear response of Fraser River silt

Liquefaction, in the form of strain softening, accompanied by loss of shear strength, was not observed regardless of the applied cyclic stress ratio or the level of pore water generated during cyclic loading. The observed behaviour suggests that Fraser River delta silt is unlikely to experience flow failure as observed in loose saturated sand deposits subjected to cyclic loading.

Under constant volume cyclic DSS loading, Fraser River silt exhibited a cumulative decrease in effective stress with the increasing number of load cycles (i.e., cyclic-mobility-type strain development mechanism), similar to the observed behaviour of dense sands. In general, the specimens initially exhibited a contractive response followed by a dilative response. Specimens tested under more severe cyclic stress ratio levels manifested phase transformation at early stages of cyclic loading, and reached a cyclic excess pore water pressure ratio ($\Delta u/\sigma'_{vc} = r_u$) of approximately 100% in a fewer number of cycles than those subjected to low CSR values.

This type of behaviour was observed regardless of the initial confining stress, σ'_{vc} , initial static shear stress bias (α), overconsolidation ratio (OCR), or applied CSR level. No strain softening and/or loss of shear strength was observed in any of the tests that were conducted under different values for the above variables. The cyclic resistance ratio (CRR) of normally consolidated Fraser River silt was not sensitive to the initial σ'_{vc} for the tested stress range of $85 \text{ kPa} < \sigma'_{vc} < 400 \text{ kPa}$. The CRR of Fraser River silt was found to increase with increasing (OCR), for $\text{OCR} > 1.3$. The test results also indicated that the cyclic resistance would decrease with an increase in initial static shear stress bias (α).

7.1.1 Cyclic shear response of other fine-grained soils

Observations on limited data available on other low plasticity fine-grained soils (i.e. reconstituted quartz rock powder and Kitimat clay) also show a behavioural pattern generally similar to that observed for low plastic Fraser River silt. For example, cumulative decrease in effective stress with increasing numbers of load cycles without strain softening or loss of shear strength were observed in both undisturbed and reconstituted specimens of these soils,. The comparison of the trend-lines obtained for cyclic resistance ratio (CRR) versus number of cycles for these materials revealed that the CRR of the materials seemed to generally increase with increasing plasticity of the soil.

7.2 Comparison of the response of undisturbed versus reconstituted Fraser River silt

Comparison of monotonic tests of undisturbed and reconstituted specimens of Fraser River silt indicate that, for the initial vertical effective confining pressures ranging between 100 to 400 kPa, the volume change tendency exhibited by specimens of reconstituted low plastic Fraser River silt is consistently more contractive than that exhibited by specimens of counterpart undisturbed material. It is important to note this behaviour was prevalent despite the fact that the undisturbed material was in a looser density under identical consolidation stress conditions. This contractive response was also reflected in the stress-strain response, in which the reconstituted specimens experienced a mild strain-softening response before regaining the shear resistance whereas the stress-strain response of undisturbed specimen was

essentially strain-hardening. Overall, the reconstituted specimens exhibited a generally weaker stress-strain response in comparison to the undisturbed specimens.

The consolidation stress state in terms of void ratio (e) and corresponding effective stress (σ'_{vc}) are commonly considered as suitable variables for representing the state of a soil. However, the experimental observations presented herein, with respect to the $e - \log \sigma'_v$ domain, suggest that the reconstituted and undisturbed silt specimens exhibit significantly different characteristics, despite their identical mineralogical origin and grain size. The observed differences further confirm that the void ratio and vertical effective stress alone are not sufficient for defining the mechanical response of this low plastic silt.

The comparison between undisturbed and reconstituted specimens of Fraser River silt under cyclic loading conditions indicate that both undisturbed and reconstituted specimens show cyclic mobility with gradual increase in pore water pressure and degradation of shear stiffness with increasing number of cycles; however, the reconstituted specimens experience cyclic excess pore water pressures and cyclic shear strains at a relatively faster rate. These observations are in agreement with the responses observed in monotonic tests for undisturbed and reconstituted specimens, that, in turn, emphasize that the influence of particle structure and aging on the silt behaviour cannot necessarily be captured by the void ratio alone.

Similar observations were made on tests conducted on undisturbed and reconstituted specimens of Kitimat clay, showing that all reconstituted specimens consistently required a lower number of cycles to reach a certain shear strain level, and that the increase in shear strain and gradual increase of the pore water pressure ratio occurred at a higher rate.

7.3 Post-cyclic reconsolidation response of low-plastic silt

The results from reconsolidation tests conducted on specimens that were initially subjected to constant volume cyclic loading indicate that post-cyclic reconsolidation volumetric strains (ε_{v-ps}) increase with the maximum pore water pressure generated during cyclic loading, as well as with the maximum cyclic shear strain to which the specimens were subjected during cyclic loading. The values of ε_{v-ps} , arising from the specimens of Fraser River silt with different overconsolidation history, particle fabric, and pre-cyclic void ratio, as well as those arising from the quartz powder correlated well with the maximum excess pore water pressure ratio (r_{u-max}).

The resulting ε_{v-ps} versus r_{u-max} trend observed in the study in combination with the relationship of r_u versus number of cycles and CSR, provided an opportunity to develop a method to estimate ε_{v-ps} using experimental data. The method would employ information from laboratory tests, as presented in this thesis, and ideas commonly used in seismic ground response analysis and liquefaction assessment. In principle, the approach has already been adopted as part of current practice by the geotechnical profession in the Greater Vancouver area of the Province of British Columbia, Canada (GVLTF 2007).

Considering that the present database is from limited tests of Fraser River silt, additional research to generate laboratory data for other silty materials and for collecting and synthesizing field data from past earthquakes would be required to confirm the applicability of the above observations and proposed approaches for general geotechnical engineering design.

7.4 Recommendations for future research

In addition to the research findings presented above, the investigation so far has also led to identifying a number of additional tasks as given below that could be undertaken in the future to enhance the current understanding of the response of fine-grained soils to cyclic shear loading:

- The findings presented in this thesis were mainly based on tests carried out on low plastic Fraser River silts obtained from a specific location in the Fraser River delta. It is recommended that additional work be undertaken to enhance the database, specifically, by conducting cyclic DSS testing on samples representing silts with relatively higher plasticity; these soils may be obtained from other locations in the Fraser River delta (or other geographic areas of seismic activity). The work should preferably include tests on fine-grained materials to cover different origins. The effects of initial confining stress level, initial static shear bias, and overconsolidation ratio should be evaluated to compare with the findings of this thesis.
- Additional research work should be undertaken with the objective of correlating laboratory observations with data from field testing (e.g., cone penetration testing), so that the response of a given low plastic soil under cyclic loading can be confidently predicted using data from field testing.
- The evaluation of the post-cyclic reconsolidation response also can be extended to obtaining data from different materials and origins. These additional data would supplement the data in Figure 6.6 for evaluating ε_{v-ps} versus r_{u-max} accompanied with

pore water pressure generation (r_u versus No. of cycles). These evaluations would improve the understanding of the post-cyclic reconsolidation response of various silts.

- There is a need to extend the study to understand the effect of fabric on the cyclic response. For example, the differences in response obtained for tests conducted with undisturbed and reconstituted specimens from a given material should be further investigated, perhaps with the assistance of scanning electron microscopy.
- Improvements to evaluation of the degree of sample disturbance should also form part of future research on low plastic fine-grained soils.
- The data from the present study was obtained from tests conducted using the direct simple shear (DSS) device, which assumes “ K_0 ” conditions. Developing a mechanism to measure the lateral stresses on DSS specimens during testing would improve the understanding of the response of soils to cyclic loading.
- Pore water generation models in silty soils are useful in liquefaction assessments and geotechnical design. The data generated from this study are useful for modeling the generation of pore water pressure of silty soils, and the available laboratory data would allow for model calibration.

REFERENCES

- Andersen, K.H. (2009). Bearing capacity under cyclic loading — offshore, along the coast, and on land. The 21st Bjerrum Lecture presented in Oslo, 23 November 2007 *Can. Geotech. J.* 46(5): 513–535
- Atkinson, J.H., and Bransby, P.L. (1978). The mechanics of soils: An introduction to critical state soil mechanics. McGraw-Hill Book Co., London and New York.
- Bjerrum, L., and Landva, A. (1966). Direct simple-shear tests on a Norwegian quick clay. *Geotechnique*, 16(1), 1-20.
- Boulanger, R.W., and Idriss, I.M. (2006). Liquefaction susceptibility criteria for silts and clays. *J. Geotech. Geoenviron. Eng.*, 132(11), 1413-1426.
- Boulanger, R.W., and Idriss, I.M. (2007). Evaluation of cyclic softening in silts and clays. *J. Geotech. Geoenviron. Eng.*, 133(6), 641-652.
- Bradshaw, A.S., and Baxter, C.D.P (2007). Sample preparation of silts for liquefaction testing. *Geotech Test. J.* 30(4), Paper ID GTJ100206, 9 pages.
- Boulanger, R.W., Meyers, M.W., Mejia, L.H., and Idriss, I.M. (1998). Behavior of a fine-grained soil during the Loma Prieta earthquake. *Can. Geotech. J.* , 35(1), 146-158.
- Bray, J.D., and Sancio, R.B. (2006). Assessment of the liquefaction susceptibility of fine-grained soils. *J. Geotech. Geoenviron. Eng.*, 132(9), 1165-1177.
- Bray, J.D., Sancio, R.B., Durgunoglu, T., Onalp, A., Youd, T.L., Stewart, J.P., Seed, R.B., Cetin, O.K., Bol, E., Baturay, M.B., Christensen, C., and Karadayilar, T. (2004). Subsurface characterization at ground failure sites in Adapazari, Turkey. *J. Geotech. Geoenviron. Eng.*, 130(7), 673-685.

- Bray, J.D., Sancio, R.B., Riemer, M.F., and Durgunoglu, T. (2004). Liquefaction susceptibility of fine-grained soils. Proceedings of the 11th International Conference on Soil Dynamics and Earthquake Engineering and 3rd International Conference on Earthquake Geotechnical Engineering, Berkeley, CA, 7-9.
- Casagrande, A. (1975). Liquefaction and cyclic deformation of sands: A critical review. *Memorias Del Congreso Panamericano De Mecanica De Suelos e Ingenieria De Fundaciones* = Proceedings of the Panamerican Conference on Soil Mechanics and Foundation Engineering, No.5, 5(5), 79-133.
- Castro, G. (1969). Liquefaction of sands. Ph.D. thesis, Harvard University, Cambridge, Mass.
- Castro, G. Poulos, S.J., France, J.W., and Enos, J.L. (1982). Liquefaction induced by cyclic mobility. Report by Geotechnical Engineering, Inc., Winchester, Mass., to the National Science Foundation, Washington, D.C., Department of Commerce, Access number PB 82-235508.
- Chalkley, M.E., and Toirac, I.L. (1997). The acid pressure leach process for nickel and cobalt laterite. Part I: Review of operation at Moa. In Proceedings of the 27th Annual Hydrometallurgical Meeting, Sudbury, Ontario. 17-20 August 1997. The Metallurgical Society of CIM, pp. 341-347.
- Chern, J. (1985). Undrained response of saturated sands with emphasis on liquefaction and cyclic mobility. PhD thesis, University of British Columbia, Vancouver, BC, Canada (CAN).
- Chu, D.B., Stewart, J.P., Boulanger, R.W., and Lin, P.S. (2008). Cyclic softening of low-plasticity clay and its effect on seismic foundation performance. *J. Geotech. Geoenviron. Eng.*, 134(11), 1595-1608.
- Clague, J.J. (1996). Paleoseismology and seismic hazards, Southwestern British Columbia. *Geological Survey of Canada*.
- Crawford, C.B., and Morrison, K.I. (1996). Case histories illustrate the importance of secondary-type consolidation settlements in the Fraser River delta. *Can. Geotech. J.*, 33(6), 866-878.
- Dyvik, R., Berre, T., Lacasse, S., and Raadim, B. (1987). Comparison of truly undrained and constant volume direct simple shear tests. *Geotechnique*, 37(1), 3-10.
- Finn, W.D.L., Bransby, P.L., and Pickering, D.J. (1970). Effect of strain history on liquefaction of sand. *Journal of the Soil Mechanics and Foundations Division*, 96(6), 1917-1934.

- Finn, W.D.L., and Vaid, Y.P. (1977). Liquefaction potential from drained constant volume cyclic simple shear tests. *Proceedings of the 6th World Conference on Earthquake Engineering*, (3), 2157-2162.
- Finn, W.D.L., Vaid, Y.P., and Bhatia, S.K. (1978). Constant volume simple shear testing. *Proceedings of the 2nd International Conference on Microzonation for Safer Construction – Research and Application*, San Francisco, CA, Vol. 2, 839-851.
- Greater Vancouver Liquefaction Task Force Report - GVLTFR. (2007). Task Force report on geotechnical design guidelines for buildings on liquefiable sites in Greater Vancouver in accordance with NBC 2005, D.L. Anderson, P.M. Byrne, R.H. DeVall, E. Naesgaard, and D. Wijewickreme eds. Vancouver, B.C., Canada. 74 pp. <http://www.civil.ubc.ca/liquefaction/>
- Green, R.A., Mitchell, J.K., and Polito, C.P. (2000). An energy-based pore pressure generation model for cohesionless soils, *Proc., John Booker Memorial Sympo. - Developments in the Theoretical Geomechanics*, D.W. Smith and J.P. Carter, eds., Balkema, Rotterdam, The Netherlands, 383-390.
- Guo, T., and Prakash, S. (1999). Liquefaction of silts and silt-clay mixtures. *J. Geotech. Geoenviron. Eng.*, 125(8), 706-710.
- Hoeg, K., Dyvik, R., and Sandbaekken, G. (2000). Strength of undisturbed versus reconstituted silt and silty sand specimens. *J. Geotech. Geoenviron. Eng.*, 126(7), 606-617.
- Hyde, A.F.L., Higuchi, T and Yasuhara, K. (2006). Liquefaction, cyclic mobility, and failure of silt. *J. Geotech. and Geoenviron. Eng.* 132(6), pp. 716-735.
- Hyde, A.F.L., Higuchi, T and Yasuhara, K. (2007). Postcyclic recompression, stiffness, and consolidated cyclic strength of silt. *J. Geotech. and Geoenviron. Eng.* 133(4), pp. 416-423.
- Idriss, I.M., and Boulanger, R. (2008). Soil liquefaction during earthquakes. Earthquake Engineering Research Institute. Pub No. MNO-12. 237 pp.
- Ishihara, K. (1996). Soil behaviour in earthquake geotechnics. Oxford Engineering Science Series, 350 pp.
- Ishihara, K. Sodekawa, M. and Tanaka, Y. (1977). Effects of overconsolidation on liquefaction characteristics of sands containing fines. *Dynamic Geotechnical Testing*. ASTM Special Technical Publication 654. Denver, Col., 28 June 1977. pp. 247-264.
- Ishihara, K. Tatsuoka, F. and Yasuda, S. (1975). Undrained deformation and liquefaction under cyclic stresses. *Soil and Foundations*, 15(1): 29-44.

- Ishihara, K., Yasuda, S., and Yokota, K. (1981). Cyclic strength of undisturbed mine tailings: International conference on recent advances in geotechnical earthquake engineering and soil dynamics; St. Louis, Mo., 26 April – 2 May 1981. University of Missouri–Rolla, St. Louis, Mo. Vol. 1, pp. 53–58.
- Ishihara, K., and Yoshimine, M. (1992). Evaluation of settlements in sand deposits following liquefaction during earthquakes. *Soils and Foundations*, 32(1), 173-188.
- Jefferies, M.G., and Been, K. (2006). Soil liquefaction – A critical state approach. Taylor & Francis Group, London and New York.
- Kammerer, A.M. (2002). Undrained response of Monterey 0/30 sand under multidirectional cyclic simple shear loading conditions. PhD thesis, University of California at Berkeley, Berkeley, CA, United States (USA).
- Kuerbis, R., Negussey, D., and Vaid, Y.P. (1988). Effect of gradation and fines content on the undrained response of sand. Hydraulic Fill Structures, Publ by ASCE, New York, NY, USA, Fort Collins, CO, USA, 330-345.
- Lee, K.L., and Albaisa, A. (1974). Earthquake induced settlements in saturated sands. *J. Geotechnical Engineering Division*, 100(GT4), 387-406.
- Lee, K.L., and Seed, H.B. (1967). Dynamic strength of anisotropically consolidated sand. *Proceedings of the American Society of Civil Engineers*, 93(SM5), 169-190.
- Leroueil, S., and Hight, D.W. (2003). Behaviour and properties of natural soils and soft rocks. Characterisation and engineering properties of natural soils, T.S. Tan, K.K. Phoon, D.W. Hight, and S. Leroueil, eds., A.A. Balkema, United States (USA).
- Long, M., Vaid, Y.P., Sivathayalan, G., Hoeg, K., Dyvik, R., and Sandbaekken, G. (2001). Strength of undisturbed versus reconstituted silt and silty sand specimens: Discussion and reply [modified]. *J. Geotech. Geoenviron. Eng.*, 127(11), 991-994.
- Lunne, T., Berre, T., and Strandvik, S. (1999). Sample disturbance effects in soft low plastic Norwegian clay. *Publikasjon-Norges Geotekniske Institutt*, (204), 81-102.
- Monahan, P.A., Byrne, P.M., Watts, B.D and Naesgaard, E. (2000). Engineering geology and natural hazards of the Fraser River delta. Guidebook for geological field trips in Southwestern British Columbia and Northern Washington. Annual Meeting of the Cordilleran Section of the Geological Society of America. Vancouver, April 2000. pp. 27-47.

- Monahan, P.A., Luternauer, J.L., Barrie, J.V., Martindale, B., and Wood, J. (1997). The topset and upper foreset of the modern Fraser River delta, British Columbia, Canada; CSPG-SEPM joint convention: Sedimentary events, hydrocarbon systems. CSPG-SEPM Joint Convention, Calgary, AB, Canada (CAN).
- NBCC 1995 (1995). National Building Code of Canada (NBCC), 11th edition, 1995, National Research Council of Canada, Ottawa, Canada.
- Negussey, D., Wijewickreme, W.K.D., and Vaid, Y.P. (1988). Constant-volume friction angle of granular materials. *Can. Geotech. J.*, 25(1), 50-55.
- Oda, M. (1972). The mechanism of fabric changes during compressional deformation of sand. *Soils and Foundations*, 12(2), 1-18.
- Park, S., and Byrne, P.M. (2004). Stress densification and its evaluation. *Can. Geotech. J.*, 41(1), 181-186.
- Polito, C., Green, R., and Lee, J. (2008). Pore pressure generation models for sands and silty soils subjected to cyclic loading. *J. Geotech. Geoenviron. Eng.*, 134(10), 1490-1500.
- Polito, C.P., and Martin II, J.R. (2001). Effects of nonplastic fines on the liquefaction resistance of sands. *J. Geotech. Geoenviron. Eng.*, 127(5), 408-415.
- Sanin, M.V. (2005). Cyclic shear loading response of Fraser River delta silt. MASc thesis, Department of Civil Engineering, University of British Columbia, Vancouver, B.C., Canada.
- Sanin, M.V., and Wijewickreme, D. (2006). Cyclic shear response of channel-fill Fraser River delta, *Soil Dynamics and Earthquake Engineering*, 26(9), 854-869.
- Schnabel, P.B., Lysmer, J., and Seed, H.B. (1972). SHAKE: a computer program for earthquake response analysis of horizontally layered sites. Berkeley: Earthquake Engineering Research Center, University of California.
- Schofield, a. N., and Wroth, P. (1968). Critical state soil mechanics. McGraw-Hill, 310 pp.
- Seed, H.B. (1979). Soil liquefaction and cyclic mobility evaluation for level ground during earthquakes. *Journal of the Geotechnical Engineering Division, ASCE*, 105(2), 201-255.
- Seed, H.B., Duncan, J.M., and Idriss, I.M. (1975). Criteria and methods for static and dynamic analysis of earth dams: Criteria and assumptions for numerical analysis of dams. Swansea, Univ. Wales, Swansea, United Kingdom (GBR).

- Seed, R.B., and Harder, L.F. (1990). SPT-based analysis of cyclic pore pressure generation and undrained residual strength. Proceedings of the H. Bolton Seed Memorial Symposium, 351-376.
- Seed, H.B., Mori, K., and Chan, C.K. (1977). Influence of seismic history on liquefaction of sands. *Journal of the Geotechnical Engineering Division, ASCE*, 103(GT4): 257-270.
- Seed, H.B., and Peacock, W.H. (1971). Test procedures for measuring soil liquefaction characteristics. *Journal of the Soil Mechanics and Foundations Division*, 97(8), 1099-1119.
- Sriskandakumar, S. (2004). Cyclic loading response of Fraser River sand for validation of numerical models simulating centrifuge tests. PhD thesis, MAsc. Thesis, Department of Civil Engineering, The University of British Columbia, Vancouver, BC.
- Suzuki, T., and Toki, S. (1984). Effect of pre-shearing on liquefaction characteristics of saturated sand subject to cyclic loading. *Soils and Foundations*, 24(2):16-28.
- Terzaghi, K., Peck, R.B., and Mesri, G. (1996). Soil mechanics in engineering practice. John Wiley & Sons, New York, NY, United States (USA).
- Thevanayagam, S., Shenthnan, T., Mohan, S., and Liang, J. (2002). Undrained fragility of clean sands, silty sands, and sandy silts. *J. Geotech. Geoenviron. Eng.*, 128(10), 849-859.
- Tokimatsu, K., and Seed, H.B. (1987). Evaluation of settlements in sands due to earthquake shaking. *Journal of Geotechnical Engineering, ASCE*, 113(8): 861-878.
- U.S., National Research Council, Committee on Earthquake Engineering, Washington, DC, United States (USA). (1985). Liquefaction of soils during earthquakes. Natl. Acad. Press, Washington, DC, United States (USA).
- Vaid, Y.P., and Chern, J.C. (1985). Cyclic and monotonic undrained response of sands. Advances in the Art of Testing Soils Under Cyclic Loading Conditions, Proceedings of the ASCE Convention, Detroit, 120-147.
- Vaid, Y.P., Chung, E.K.F., and Kuerbis, R.H. (1989). Preshearing and undrained response of sand. *Soils and Foundations*, 29(4), 49-61.
- Vaid, Y.P., and Finn, W.D.L. (1979). Static shear and liquefaction potential. *Journal of the Geotechnical Engineering Division, ASCE*, 105(GT10): 1233-1246.
- Vaid, Y.P., Sivathayalan, S., and Stedman, D. (1999). Influence of specimen-reconstituting method on the undrained response of sand. *Geotech Test J*, 22(3), 187-195.

- Vaid, J.P., Stedman, J.D., and Sivathayalan, S. (2001). Confining stress and static shear effects in cyclic liquefaction. *Can. Geotech. J.* , 38(3), 580-591.
- Vaid, Y.P., and Thomas, J. (1995). Liquefaction and postliquefaction behavior of sand. *Journal of Geotechnical Engineering, ASCE*, 121(2), 163-173.
- Vucetic, M., and Dobry, R. (1991). Effect of soil plasticity on cyclic response. *J. Geotech. Eng.*, 117(1), 87-107.
- Wijewickreme, D., Sanin, M.V., and Greenaway, G.R. (2005a). Cyclic shear response of fine-grained mine tailings. *Can. Geotech. J.* , 42(5), 1408-1421.
- Wijewickreme, D., Srisankandakumar, S., and Byrne, P. (2005b). Cyclic loading response of loose air-pluviated Fraser River sand for validation of numerical models simulating centrifuge tests. *Can. Geotech. J.* , 42(2), 550-561.
- Wu, J. (2002). Liquefaction triggering and post-liquefaction deformation of Monterey 0/30 sand under unidirectional cyclic simple shear loading. PhD thesis, University of California, Berkeley, California, U.S.
- Yasuhara, K., Murakami, S., Toyota, N., and Hyde, A.F.L. (2001). Settlements in fine-grained solids under cyclic loading. *Soils and Foundations*, 41(6), 25-36.
- Youd, T. L., Idriss, I. M., Andrus, R. D., Arango, I., Castro, G., Christian, J. T., Dobry, R., Finn, W. D. L., Harder, L. F. J., Hynes, M. E., Ishihara, K., Koester, J. P., Liao, S. S. C., Marcuson, W. F. I., Martin, G. R., Mitchell, J. K., Moriwaki, Y., Power, M. S., and Robertson, P. K. (2001). Liquefaction Resistance of Soils: Summary Report from the 1996 NCEER and 1998 NCEER/NSF Workshops on Evaluation of Liquefaction Resistance of Soils. *J. Geotech. Geoenviron. Eng.*, 127(10), 817-833.
- Zergoun, M., and Vaid, Y.P. (1994). Effective stress response of clay to undrained cyclic loading. *Can. Geotech. J.* , 31(5), 714-727.
- Zhang, G., Robertson, P. K., and Brachman, R.W.I. (2002). Estimating liquefaction-induced ground settlements from CPT for level ground. *Can. Geotech. J.*, 39(5), 1168-1180.